ENGINEERED γδ T CELLS FOR MULTIPLE MYELOMA

TAC ENGINEERED γδ T CELLS FOR MULTIPLE MYELOMA

By SARAH ASBURY, B.Sc. (HONS)

A Thesis
Submitted to the School of Graduate Studies in
Partial Fulfillment of the Requirements for the Degree

Master of Science

McMaster University

MASTER OF SCIENCE (2021) McMaster University
(Biochemistry & Biomedical Science) Hamilton, Ontario

TITLE: TAC Engineered γδ T Cells for Multiple Myeloma

AUTHOR: Sarah Asbury, B.Sc. (McMaster University)

SUPERVISOR: Dr. Jonathan L. Bramson

NUMBER OF PAGES: 143

Abstract

Engineered T cell therapies have had unprecedented success in treating hematological malignancies. However, their use is limited by expensive treatment costs – priced at approximately $500,000 CAD for a single-dose of CAR-T cell therapy. γδ T cells are a candidate for allogeneic engineered T cell therapies, which can be mass manufactured to reduce the cost of goods. In this thesis we investigate γδ T cells engineered with a T cell Antigen Coupler targeting BCMA (BCMA-TAC) for the treatment of Multiple Myeloma – an incurable hematological malignancy. We optimized a manufacturing method to transduce γδ T cells with a GaLV-pseudotyped γ-retrovirus encoding BCMA-TAC and demonstrated that BCMA-TAC γδ T cells rapidly and specifically kill Multiple Myeloma tumour cells. We also investigated the potential for a combination therapy using engineered γδ T cells and monoclonal antibodies. Such a combination therapy may be synergistic, because γδ T cells express CD16 and can respond to antibody opsonized cells via direct cytotoxicity or phagocytosis. While degranulation of BCMA-TAC γδ T cells was enhanced by CD16 stimulation, we did not observe any improvements in direct cytotoxicity against antibody-opsonized tumour cells. Overall, our results demonstrate that BCMA-TAC γδ T cells can directly target and kill Multiple Myeloma tumour cells, but whether monoclonal antibodies can be used to further enhance their anti-tumour properties remains unclear.

Acknowledgements

Thank you to Dr. Jonathan Bramson for your mentorship and support over the last 2 years. I am grateful for both the encouragement and the feedback you've provided throughout this project; I have learned from you both as a scientist and as a professional. I have a deep respect and admiration for your approach to science. The culture of creativity and intelligent risk-taking you've cultivated in the lab has made my time in the Bramson lab exciting, and full of novel opportunity. Thank you for giving me the freedom in this project to pursue my interests, whether it be the esoteric functions of γδ T cells, or bioinformatics. I am fortunate to have been one of your students.

The Bramson lab has always truly felt like a community during my time here, and that's because of all the wonderful and supportive people in the lab. I would like to thank SeungMi Yoo, in my first few months of graduate school you took me under your wing and made sure I understood everything I needed to know. You were an advocate, a teacher, a mentor, and a cheerleader – I am very thankful for all the support you gave me. I would also like to thank Arya Afsahi. You have been an incredible source of help, whenever there was a new lab technique I was planning, I knew I could rely on you to provide direction. Your efforts to unite all the grad students in the lab has been such a key part of the positive community here, especially during the pandemic. Thank you for all the encouragement, but even more importantly, thank you for all the commiseration. To Rebecca Burchett, you have been such a delight to spend late-nights running experiments in TC alongside. Thank you for all the fun and whacky memories, and having impeccable taste in Christmas music. Most importantly, thank you for your kindness in

all that you do. I am so grateful you reached out and offered to help with that one incredibly long flow-sort experiment, just because you saw the booking was long. I, quite literally, could not have done it without you. I would also like to thank those in the Bramson lab who helped along the way. Thank you, Derek Cummings, Joni Hammill, and Bonnie Bojovic, for helping me with the day-to-day around the lab. Thank you to Ying Wu for helping me source 10 blood donors for my experiments, and your unending patience. Finally, thank you to Ksenia Bezverbnaya, Jamie McNicol, Duane Moogk, and Carly Graham for technical advice in my experiments. It has been a pleasure working among bright scientists, who also have the best interest of their colleagues at heart.

I would also like to thank both of my parents. To my mother, you have always believed in me, and been supportive of my somewhat nonlinear paths in pursuit of what I'm passionate about. To my father, you have always encouraged curiosity about the world around us, and to critically question our understanding of it. Thank you both for encouraging my scientific endeavours.

Most importantly, thank you to my partner, Stefano Lopiccolo. Completing this project in the pandemic has not been easy, but I could not have asked to have someone more encouraging, thoughtful, and compassionate by my side. In the hard times you have kept me grounded, and always taken care to remind me of the big picture. In the good times you have always cheered me on, celebrating my wins with me. The way in which you believe in me, allows me to believe in myself. Thank you for your love, your patience, and your support.

Table of Contents

List of Tables and Figures

List of Abbreviations

aAPC	Artificial antigen presentation cell
ACT	Adoptive T Cell Therapy
ADCC	Antibody-dependent cytotoxicity
ADCP	Antibody-dependent phagocytosis
alloHSCT	Allogeneic hematopoietic stem cell transplant
APC	Antigen presentation cell
BCMA	B-Cell Maturation Antigen
BTN2A1	Butyrophilin Subfamily 2 Member A1
BTN3A1	Butyrophilin Subfamily 3 Member A1
CAR	Chimeric Antigen T Cell Receptor
CRS	Cytokine release syndrome
DEG	Differentially expressed genes
FcγRIII	Fc gamma receptor III
gRV	γ-retrovirus
GSEA	Gene set enrichment analysis
GvHD	Graft-versus-host disease
HMBPP	(E)-4-Hydroxy-3-methyl-but-2-enyl pyrophosphate (HMBPP)
hV	High viral supernant manufacturing condition
hVR	High viral supernant and retronectin manufacturing condition
IgG	Immunoglobulin G
IPP	Isopentenyl pyrophosphate
ITAM	Killer cell immunoglobulin-like receptor 2DS2
JTM	Juxtatransmembrane
KIR	Killer Ig-Like Receptor
KIR2DS2	Killer cell immunoglobulin-like receptor 2DS2
LFC	Log2 fold change
LV	Lentivirus
mAb	Monoclonal antibody
MM	Multiple Myeloma
NGFR	Nerve growth factor receptor
NKR	Natural Killer Receptor
NT	Non-transduced
pAg	Phosphoantigen
PBMC	Peripheral blood mononuclear cell
PCA	Principal component analysis
SLC	Solute carrier family
TAA	Tumour-associated antigen
TAC	T Cell Antigen Coupler
TCR	T Cell Receptor
TF	Transcription factor

Declaration of Academic Achievement

Dr. Jonathan Bramson and I designed the experiments in this thesis. Experiments were carried out by myself, with technical assistance from Rebecca Burchett for RNA-Seq flow-sorting and Tianning Yu for the tumour ICS. The conceptual design for the KIR-TAC construct was developed by Dr. Galina Denisova, Dr. Joanne Hammill, and Dr. Jonathan Bramson. I completed the KIR-TAC construct cloning and generation of a stable gRV-producing PG13 cell line, as well as γδ T cell manufacturing. Transduction of γδ T cells with commercial lentivirus data was collected by Seungmi Yoo.

Background

Multiple Myeloma

Multiple Myeloma (MM) is a hematological malignancy characterized by malignant plasma cells in the bone marrow[1]. MM originates from developing B cells that undergo transformation after an erroneous VDJ recombination event. Double-stranded breaks, inherent to the recombination process, facilitate a random chromosomal translocation in the transformed MM precursor, relocating oncogenes under the control of constitutively expressed B Cell Receptor promoter[2]. The primary site of MM is the bone marrow niche, which is critical for providing a microenvironment that supports MM cell survival, in a similar manner to long-lived plasma cells[3]. Indeed, stromal cells in the bone marrow that interact directly with MM cells can produce pro-inflammatory cytokines activating growth-related signaling cascades,[3] and upregulate checkpoint molecules that prevent MM cell apoptosis[4].

Multiple Myeloma Conventional Therapies

MM is conventionally treated using high-dose chemotherapy followed by autologous stem cell transplant for patients healthy enough to withstand the chemotherapy and transplant procedure[5], however this method is not curative and requires indefinite maintenance treatment with the immunomodulatory drug, lenalidomide[6]. For patients ineligible for autologous stem cell transplant, MM can be treated using triplicate therapies. The first-line triplicate therapy uses a combination of immunomodulators and a steroid: bortezomib, lenalidomide and dexamethasone (VRd)[7]. MM patients treated with VRd triplicate therapy have a median overall survival of 6 years, compared to only 5.3 years with the previous standard of

care – lenalidomide and dexamethasone. However, a treatment course of VRd and other triplicate therapies is not curative, and MM must also be indefinitely managed with lenalidomide[7].

While indefinite treatment with lenalidomide improves MM progression-free survival, its use is not inconsequential. There are a number of adverse events affecting quality of life including fatigue, gastrointestinal disturbances, muscle pain, and increased susceptibility to infection[6]. Lenalidomide also increases risk of developing secondary primary malignancies[6]. Furthermore, the total cost of maintaining a patient on lenalidomide treatment has been estimated at $130,000 yearly to the Canadian healthcare system[8]. Given this treatment is usually maintained indefinitely in patients with MM, novel alternative therapies represent significant potential for improving patient health and quality of life, while reducing treatment cost.

Multiple Myeloma Contemporary Therapies

MM Antibody Therapies

The efficacy of immunomodulators and steroids in VRd treatment underscores the potential for treatments that modify the interaction between the immune system and MM cells. Several clinical trials for antibody-dependent MM immunotherapies, including monoclonal antibodies, BiTEs, and bispecific antibodies, have been completed and demonstrated some efficacy, or are underway[9]. Common targets for MM-specific antibody therapies include anti-CD38 and B-Cell Maturation Antigen (BCMA)[9]. Such therapies can benefit patients as a monotherapy, or improve outcomes for patients when used in combination with

traditional MM treatment regimens[9]. For example, treatment with anti-CD38 (Daratumumab) in combination with lenalidomide and dexamethasone (Rd), improved progression-free survival in MM patients compared to Rd alone in a phase 3 clinical trial[10]. Anti-CD38 is used as a target for mAb MM immunotherapies because CD38 is highly expressed on MM cells[11], and high expression levels are an important factor for increasing the probability of antibody-dependent cell cytotoxicity directed against the tumour target[12]. However, CD38 can also be expressed in a number of cells in both the myeloid and lymphoid lineages[13], thus anti-CD38 mAb treatment can cause hematopoietic cell cytopenias including lymphopenia, neutropenia, anemia, and thrombocytopenia[14].

MM CAR-T Cell Therapies

Recent success of CAR-T cell therapies for otherwise incurable leukemias[15] has invigorated the possibility for engineered T cell therapy targeting other hematological malignancies, such as MM. A well-designed CAR should target a tumour-associated antigen that is ubiquitously expressed on tumour cells and has limited expression on healthy cells, thereby reducing the likelihood on-target off-tumour toxicity. While CD38 is highly expressed on MM cells, it is also expressed on several hematopoietic cells[11,12]. Comparatively, BCMA is also upregulated in MM cells, but only has normal expression in plasma cells and plasmacytoid dendritic cells[16]. Indeed, a number of CAR-T cell clinical trials for MM have focused on targeting BCMA, and have demonstrated an overall response rate of 64 – 94%[9]. However, the current iterations of BCMA-specific CAR-T cells are often not curative for MM, with a median progression-free survival of only 4.4 months using a CD3ζ-CD28 2nd generation CAR[17] or 11.8 months in phase 1 trials for a CD3ζ-4-1BB 2nd generation CAR – idecabtagene vicleucel [18].

Recently, idecabtagene vicleucel completed phase 2 trials and received FDA approval for the treatment of Multiple Myeloma. However, their phase 2 trials the median progression free survival was only 8.8 months, with a 33% complete response rate[19]. Ciltacabtagene autoleucel, a BCMA-specific 4-1BB-CD3ζ 2nd generation CAR, had higher response rates in their phase 2 trials, with 67% of patients achieving complete response. While progression free survival was not reached – indicating durable remission – the progression free rate at 12-months was 77%[20]. Ciltacabtagene autoleucel is engineered with two single-domain antibodies that target BCMA, as opposed to idecabtagene vicleucel which uses a BCMA-specific scFv[19,20]. Despite ciltacabtagene autoleucel having high response rates, it also has high toxicities with 95% patients experiencing CRS (4% ≥ grade 3) and 21% of patients experiencing neurotoxicities (9% ≥ grade 3)[20]. While the overall response rates of BCMA-specific CAR-T cells suggest that engineered T cells can be used to specifically target MM cells, the incidence of relapse with idecabtagene vicleucel and serious neurotoxicities in ciltacabtagene autoleucel suggests there is a need to improve the efficacy and safety of the engineered T cell products.

T cell Antigen Coupler (TAC)

The Bramson Lab has developed a novel chimeric receptor, referred to as T cell Antigen Coupler (TAC) receptors. Like CARs, the TAC receptor uses a single-chain variable fragment to garner specificity to a tumour-associated antigen. However, instead of using a synthetic CD3ζ domain, the TAC interfaces directly with CD3 using anti-CD3 UCHT1 scFv[21]. By interfacing with CD3 rather than stimulating signaling via an artificial CD3ζ domain, the TAC receptor may be able to better replicate endogenous regulation within the TCR-CD3 interface – which enhances or represses TCR signaling depending on the danger context of the target. In accordance with

this, our lab has shown that αβ T cells engineered with TAC to target HER2 have lower toxicity *in vivo* compared to 2nd generation HER-2 specific CARs, while maintaining equivalent tumour clearance efficacy[21].

TAC for MM

Our group has developed BCMA-specific TACs for multiple myeloma. Recently published data from our lab has shown that BCMA-specific αβ TAC T cells can clear tumours in a MM (KMS-11) xenograft mouse model[22]. This *in vivo* efficacy has been demonstrated in 2 lentiviral BCMA-specific TAC constructs that differ by their leader sequences: LV-BCMA-TAC#898 which uses an Igκ leader sequence, or LV-BCMA-TAC#1072 which uses a CD8α leader sequence. When transduced into αβ T cells LV-BCMA-TAC#1072 has higher TAC surface expression in comparison to LV-BCMA-TAC#898. While TAC surface expression impacts some *in vitro* features of the TAC T cells, surface expression had no bearing on the *in vivo* efficacy of BCMA-TAC T cells. The robust therapeutic effect of the BCMA-TAC T cells has prompted the development of a clinical trial to test the tolerability and therapeutic efficacy of engineered autologous αβ T cells expressing a fully humanized BCMA-TAC with a CD3a leader sequence.

Introduction to γδ T Cell Biology

General γδ T Cell Biology

Previous work in the Bramson lab has focused on conventional αβ T cells. My project aims to explore the utility of non-canonical γδ T cells as substrates for the generation of TAC-T cells. We believe the TAC receptor will be particularly well suited for γδ T cells based on data showing that UCHT1 robustly activates the Vγ9Vδ2 TCR[23]. γδ are considered a rare non-

conventional T cell subsets because they only make up 0.5 – 16% of CD3+ cells in peripheral blood[24]. However, during an infection, they may expand to comprise up to 60% of CD3+ T cells in peripheral blood[24]. Additionally, in mucosal and epithelial tissues, γδ T cell can comprise up to 20 - 50% of CD3+ cells[25]. γδ T cells are thought to play a critical role in bridging the innate and adaptive immune systems in an immune response, as they have characteristics of both systems. There is limited research on γδ T cells compared to αβ T cells likely in part because the development and subsets of γδ T cells differ between primates and rodents[25], and therefore access to a model systems to study human γδ T cells is limited.

γδ T Cell Subsets

γδ T cells are be broadly defined by their delta and gamma T cell receptor (TCR) chains, and the most common subsets in humans are Vδ2 and Vδ1. Single cell RNA-sequencing analysis of Vδ1 and Vδ2 using dimension reduction technique t-SNE demonstrates that these two subsets can be transcriptomically separated into 2 clusters distinguished by 37 differentially expressed genes[26]. Consequently, Vδ2 and Vδ1 subsets do have unique functional capabilities and tissue distributions. The Vγ9+Vδ2+ subset is often considered the most common γδ T cell in peripheral blood, although this phenotype is not conserved across all populations – a study conducted comparing individuals from Denmark and Ghana demonstrated that the Adult Africans had a slight Vδ1 predominance in peripheral blood[27]. A separate study in the United States demonstrated that African Americans also have a lower proportion of circulating Vδ2+ T cells compared to Caucasian Americans, although Vδ1 subsets were not characterized[28]. These studies demonstrate that there are genetic and/or regional environmental factors (i.e. regional

antigen exposure) that can influence the circulating γδ repertoire. However, the overall TCR repertoire of γδ T cells appears to be primarily shaped by environment rather than genetics[29,30].

Vγ9Vδ2 Biology

Vγ9Vδ2 Repertoire Tissue Localization and Development

The Vγ9Vδ2 subset represents a rational candidate for MM-specific engineered γδ T cell therapy. They are the primary γδ T cell subset circulating in peripheral blood and have demonstrated bone marrow homing capability[31]. Indeed, MM patients have a Vγ9Vδ2 cell infiltrate, although T cell infiltrates are exhausted due to bone marrow niche-induced upregulation of PD-1 on MM cells[32]. Healthy engineered Vγ9Vδ2 T cells may have advantages in accessing and destroying MM cells compared to conventional engineered αβ T cells due to their inherent bone marrow homing capabilities.

Vγ9Vδ2 T cells are the first T cell to appear during fetal development, and are generated at this stage within the fetal liver rather than the fetal thymus[29]. The Vγ9Vδ2 subset is considered innate-like because Vγ9Vδ2 TCR diversity is oligoclonal at birth and remains relatively invariant throughout life. However when considering all γδ subsets, there is greater γδ TCR diversity in cord blood compared to adult peripheral blood, indicating adaptive postnatal restriction of γδ repertoire[30]. Antigen-experienced Vγ9Vδ2 T cell expand to become the most prominent γδ T cell subset in peripheral blood by adulthood, despite greater diversity of Vδ1 in the thymus[33], demonstrating the role of adaptive antigen-specific expansion in shaping the γδ repertoire.

Vγ9Vδ2 Phosphoantigen Recognition

The Vγ9Vδ2 TCR recognizes nonpeptide phosphoantigens accumulated in target cells either due to bacterial infection or metabolic disruptions inhibiting the mevalonate synthesis pathway. The downstream products of the mevalonate pathway include cholesterol and farnesyl pyrophosphate, which is required for post-translation modification in the Ras/rho pathway[34]. Transformed cells often have dysregulation of the mevalonate pathway, leading to recognition and destruction by Vγ9Vδ2 cells[35]. Vγ9Vδ2 T cells recognizes the accumulation of phosphoantigens (pAgs) such as isopentyl pyrophosphate (IPP), which is an intermediate in the mevalonate pathway – or in the case of bacterial infection, (E)-4-Hydroxy-3-methyl-but-2-enyl pyrophosphate (HMBPP) – via butyrophilin molecules expressed on the surface of the target cells, as opposed to the MHC molecules that are ligands for αβ TCRs[36]. Both BTN3A1 and BTN2A1 are required for Vγ9Vδ2 TCR signaling[37], however the precise receptor-ligand interaction has yet to be fully elucidated. It is known that the B30.2 domain on the cytoplasmic tail of BTN3A1 binds to intracellular phosphoantigens in the target cell, leading to a conformational change in the juxtatransmembrane (JTM) region of target cell BTN3A1[36] – which modulates the strength of γδ TCR signaling[38]. However, while BTN3A1 and cell-to-cell contact[36] are necessary for accumulated pAg recognition by Vγ9Vδ2 TCRs, there is no evidence that the TCR interacts with BTN3A1 directly[36]. A recently published study demonstrated that BTN2A1 can bind directly to Vγ9 and is required for Vγ9Vδ2 TCR recognition of pAg in target cells[37]. Using FRET, Rigau et al. also demonstrated that both the intracellular and extracellular domains of BTN2A1 and BTN3A1 co-localize on the cell-surface, indicating the possibility that they assemble a complex mediating Vγ9Vδ2 TCR recognition[37].

γδ T Cell Cytotoxicity

The effector functions of human γδ T cells, including the Vγ9Vδ2 subset, are acquired in the periphery in response to cytokine and antigen stimulation. This is unlike in rodent γδ T cell effector functions, which are pre-programmed in the thymus[25]. Both human and rodent γδ produce either IFNγ+, indicating a Th1-like effector functions, or IL-17+, indicating a Th17-like effector functions. IFNγ expressing γδ T cells are associated with cytotoxic anti-tumour functions, whereas IL-17 expressing γδ T cells are associated with pro-tumour inflammation[25]. In humans, IL-17+ γδ T cells are rare in healthy individuals and are typically only found in immunosuppressive microenvironments such as tumours[25] and TB granulomas[39,40], or in response to bacterial infections that depend on neutrophil recruitment for clearance[41]. Th1-like IFNγ+ T cells can mediate tumour clearance via a number of direct cell-mediated cytotoxicity methods including TRAIL, and FasL and cytotoxic granule release mediated by TCR, NKR, or FcγRIII signaling[35].

While cytokine stimulation can generate an IFNγ effector phenotype in the periphery, cytokine signaling alone is not sufficient to activate effector functions and cytotoxicity in Vγ9Vδ2 cells – this subset also requires CD3 stimulation via TCR-dependent phosphoantigen recognition[42]. The requirement of CD3 for activation does not appear as stringent in Vδ1 cells, which can exhibit effector functions and cytotoxicity from cytokine stimulation alone[42].

γδ TCR signaling is important to Vγ9Vδ2 cytotoxicity for certain tumour cell types, but TCR activation it is not universally required for killing. As an example, γδ TCR signaling is critical is in neuroblastoma cell line SH-SY-5Y, as anti-Vγ9 monoclonal antibody (mAb) or mevastatin – which prevent accumulation of IPP – inhibits cell lysis by Vγ9Vδ2 cells[43]. However, Vγ9Vδ2

cytotoxicity can also be triggered by innate-like receptors such as NKRs and the KIR system. Vγ9Vδ2 cells express NKG2D, which recognizes a host of stress ligands including MICA, MICB, and ULBP proteins and transduces signals via adaptor protein Dap10[44–46]. NKG2D can either co-stimulate Vγ9Vδ2 TCR signaling to improve γδ T cell cytotoxicity as demonstrated in lymphoma cell line Daudi[45], or induce cytotoxicity independent of TCR stimulation as demonstrated in Jurkat and Molt-4 leukemia cell lines[45]. Another NKR, DNAM-1 – which recognizes PVR and nectin-2 – can also co-stimulate CD3 γδ TCR signaling[31]. Similar to NK cells, Vγ9Vδ2 cytotoxicity that relies on activating NKRs can be regulated by the inhibitory receptors within the Killer cell Immunoglobulin-like Receptor (KIR) system, whereby MHC I expression increases inhibitory KIR signals and consequently the threshold for cell-mediated cytotoxicity[47]. Activating KIR receptor KIR2DS2 expression has also been shown in Vγ9Vδ2 cells of some chronic lymphocytic leukemia patients, although expression seems to be variable and no efforts were made to characterize the role of KIR2DS2 in Vγ9Vδ2 cytotoxicity[48]. There is one report demonstrating KIR2DS2-mediated cytotoxicity in a Vδ2- γδ T cell clone, although the clone has puzzlingly low gene expression of KIR system adaptor protein DAP12 – an adaptor protein thought to be critical for KIR2DS2 signaling transduction[49]. Overall, Vγ9Vδ2 T cells may be activated by TCR and NKR-dependent signaling in either an independent or cooperative manner depending on the tumour or cell line; the exact nature of activation is likely dictated by which TCR or NKR ligands are expressed by target cells[45].

FcγR Functionality in γδ T cells

FcγR Signaling

γδ T cells are capable of antibody-dependent cytotoxicity (ADCC) and antibody-dependent phagocytosis (ADCP) via multivalent Fcγ Receptor (FcγR) interactions with antibody opsonized target cells. FcγR's, which mediate effector functions in response to Ig Fc binding of antibodies, are expressed on pAg expanded γδ T cells; specifically, CD16[50–54] and CD32[50]. Similar to TCRs, FcγR ultimately have an antigen-specific response through antibody opsonization, but most FcγRs cannot independently transduce activation signals[55,56]. Rather, adaptor molecules are required for signal transduction in response to multivalent Ig-Fc binding, and include CD3 molecules, DAP12, and FcRγ[55]. ITAM phosphorylation of these adaptor proteins leads to downstream phosphorylation for Zap-70, ERK, PLCγ, PI3K, and Akt pathways[55,57]. Indeed, inhibition of MAPK or MEK phosphorylation in Vγ9Vδ2 cells prevents TNFα production in response to anti-CD16 stimulation, outlining the importance of the Ras-Raf-MEK-ERK pathway for FcγR signaling in γδ T cells[54]. Although CD3 and FcγR activate similar signaling pathways, the tyrosine phosphorylation patterns generated by CD3 or CD16 stimulation in γδ T cell is unique, suggesting the potential for unique downstream effector functions in response to each pathway[54].

Importantly, monovalent interaction between FcγR-expressing cells and Ig-Fc has been associated with inhibition of immune effector functions. Monovalent Ig-Fc interaction is proposed to induce weak phosphorylation of downstream signaling components, including low phosphorylation of Erk, and the recruitment of SHP-1 to the cell membrane[58]. This recruitment

leads to dephosphorylation of ITAMs on signaling proteins associated with FcγR signaling transduction[55]. The potential inhibitory function of Fc-mediated response to mAb in immune cells outlines the importance of using appropriate mAb concentrations when assessing their immunotherapeutic value.

Vγ9Vδ2 ADCC

γδ T cell cultures expanded using pAg stimulation respond to FcγR stimulation via ADCC, as evidenced by enhanced cytotoxicity and degranulation. For example, γδ T cells stimulated with Rituximab cross-linked via anti-human IgG upregulate FcγR activation signals: p-Zap70 and p-ERK1/2[50]. Phosphorylation of Zap-70 and ERK/12 1-hour post-stimulation is most potent when mAb stimulation is combined with pAg stimulation, suggesting synergistic effects of FcγR and TCR activation pathways in γδ T cells. Accordingly, CD107a expression in response to tumour targets is highest in presence of both pAg and mAb stimulation. Generally, tumour cytotoxicity followed the same pattern, whereby the presence of both signals enhances tumour killing. However, CD20+ tumour cell lines that were inherently sensitive to TCR-mediated γδ T cell killing did not have improved specific tumour lysis when co-cultured with mAbs across multiple E:T conditions[50]. This may suggest that the maximum cytotoxic potential of the effector γδ T cells in the 4h cytotoxicity assay had already been reached by TCR stimulation alone. Rituximab-mediated cytotoxicity in other tumour cell lines was abrogated by using Fab'2-only Rituximab or preventing cytotoxic granule release[50], indicating that ADCC mechanisms are responsible for the improvements in γδ T cell cytotoxicity, as opposed to other biological factors such as increased tumour target binding. γδ T cell ADCC has also been reported in a separate study using Rituximab or Ofatumumab bound to a CD20+ B Cell Lymphoma cell line,

and in some cases against patient-derived tumour cell lines[59]. Similarly, γδ T cells ADCC was reported by Capietto et al. when γδ T cells were co-cultured with HER2+ tumour cell lines and Trastuzumab (anti-HER2). Increased γδ T cell cytotoxicity was correlated to higher expression of HER2 on tumour cell lines[60]. Importantly, Capietto et al. demonstrated that *in vivo* combination treatment of trastuzumab and adoptively transferred γδ T cells in HER2+ tumour-bearing xenograft mice was more effective for reducing tumour growth than adoptive γδ T cell or trastuzumab treatment alone, indicating *in vivo* synergy of these treatments[60].

Vγ9Vδ2 ADCP

Furthermore, γδ T cell APC functions are enhanced by target antibody opsonization, including enhanced phagocytic activity via Antibody-Dependent Phagocytosis (ADCP). In addition to demonstrating increased anti-tumour cytotoxicity by Vγ9Vδ2 cells co-cultured with rituximab-coated Daudi cells, Himoudi et al. demonstrate that antibody opsonized tumour cells are phagocytosed and cross-presented by γδ T cells[61]. Specifically, opsonization of tumour cells with Rituximab (Daudi cells), anti-GD2 (Lan-1 cells), or anti-CD45 (K562 cells) mAbs induced antigen cross-presentation of tumour antigens by γδ T cells, leading to αβ T cell clonal expansion. Cross-presentation requires cytotoxic activation of γδ T cells against mAb opsonized target cells, HLA-A2 expression on γδ T cells, and cell-to-cell interactions between γδ T cells, αβ T cells, and tumour cells[61]. Barisa et al. followed up on Himoudi et al.'s study, demonstrating the importance of mAb opsonization of target cells for γδ T cell APC phagocytosis, a necessary stage for antigen presentation[62]. γδ T cells were shown to only uptake 0.5μM beads, but not 1μM beads nor *E. Coli* in the absence of mAb opsonization. Comparatively, opsonization via mAb allows more than 50% of zoledronate expanded γδ T cells in culture to phagocytose 1μM

labeled beads or labeled *E. coli*. Furthermore, opsonization increases the proportion of *E. coli* entering acidic phagosomes[62], where breakdown of phagocytosed material occurs prior to antigen presentation[63]. Although γδ T cell phagocytic activity requires mAb opsonization large cells and materials requires, the efficiency of phagocytic activity is reduced by blocking TCR activation[62] – in accordance with TCR-stimulated cytotoxicity licensing APC function in γδ T cells previously described by Himoudi et al[61].

Vγ9Vδ2 APC Functions

The Vγ9Vδ2 subset can act as professional antigen presenting cell (APC), particularly after ADCP. Unlike the Vδ1 subset, Vγ9Vδ2 maintain expression of CCR7 – a chemokine receptor required for lymph node homing – throughout their developmental trajectory[26]. Vγ9Vδ2 have been shown to phagocytose bacteria and present bacterial epitopes to CD4+ T cells via MHC-II[64]. They have also been shown to cross-present peptides on MHC-I stimulating CD8+ αβ T cell responses[61,65]. Furthermore, in response to tumour cell co-culture, Vγ9Vδ2 cells upregulate co-stimulatory molecules CD80 and CD86 as well as HLA-DR (MHC-II) – which are characteristic APC markers. They also upregulate APC marker CD40, a surface ligand required for activation of antigen presenting cells[61]. However, up regulation of APC markers does not necessarily indicate antigen presentation is possible, as upregulation of APC machinery and antigen presentation itself appear to occur independently in Vγ9Vδ2 cells[61]. Specifically, antibody recognition of tumour-associated antigens (TAAs) on the surface of tumour cells via FcγRIII (i.e ADCP) seems to be critical for antigen presentation in Vγ9Vδ2[61].

Phenotype of CD16+ Vγ9Vδ2 T Cells

CD16 is expressed following γδ TCR stimulation[54], and its expression is typically associated with the low-proliferation CD27- TEMRA phenotype[66,67] – although CD27+ CD16+ γδ T cell phenotypes have been reported[33]. Indeed, single-cell sequencing of Vδ2 subsets analyzed using pseudotemporal trajectories indicate that Vδ2 cells express FcγRIII at later cell pseudotimes[26]. In accordance with a TEMRA phenotype, Ryan et al. demonstrated that the phenotypic profile of γδ T cells they defined as CD16+ have lower proliferative capacity compared to other phenotypic profiles of γδ T cells[67]. However, they gated their CD16+ γδ T cell subsets as CD28- CD27- CD16+, thereby excluding any CD27+ CD16+ γδ T cells that may have higher proliferative capacity. Regardless, given the predominantly CD27- TEMRA phenotype of CD16+ γδ T cells, these cells would be expected to have lower proliferative potential. While their proliferative capacity is expected to be limited, CD16+ γδ T cells have a highly cytotoxic phenotype, with increased anti-tumour cytotoxicity against several tumour cell lines[66,67]. Accordingly, CD16+ γδ T cells upregulate perforin and granzyme, as well as NKR receptors capable of recognizing stress ligands and MHC-downregulation – NKG2 receptors and KIRs[66,67]. Despite increased anti-tumour cytotoxicity, Angelini et al. show that CD16+ γδ T cells have decreased phosphorylation of the ERK signalling pathways and lower IFNγ production following TCR stimulation[66], although Ryan et al. show that degranulation in response to TCR stimulation is highest in the CD16+ γδ. T cells[67]. Taken together, these results may indicate that CD16+ γδ T cells have an altered signalling response to TCR stimulation leading to lower cytokine production and higher direct cytotoxicity and degranulation. CD16+ γδ. T cells also have altered chemokine expression, upregulating CXCR3 and downregulating CCR6[66,67]. Furthermore, CD16+

γδ T cells downregulate Th17-associated cytokines and the transcription factor RORC[67]. Ryan et al. further investigate this finding and demonstrated that low level of IL-17 production in response to PMA stimulation only occurs within the CD16-CCR6+CD28+ fraction of γδ T cells[67], suggesting that this subset harbours the small subset of Th17 γδ T cells. Overall, results from the literature suggests that CD16+ γδ T cells – capable of ADCC and ADCP – are associated with a highly cytotoxic Th1-like phenotype with a limited proliferative capacity TEMRA phenotype.

γδ T Cell Engineering

Allogeneic γδ T Cells for Engineered ACT

Engineered adoptive T-cell therapies (ACT), such as CAR-T cells, have revolutionized cancer therapy for patients with relapsed refractory hematological malignancies, with unprecedented 67% response rates in B-Cell malignancies[15]. However, one of the challenges impeding widespread clinical use of CAR-T cell therapy is the prohibitively expensive treatment cost – beginning at $500,000 CAD for the CAR-T cell product alone, excluding any additional medical costs associated with treatment[68].

For engineered ACT to be sustainable within the Canadian health care system, the manufacturing cost of CAR-T cell products must be reduced. One way to achieve this is by scaling up from individualized single-batch manufacturing on a per-patient basis, to mass manufacturing CAR-T cells for allogeneic use. However, CAR-T cells are traditionally manufactured in the αβ T cell subset, which are restricted to autologous adoptive transfer because, as allogeneic hematopoietic stem cell transplant (alloHSCT) research has shown, allogeneic αβ T cells cause graft-versus-host disease (GvHD). GvHD occurs when there is a HLA

mismatch between donor and recipient[69]. HLA-mismatched donor αβ TCRs have more promiscuous activation and pro-inflammatory cytokine production in response to recipient epitopes presented on foreign MHC, leading to widespread tissue inflammation across multiple organs[69]. Consequently, αβ T cells are now routinely depleted from alloHSCT transplants to reduce the likelihood of GvHD[70].

γδ T cells are promising candidates for allogeneic engineered ACT because unlike αβ T cells, γδ T cells do not rely on MHC for TCR target recognition and consequently do not pose a risk for GvHD[71]. Furthermore γδ T cells have innate tumour cytotoxicity[25] – tumour-infiltrating γδ T cells were shown to be the most favorable prognostic marker in a pan-cancer analysis[72]. Allogeneic γδ T cells have already been safely administered as cancer immunotherapy[73,74] and are routinely transferred during alloHCST – both directly within the αβ-T cell depleted HSCT grafts and during immune cell reconstitution by donor hematopoietic stem cells[75,76]. In fact, expansion of allogeneic γδ T cells improves overall and disease-free survival and prevents relapse in leukemia patients receiving alloHCST, because expanded donor γδ T cells recognize and kill leukemic blasts[77].

γδ T Cell Manufacturing Strategies

Protocols for manufacturing γδ T cell differ depending on the desired the cell product. Vγ9Vδ2 T cells can be specifically cultured using drugs, such as Zoledenorate (Zol)[78,79] and BrHPP[80,81], that induce intracellular pAg accumulation by interrupting the mevalonate pathway or through direct stimulation with pAgs, such as HMBPP[82]. They can also be expanded using the plant mitogen Concavalin A, however this protocol generates a mix of Vδ1 and Vγ9Vδ2 T cells[78]. Regardless of the protocol, γδ T cell culture media is supplemented with either IL-2 or IL-15,

which can both support proliferation and acquisition of IFNγ effector functions[83]. However, IL-15 may provide more consistent and greater expansion of Vγ9Vδ2 T cells (Table 1)[79,84–86] while maintaining a less differentiated central memory T cell subset phenotype[87]. More complex protocols using artificial Antigen Presenting Cells (aAPC) can also be used to enhance expansion of Vγ9Vδ2 cells. For example, Xiao et al.'s Vγ9Vδ2 expansion protocol uses aAPCs that are irradiated erythroleukemia cell line, K562, transduced with monocyte surface protein CD64, and costimulatory ligands CD86 and CD137L, in addition to an initial Zol and IL-2 manufacturing protocol[52].

Table 1: γδ T Cells Manufactured Using IL-15

Year	First Author	[IL-15]	Starting Cells	pAg Drug	IL-2 Comparison
2013	Cairo[87]	10 ng/ml	Cord blood Mononuclear Cells	Alendronate	IL-2: Viability 70% IL-15: Viability 90% IL-2: Annexin V+ 35% IL-15: Annexin V+ 20% Higher concentration of Vδ2 at D21 and D28. IL-15: 75% Tcm IL-2: 70% Tcm
2018	Domae[85]	1ng/mL (Low) or 3 ng/mL (High)	PBMC	Zolendronate	Il-2: 10% Proliferate IL-15: 20% (IL-15 Low) or 30% (IL-15 High) Proliferate.
2008	Viey[86]	20ng/mL	PBMC	BrHPP	4x Higher expansion of Vδ2 from TILs with IL-15
2016	Van Acker[84]	12.5 ng/mL	PBMC	Zolendronate	IL-2: 10% Proliferate IL-15: 30% proliferate
2014	Ribot[83]	10 ng/mL	PBMC	Anti-CD3 + Anti-CD28	IL-2 and IL-15 proliferation (CFSE) is the same.
2017	Nada[79]	50 - 100ng/mL	PBMC	Zolendronate or HMBPP	IL-15 expansion leads to greater proportion of Vδ2 and Tcm γδ T cells.

γδ CAR-T Cell Therapies

Vγ9Vδ2 T cells are capable of killing multiple myeloma cell lines and patient-derived multiple myeloma cells *in vitro*[88], however non-engineered Vγ9Vδ2 adoptive cell therapy (ACT) or *in vivo* expansion therapies have failed as a cancer immunotherapies in 20 clinical trials, including a clinical trial for MM patients[89]. Given the success of engineered αβ T cells CAR-T cells for hematological malignancies, it is worthwhile to examine the potential of improving Vγ9Vδ2 cancer immunotherapy by reprogramming Vγ9Vδ2 target recognition – thereby also producing an allogeneic CAR-T product.

Recent attempts to use CD3ζ-CD28 CARs in Vγ9Vδ2 T cells have showed improved efficacy for *in vitro* tumour killing compared to non-transduced Vγ9Vδ2 cells[52,78]. Furthermore, αβ and Vδ1 or Vδ2 T cells engineered with Cd3ζ-CD28 CARs expanded using the same ConA protocol showed similar *in vitro* cytotoxic potential[78]. Recently, Ang et al. described RNA electroporated γδ T cells with mRNA encoding an CD3ζ CAR with a NKG2D tumour recognition domain, capable of recognizing NKG2D stress ligands upregulated on tumour cells. The NKG2DL-specific γδ CAR-T were tested *in vivo*, and initially reduce tumour burden, but tumour volumes eventually progress, especially after repeated γδ CAR-T injections are halted[90]. Another study by Rozenbaum et al. demonstrated their CD19-specific γδ CAR-T cells nearly eradicate leukemia burden in the bone marrow, albeit to a lesser degree than αβ CD19-specific CAR T cells[91]. While Rozenbaum et al. appear to have higher *in vivo* efficacy for their γδ CAR-T cells compared to Ang et al., they also used a less challenging tumour model. Rozenbaum et al. tested their CD19 γδ CAR-T cells in mice injected with a 10x lower inoculation of tumour cell than Ang et al., and the tumour were less established – with treatment beginning Day 2 as

opposed to Day 7 post-tumour injection[90,91] . Rozenbaum et al.'s result also observed an initial eradication of tumour cells in response to γδ CAR T cells, but only record 14 days post-treatment and therefore do not evaluate the potential for long-term tumour progression after γδ CAR-T cell therapies are halted,[91] as observed by Ang et al[90]. Both Rozenbaum et al. and Ang et al.'s studies indicate that engineered γδ T cell therapies benefit from *in vivo* zoledronate combination therapy, and that γδ CAR T cell prone to poor *in vivo* persistence limiting their ability to induce a complete response[90,91]. More recently, Park et al. tested a novel anti-tumour bispecific antibody conjugated with γδ T cells and demonstrated that *in vivo* γδ T cell expansion and anti-tumour efficacy could be improved by exogenous administration of IL-2 and IL-15 – although IL-15 treatment was superior for both metrics[92]. These results indicate that co-administration of exogenous IL-15, or co-expression of the IL-15 cassette in engineered γδ T cells may address the poor *in vivo* persistence of engineered γδ T cells.

CD3ζ engineered Vγ9Vδ2 cells are still likely to be susceptible to another major challenge facing CAR-T cell therapy – cytokine release syndrome toxicity. In response, Fisher et al. developed a co-stimulatory DAP10 CAR γδ T cell, the co-adaptor for NKG2D. The DAP10 CAR only provides a co-stimulatory signal to Vγ9Vδ2 cells upon CAR ligand recognition. Direct cytotoxicity of DAP10 CAR γδ T cells therefore requires both endogenous Vγ9Vδ2 TCR signaling via recognition of tumour phosphoantigen accumulation and CAR ligand recognition[93]. While this model is ideal for preventing toxicity caused by off-tumour CAR-mediated cytotoxicity, not all tumours are capable of activating Vγ9Vδ2 TCR-mediated killing[45]. Additionally, the DAP10 co-stimulatory CARs would be expected to be more susceptible to antigen loss, as CAR-T cells would become non-responsive upon downregulation of either the CAR or Vγ9Vδ2 TCR ligand.

γδ TAC T cells

Our group has been developing TAC γδ T cells with the intention of generating an engineered cell product for allogeneic use. The αβ TAC T cell platform can be adapted, as Vγ9Vδ2 T cells also require CD3 stimulation for activation and effector functions[42]. Furthermore, Dopfer et al. have shown that UCHT1-mediated γδ TCR signaling, which is the anti-CD3 mAb used in our current generation of TACs, is a more potent activator of Vγ9Vδ2 cells and anti-tumour cytotoxicity compared to the alternative common anti-CD3 antibody, OKT3[23]. UCHT1-mediated γδ TCR signaling integrates the CD3ε chain via a CD3 conformational change, affecting which pathways the TCR signaling cascade activates[23]. This demonstrates how additional CD3 chains other than CD3ζ can modulate TCR signaling, which γδ TAC T cells can utilize.

Our lab has developed protocols for manufacturing γδ T cells using Zoledenorate and IL-2, and purifying cultures using MACS columns. Prior to this project, Vγ9Vδ2 cells had been engineered in our lab using commercially produced (Lentigen) CD19- and HER2-specific TAC lentiviral vectors, and these TAC γδ T cells have demonstrated potent *in vitro* cytotoxicity.

Scientific Aims

There is currently a need for both improvements in MM-specific engineered T cell and allogeneic therapies. Consequently, my project will focus on evaluating methods to enhance BCMA-specific TAC γδ T cell functionality and optimizing engineered TAC Vγ9Vδ2 manufacturing protocols in our BCMA-TAC constructs.

Aim 1: Optimization of engineered γδ TAC T cells manufacturing

We aim to optimize the manufacturing of engineered TAC γδ T cells from the zoledronate and IL-2 manufacturing protocol developed in our lab. Previously, our lab used commercial Lentigen lentiviruses to manufacture TAC γδ T cells. We will assess whether γδ T cells can be engineered with in-house lentiviral and γ-retroviral BCMA-TAC vectors. We will also optimize the transduction protocol to select a transduction time yielding the highest level of TAC expression, and optimization of retronectin and cell density parameters. Furthermore, we aim to increase engineered γδ T cell yield by increasing cell density at early culture timepoints and testing IL-15 supplemented culture conditions. As a side project, we aimed to generate a TAC with a cytoplasmic KIR2DS2 signalling domain and co-expression of DAP12 with the intention of engaging Natural Killer receptor-based activation – which are often identified as activating receptors for γδ T cells – to enhance engineered γδ T cell function. We will also optimize the cell density of stable γ-retrovirus producing PG13 cells for retroviral harvest conditions, to increase transduction and minimize impact on γδ T cell culture composition. Furthermore, we aim to develop a manufacturing strategy expanding γδ T cells from αβ-

depleted PBMCs. Finally, we will assess the *in vitro* anti-tumour functionality of our manufactured BCMA-TAC γδ T cells.

Aim 2: Investigation of CD16 functionality in BCMA-TAC γδ T cells

To take advantage of CD16 expression and the recent integration of monoclonal antibodies as a cancer immunotherapy, we will investigate the potential of an engineered γδ T cell and monoclonal antibody combination therapy. A synergistic combination therapy would be beneficial not only to increase the cytotoxic activity of the engineered γδ T cells but may also help prevent relapse associated with antigen loss of the engineered receptor target. First, we will assess whether our BCMA-TAC γδ T cells expressed and responded to CD16 stimulation. We will also assess whether CD16 stimulation could synergize with TAC signalling in γδ T cells. Furthermore, we aim to determine whether Daratumumab (anti-CD38) can enhance the functionality of engineered BCMA-TAC γδ T cells against Multiple Myeloma tumour cell lines that express BCMA and CD38. Beyond characterizing the functionality of BCMA-TAC γδ T cells stimulated with CD16, we will also further investigate the phenotype of CD16+ γδ T cells, to understand the nature of engineered γδ T cells that would potentially respond to a monoclonal antibody combination therapy.

Methods

Cell Culture Media

Media	Purpose	Components
TRPMI	*γδ T cell culture* *In vitro cytotoxicity* *In vitro cytokine production* *Plate-bound ICS*	500mL RPMI 1640 50mL Heat-inactivated Sterile FBS 5mL 1M HEPES 5mL 0.2M L-Glutamine 5mL Sodium Pyruvate 5mL 100X NEAA 5mL 100U/mL Penicillin/100µg/mL Streptomycin 500µL 55mM 2-Mercaptoethanol
HEK	*HEK293TM cell culture* *PG13 cell culture*	500mL DMEM 50mL Heat-Inactivated Sterile FBS 5mL 1M HEPES 5mL 0.2M L-Glutamine 5mL 100U/mL Penicillin/100µg/mL Streptomycin 10µg/mL Puromycin
cRPMI	*K562 cell culture* *Jurkat cell culture* *Tumour ICS*	500mL RPMI 1640 50mL Heat-inactivated Sterile FBS
Multiple Myeloma	*MM.1S cell culture* *KMS-11 cell culture* *U266 cell culture* *RPMI-8226 cell culture*	500mL RPMI 1640 50mL Heat-inactivated Sterile FBS 5mL 1M HEPES 5mL 0.2M L-Glutamine 5mL Sodium Pyruvate 5mL 100X NEAA 5mL 100U/mL Penicillin/100µg/mL Streptomycin
Daudi	*Daudi cell culture*	500mL RPMI 1640 50mL Heat-inactivated Sterile FBS 5mL 0.2M L-Glutamine 5mL 100U/mL Penicillin/100µg/mL Streptomycin

TAC γδ T Cell Culture

Engineered γδ T cells were manufactured by activating γδ T cells from PBMCs with 1ng/µL Zoledronate and 660IU/mL IL-2. The TAC transgene was introduced using either VSV-G pseudotype lentivirus or GaLV-psuedotyped γ-retrovirus vectors. Through optimization studies, we determined transduction was highest 24 hours post-activation for lentivirus and 72 hours post-activation for γ-retrovirus. Cultures were fed with 660 IU/mL IL-2 supplemented media every 2 – 3 days, unless otherwise indicated. 5E6 – 2E7 cells were cryopreserved on D14 in 1mL Cryostor CS10 (Stem Cell Technologies). Some cultures were also γδ-enriched on D14 prior to cryopreservation.

Non-purified γδ T cells were used for flow-based assays, including *in vitro* plate-bound stimulation and tumour stimulation ICS assays. γδ T cells were enriched on Day 14 to >99% γδ T cell purity using CD4/CD8 magnetic-activated cell sorting depletion (Miltenyi Biotec) for *in vitro* cytotoxicity and cytokine production assays. Non-purified cells were used for other functional assays. For these cultures, a flow phenotype was performed on D12 or D13 of culture to assess pre-purification γδ purity. Depletion was performed at room temperature using reagents (buffers, TRPMI, CD4/CD8 beads) pre-warmed in 37°C water bath. Cells were incubated with CD4/CD8 beads for 15 minutes at 37°C using 100µL of each CD4 and CD8 beads per 5E7 cells. Beads were also adjusted for D13 γδ purity after calculating the required bead volume for the number of cells. If %γδ was <78% then 30% more beads were added; if %γδ was <65% then 50%

more beads were added. Following manufacturing recommendations, we purified 0 – 1E7 cells with MS columns, or 1E7 – 2E9 cells using LS columns.

Flow Cytometry Culture Phenotype

Cultures were phenotyped on Day 10 and Day 14 of culture unless otherwise indicated. Either Vδ2TCR or γδTCR antibodies were used to stain for γδ T cells. We identified γδ T cells by gating on CD3+ γδ/Vδ2TCR+ αβTCR- population. The CD3+ αβTCR+ population was used as a negative control to set the CD16 gate. TAC T cell transduction was measured by assessing NGFR positivity. Surface TAC expression was measured using BCMA-Fc (R&D Systems, TNFRSF17 Met1-Ala54) and huIgG-PE. In some cases, other features of γδ T cell phenotype (e.g CD32, CD64, CD27, CD56, intracellular DAP12) were assessed.

The following antibodies were used for flow cytometry: CD3-BV605 (Biolegend, Clone UCHT-1), γδTCR-APC (Biolegend, Clone B1), Vδ2TCR-APC (Biolegend, Clone B6), αβTCR-FITC (Biolegend, Clone IP26), NGFR-BV421 (BD Biosciences, Clone C40-1457), huIgG-PE (Jackson Laboratory, polyclonal), CD16-SB780 (eBioscience, Clone CB16), CD32-AF700 (R&D Systems, Clone 190723), CD64-BV480 (BD Biosciences, Clone 10.1), CD27-APC-eFluor780 (eBioscience, Clone O323), CD56-PE-Cy7 (BD Biosciences, Clone B159), and DAP12-AF647 (BD Biosciences, Clone 406288).

Lentivirus Production

VSV-G pseudotyped lentiviruses encoding the TAC transgene and NGFR transduction marker were harvested from transfected HEK293TM according to Bramson Lab SOP-LV-AM-004 for the purpose of engineering γδ T cells. HEK293TM cells were cultured for 5 days prior to viral transfection. Lentiviral components pMD2.G (VSV-G envelope), pRSV-Rev, pMDLg/pRRE (Gag,

Pol), and pCCL encoding the TAC transgene and NGFR transduction marker were mixed with Opti-MEM and Lipofectamine 2000, and then added to HEK293TM cells for viral transfection. Media was changed 12 – 16 hours after transfection with sodium butyrate-supplemented media. 26 – 36 hours after media change, lentivirus was harvested by filtering via 0.45µM PES filter and Amicon Ultra-15 100 kDa centrifugal filter, and then frozen at -80°C. Lentiviral MOI was determined by transfecting 30,000 fresh HEK293TM cells at 1:100 to 1:50000 dilutions and assessing NGFR positivity 3 – 4 days later via flow cytometry.

Retroviral Production

GaLV-pseudotype γ-retroviruses encoding the TAC transgene were generated by establishing a stable gRV-producing PG13 cell line according to Bramson Lab SOP-gRV-PLAT-E-001 and SOP-gRV-PG13-001. Retroviral constructs were engineered to co-express either an NGFR transduction marker or DAP12. Co-expressed transgenes are translated under the same promoter as the TAC transgene but separated via T2A, which is cleaved post-translation. High titre MoMuLV-psuedotyped γ-retrovirus is generated prior to PG13 transduction by transfecting PLAT-E cells. The γ-retrovirus harvested from PLAT-E was then used to transduce PG13 cells. PLAT-E cells are cultured for 5 days before transfection with Opti-MEM and lipofectamine, mixed with plasmids pCL-Eco and pRV100G encoding the TAC transgene and NGFR or DAP12. MoMuLV-psuedotype γ-retrovirus is harvested from PLAT-E cells 2 days post-transfection using a 0.45µM PES filter and Amicon Ultra-15 100 kDa centrifugal filter and frozen at -80°C. PG13 cells were cultured for 1 week prior to transduction with thawed MoMuLV-psuedotype γ-retrovirus. The stable gRV-producing PG13 cell line was expanded for 7 – 10 days post-transduction. For γδ T cell transduction, gRV-producing PG13 cell lines were thawed 1 week

prior to transduction and cultured in HEK media. PG13 cells producing gRV were prepared for retroviral harvest by seeding 2E6 cells in a T75 and culturing in HEK media 3 days prior to transduction, such that T75 flasks were approximately 90% confluent on the day of transduction. Hours before γδ T cell transduction, γ-retrovirus was harvested from gRV-producing PG13 cells culture using a 0.45µM PES filter and directly added to 24-well tissue culture plate coated overnight in 600µL 50µg/mL retronectin. The viral supernatant was centrifuged in the plate for 2 hours at 2000xg at 32°C. Following centrifugation, the viral supernatant was aspirated, and 2E6 cells from γδ T cell cultures were immediately added to each well.

Luciferase-Based Cytotoxicity Assay

Purified BCMA-TAC γδ T cells and NT cells were co-cultured with tumour cell lines (MM.1S, KMS-11, and K562) transduced with enhanced firefly luciferase (effluc). BCMA-TAC or NT γδ T cells were thawed in 660IU/mL IL-2 supplemented TRPMI 16 – 20 hours prior to functional assay. Tumour cell lines were cultured for at least 5 days prior to functional assay. The E:T range was prepared by serial dilution of γδ T cells prior to adding 5E5 tumour cells each well in a 96-well Costar white plate. D-Luciferin was added 10 minutes prior to the first luminesce reading on the i3 SpectraMax. For antibody opsonized killing assays, tumour cells were resuspended in TRPMI with Daratumumab during setup, and then immediately added to γδ T cells in the 96-well plate. % Lysis was calculated using the following formula:

$$\%\ Lysis = 1 - \frac{Sample\ luminesence - Media\ only\ luminesence}{Tumour\ only\ luminesence}$$

Plate-bound Stimulation Assay

Non-purified BCMA-TAC or NT γδ T cells were thawed in 660IU/mL IL-2 supplemented TRPMI 14 – 18 hours prior to the functional assay. Functional grade anti-CD16 (10ng/µL, 25ng/µL, 50ng/µL or 100ng/µL) (eBiosciences, Clone B73.1) and/or human BCMA-Fc (0.5ng/µL or 200ng/µL)(R&D Systems, TNFRSF17 Met1-Ala54) diluted in PBS were added to the wells of a 96-well plate at 4°C overnight. Where indicated, anti-CD3 (0.63, 1.25, 2.5, 5, or 10ng/µL)(eBioscience, Clone UCHT-1) was used instead, and coated with anti-CD16 overnight at 4°C. Anti-CD16, BCMA-Fc, and/or anti-CD3 was aspirated from the plate prior to stimulation and the wells were washed with PBS. A master mix of 2E6 cells/mL BCMA-TAC γδ T cells and NT with Monensin (BD Biosciences), Brefeldin A (BD Biosciences), and CD107a-AF488 (BioLegend, Clone H4A3) was generated. 100µL of the master mix (2E5 BCMA-TAC or NT γδ T cells) was added to each well and incubated at 37°C for 4 – 5 hours. 0.02M EDTA was added at the end of stimulation prior to flow cytometry staining. Stimulated γδ T cells were stained using our standard phenotype antibodies for CD3, Vδ2, CD16, and NGFR. Cells were fixed and permeabilized using BD Cytofix/Cytoperm (BD Biosciences), and then stained for intracellular TNFα-PE-Cy7 (BD Biosciences, Clone MAb11).

Tumour ICS Assay

Non-purified BCMA-TAC or NT γδ T cells were thawed in 660IU/mL IL-2 supplemented TRPMI 14 – 16 hours prior to functional assay. Tumour cells were cultured for at least 5 days prior to stimulation assays. Tumours cells were stained with CellTrace Violet (Life Technologies), and 2E5 tumour cells were plated in each well of a 96-well plate. Daratumumab was incubated with

tumour cells in each well for 30 minutes at 37°C in TRPMI or Multiple Myeloma media. Meanwhile, a master mix of 2E6 cells/mL BCMA-TAC γδ T cells and NT with Monensin (BD Biosciences), Brefeldin A (BD Biosciences), and CD107a-AF488 (BioLegend, Clone H4A3) was generated. The γδ T cell mastermix (50µL; 2E5 BCMA-TAC or NT γδ T cells) was directly added to tumour cell and Daratumumab mixture. For Daratumumab pre-loaded samples, a PBS wash included to remove excess soluble Daratumumab from the wells prior to adding γδ T cells. Samples were washed with 200µL PBS, centrifuged at 500xg for 5 min at room temperature, and the volume in the well was aspirated prior to addition of γδ T cells. Tumour and γδ T cells were co-cultured for 4 – 5 hours at 37°C. 0.02M EDTA was added at the end of stimulation prior to flow cytometry staining. The co-culture was stained with LIVE/DEAD Near-IR (Invitrogen), and then our standard phenotype antibodies for CD3, Vδ2, CD16, and NGFR-PE-CF594 (BD Biosciences, Clone C40-1457). Cells were fixed and permeabilized, and then stained for intracellular TNFα-PE-Cy7 (BD Biosciences, Clone MAb11).

Tumour Cell Phenotype

Tumour cell lines were separately phenotyped for BCMA, CD38, and Daratumumab binding. Daratumumab binding was assessed by staining tumour cells with Daratumumab at 37°C in Multiple Myeloma media, followed by huIgG-PE (Jackson Laboratory, polyclonal). BCMA-AF647 (Biolegend, Clone 19F2) and CD38-BV510 (BD Biosciences, Clone HIT2) were stained separately from Daratumumab binding for each tumour cell line and performed using a standard 30-minute room temperature stain in FACS-EDTA buffer.

RNA-Seq Sample Preparation

CD16+ and CD16- γδ T cells were prepared for RNA-sequencing by Fluorescence-activated Cell Sorting (FACS) of D14 BCMA-TAC γδ T cell cultures. 7.5E6 cells from each culture were stained using Live/Dead Near IR (Invitrogen), Vδ2TCR-APC (Biolegend, Clone B6), αβTCR-FITC (Biolegend, Clone IP26), and CD16-PE-Cy7. CD16 gates were initially set using αβTCR+ cells as a negative control and validated using a CD16-PE-Cy7 FMO. Live Vδ2 CD16+ and CD16- sorted fractions were collected in polypropylene tubes pre-coated with tRPMI for 2 hours. Most of the tRPMI was decanted from tubes before collection. RNA was immediately extracted from CD16+ and CD16- fractions using RNeasy Plus Mini Kit (Qiagen) and QIAshredder (Qiagen) according to the manufacturer's instructions.

NT and BCMA-TAC γδ T cell samples were prepared for RNA-seq by purifying D12 cultures from 4 donors using a CD4/CD8 magnetic-activated cell sorting (MACS) depletion kit (Miltenyi Biotec). A small sample of purified cells was set aside for flow cytometry using CD3, Vδ2TCR, and αβTCR standard phenotype antibodies to confirm >99% γδ (αβTCR-) purity. RNA was extracted from purified samples immediately after depletion using RNeasy Plus Mini Kit (Qiagen) and QIAshredder (Qiagen) according to the manufacturer's instructions.

Samples were sent to Mobix for single-end 50bp read length RNA-sequencing at a sequencing depth of 18.8 million. Their protocol uses NEBNext Poly(A) mRNA Isolation Module for polyA enrichment and NEBNext® Ultra™ II Directional RNA kit (reverse strandedness) for DNA library generation prior to next generation sequencing with Illumina HiSeq.

RNA-Seq Analysis

RNA-seq pre-processing largely followed the parameters set by NASA GeneLab RNA-Seq consensus pipeline[94]. Unprocessed FASTQ files were analyzed via FASTQC and MultiQC. Adapter sequences were trimmed using TrimGalore[95]. Trimmed files were analyzed again using FASTQC[96] and MultiQC[97] to ensure sample quality. Trimmed FASTQ files containing reads from the same sample, but recorded in two separate lanes, were concatenated using bash. Reads were aligned to the human reference genome – retrieved from the GeneLab consensus pipeline[94] – using STAR[98]. Alignment quality was manually quality controlled, ensuring uniquely mapped genes was >80% for each sample. Aligned BAM files were input into RSEM[99] to generate the gene count matrix. PCA values were generated after DESeq2's[100] variance stabilizing transformation and corrected for donor effects using limma[101] batch correction. Differential abundance analysis was performed using DESeq2 (negative binomial distribution) in R. We used DESeq2's Likelihood Ratio Test with donor as a covariate to assess significantly differentially expressed genes. Log2 Fold Change (LFC) was manually calculated from mean DESeq2 normalized counts of each group with a pseudocount of 1. Differentially expressed genes meeting the cut-off of absolute log2FC > 0.5 and adjusted p-value < 0.05 were plotted using the EnhancedVolcano package[102]. Log2fc values from the unfiltered full gene list were used for Gene Set Enrichment Analysis (GSEA), implemented using the clusterProfiler R package[103] for both GO and KEGG terms. Transcription factor prediction was performed using the DoRothEA package viper wrapper[104]. Predictions were calculated from differentially expressed gene normalized counts (variance stabilizing transformation) for each sample. The

DoRothEA transcription factor database was filtered to only A or B quality gene-transcription factor associations, which don't require experimental validation. DoRothEA predictions are reported as the average normalized enrichment score for each transcription factor of CD16+ or CD16- samples. Transcription factor prediction were also performed using log2fc of differentially expressed genes as input into the TFEA.ChIp R package[105], which uses the GSEA algorithm and ChIp-Seq annotated database. All data wrangling in R was performed using Tidyverse[106].

Statistics

Significance of CD107a MFI and TNFα MFI from dual stimulation assays was determined using Wilcoxon signed-rank test in R. Spearman correlations were calculated in R to identify correlations between D0 or D14 culture features and CD16 expression. P-values were adjusted for multiple comparisons using Benjamini-Hochberg correction. Stepwise forward linear regression[107] was used as a feature selection method to determine if any D0 or D14 predictor variables were important for CD16 expression. The importance of selected predictor variables was validated using a linear model in R. CD16 expression is a proportion, therefore we also used a generalized linear models (beta distribution) from the betareg R package[108] to test the significance of each predictor variables for CD16 expression. P-values were adjusted for multiple comparisons using Benjamini-Hochberg correction.

Results

Manufacturing

BCMA-TAC Transduction of γδ T cells Using Lentivirus

We first wanted to test whether γδ T cells could be transduced with our in-house lentivirus constructs encoding BCMA-specific TACs. All BCMA-TAC constructs used in this experiment and the following experiments use anti-CD3 scFv huUCHT1(Y54T)[22] for T cell activation and NGFR as a transduction marker. BCMA-TAC#1072 and BCMA-TAC#898 includes a CD4 cytoplasmic tail and differ by their leader sequence. BCMA-TAC#898 uses muIgGκ leader sequence, while BCMA-TAC#1072 uses the CD8α – associated with increased TAC expression in αβ T cells. BCMA-TAC#1040 is a derivative of BCMA-TAC#898 that lacks a CD4 cytoplasmic tail[42]. Importantly, most γδ T cells do not typically use CD4/CD8 for TCR signaling, thus it's unknown whether the presence of the CD4 cytoplasmic tail will influence signaling in γδ T cells.

γδ T cells transduced with in-house lentivirus can be expanded using Zolendronate and IL-2. The tailless TAC (BCMA-TAC#1040) has a unique expansion profile, appearing to begin exponential expansion at approximately Day 11. Expansion of BCMA-TAC#1040 and BCMA-TAC#1072 cultures was not as pronounced as expansion in BCMA-TAC#898 cultures at earlier timepoints (Day 10/11) (Fig. 1).

BCMA-TAC#898 and BCMA-TAC#1072 lentiviruses appear to promote αβ T cells in culture (Fig. 2A). Comparatively, tailless BCMA-TAC#1040 appears to support both αβ T cells – as evidenced by increased αβ T cells counts in comparison to NT controls – as well as supporting exceptional γδ T cells growth in culture (Fig 2A and 1B). Percentage of transduced αβ in BCMA-

TAC#1040 is higher than transduced γδ T cells (data not shown), yet despite this, the total number of transduced γδ T cells is higher than transduced αβ T cells (Fig. 2C and 2D) because γδ T cells dominate the BCMA-TAC#1040 culture (Fig. 3). However, due to limited flow cytometry data collection, whether BCMA-TAC#1040 is less inhibitory of γδ T cell growth compared to other tested BCMA-TAC lentiviruses remains to be reproduced and validated.

Regardless of the TAC lentiviral construct used (BCMA-TAC#898, BCMA-TAC#1072, and BCMA-TAC#1040), the ratio of γδ T cells:αβ T cells decreases proportional to the amount of lentivirus added. The effect of lentivirus on γδ/αβ ratio is especially pronounced at MOI 10 in BCMA-TAC#898 and BCMA-TAC#1072, wherein γδ T cells make-up less than 10% of the culture (Fig. 3).

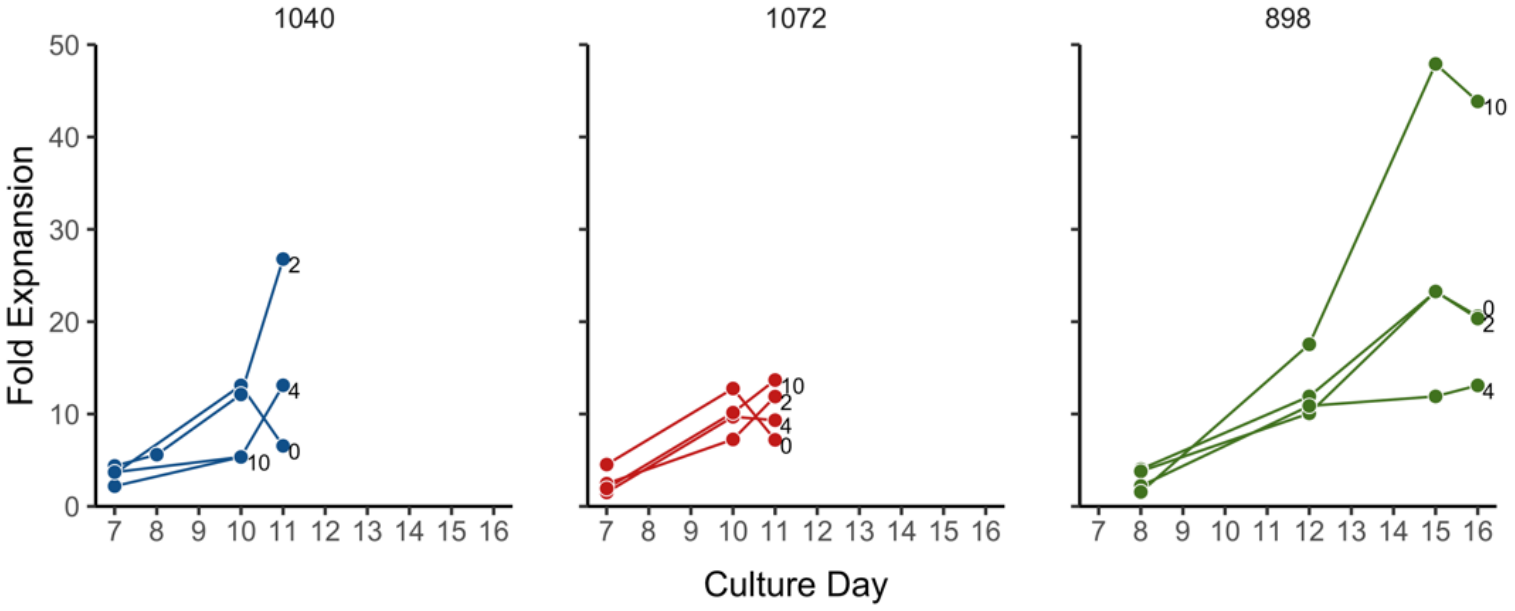

***Figure 1**: Engineered (LV-BCMA-TAC#1040, LV-BCMA-TAC#1072, and LV-BCMA-TAC#898) and non-transduced (MOI = 0) γδ T cells can be expanded from PBMCs using a combination of zoledronate and IL-2. MOI (0, 2, 4, 10) is labeled at terminus of each line. γδ T cells transduced with BCMA-TAC#1040 and BCMA-TAC#1072 were cultured concurrently until Day 12, whereas BCMA-TAC#898 transduced γδ T cells were seeded a week prior and cultured until Day 16. Fold expansion was calculated relative to PBMC seed number at D0.*

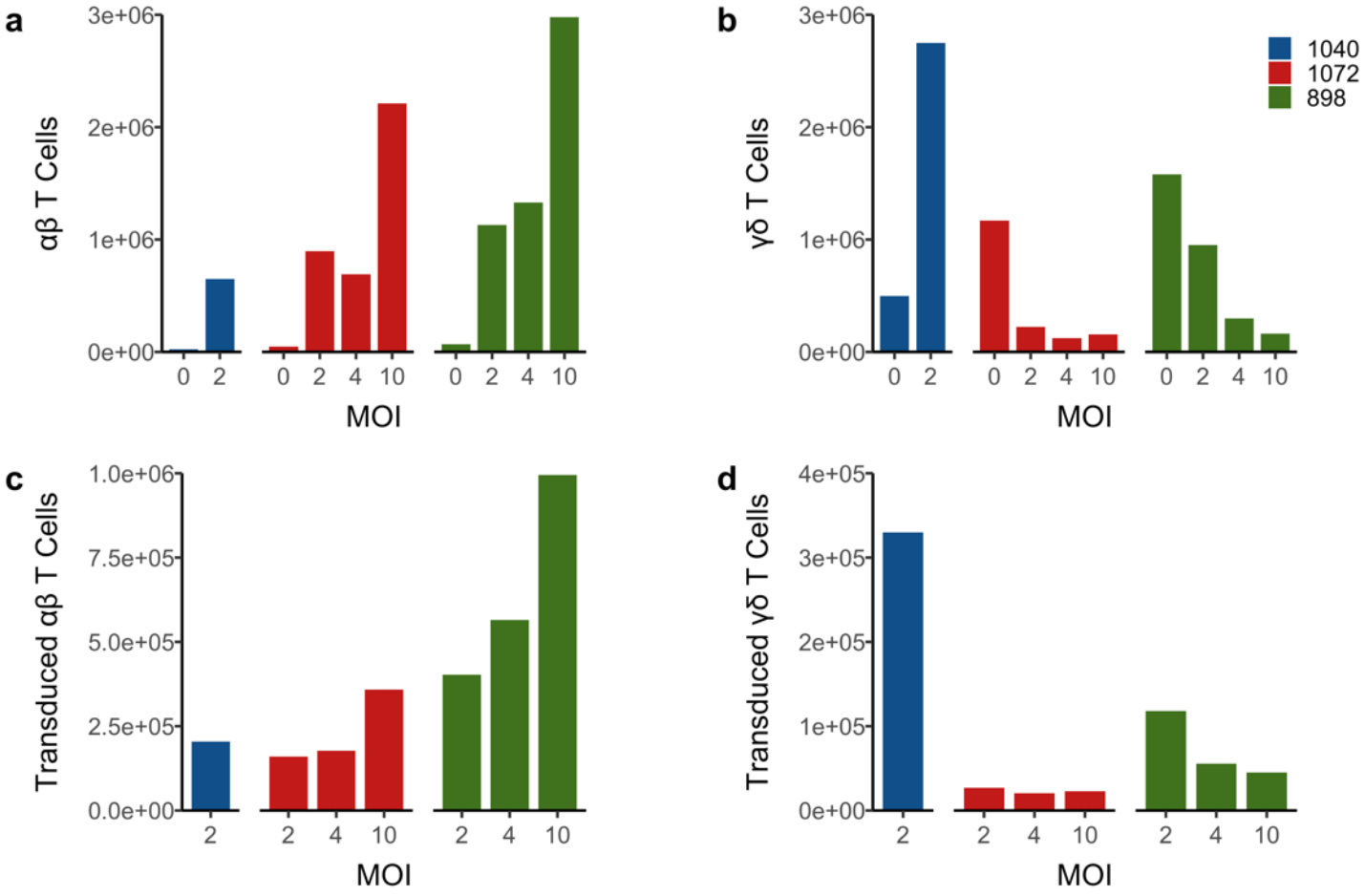

***Figure 2**: Normalized total and transduced γδ T cell vs. αβ T cell counts demonstrate that BCMA-TAC#898 and LV-NGFR#531 differentially affect γδ/αβ composition of the cell product. Day 9 flow cytometry data was used for calculations (αβ, γδ, and transduction counts). Flow data was not obtained for BCMA-TAC#1040 MOI 4 and MOI 10. The number of 96-well starting wells and therefore starting PBMC numbers differed between MOIs due to limited virus (NT = 5 starting wells; 1E6 PBMCs, MOI 2 and MOI 4 = 3 starting wells; 6E5 PBMCs, MOI 10 = 1 starting well; 2E5 PBMCs). **A, B**) Absolute αβ and γδ counts were first determined by multiplying the cell count for the culture by the percent αβ+ or %γδ+. Counts were then normalized by the number of starting wells. **C, D)** Transduced αβ and γδ counts were first calculated by multiplying αβ and γδ cell counts calculated in A and B, by the sum of the percent of BCMA+, NGFR+, and double-positive NGFR+BCMA+ αβ or γδ T cells. Counts were then normalized based on number of starting wells.*

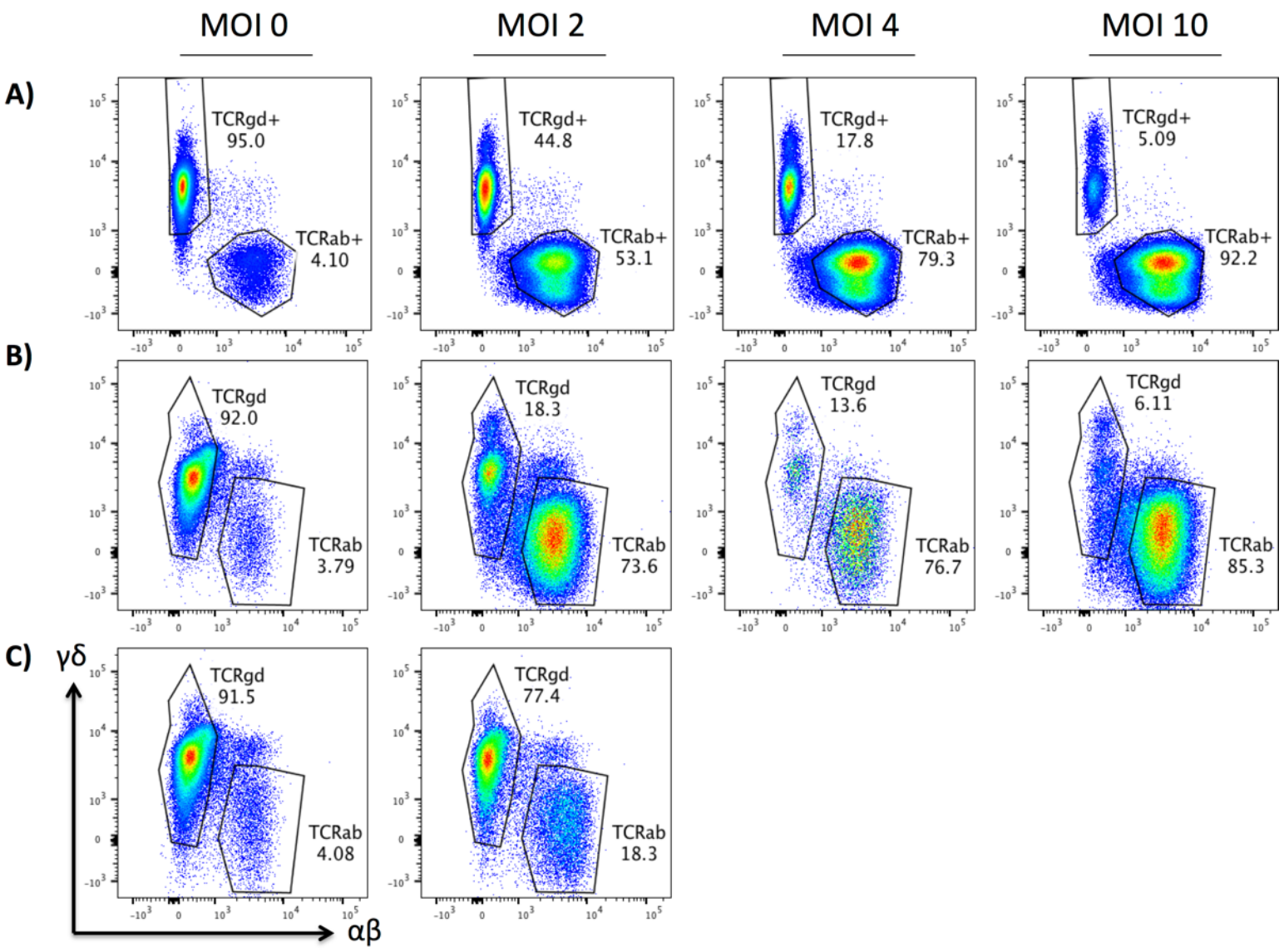

***Figure 3**: Percentage of γδ and αβ T cells for BCMA-TAC#898, BCMA-TAC#1072, and BCMA-TAC#1040 in zoledronate + IL-2 culture differs by MOI. Flow cytometry was run on Day 9. Flow data was not obtained for BCMA-TAC#1040 MOI 4 and MOI 10. **A)** BCMA-TAC#898 **B)** BCMA-TAC#1072 **C)** BCMA-TAC#1040.*

The Influence of TAC-LV on Cell Product Composition

We next wanted to determine whether the decrease in percentage of γδ T cells in culture relative to increasing MOIs of lentivirus was related to the lentiviral constructs with the TAC receptor. Consequently, an NGFR-only lentivirus (LV-NGFR#531) – lacking the BCMA-TAC receptor – was compared to lentivirus construct BCMA-TAC#898.

Similar to the results in experiment 1, transducing the cultures with BCMA-TAC#898 leads to a decrease in γδ/αβ ratio proportional to the amount of lentivirus added (Fig. 4). However, in LV-NGFR#531 there does not appear to be a relationship between the percent γδ in culture and lentivirus added, although the percentage of γδ T cells in the LV-NGFR#531 cultures is still lower than NT (Fig. 4).

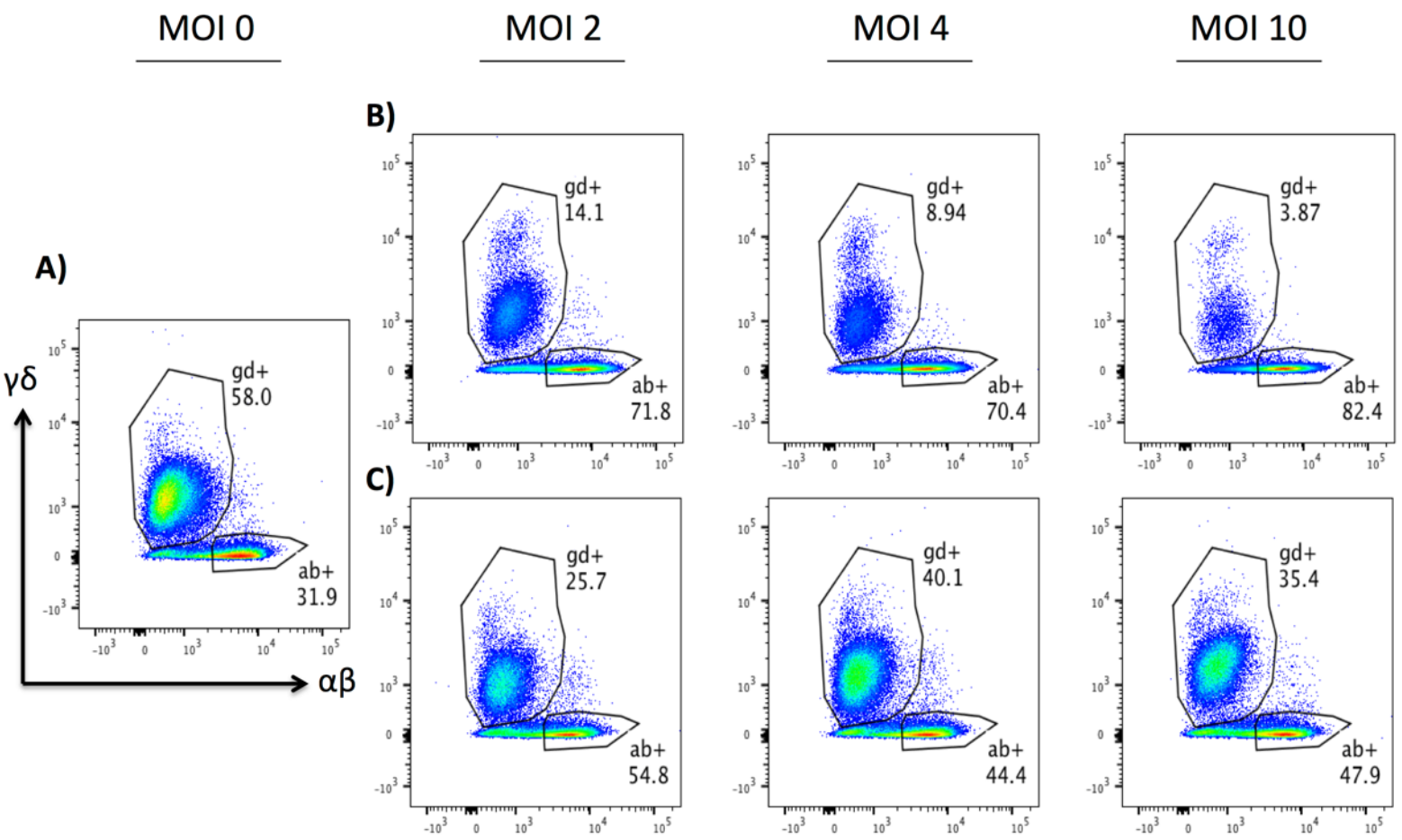

Figure 4: *Percentage of γδ and αβ for BCMA-TAC#898 and LV-NGFR#531 transduced zoledronate + IL-2 cultures. Flow cytometry was run on Day 9. A) Non-transduced culture B) BCMA-TAC#898 C) LV-NGFR#531*

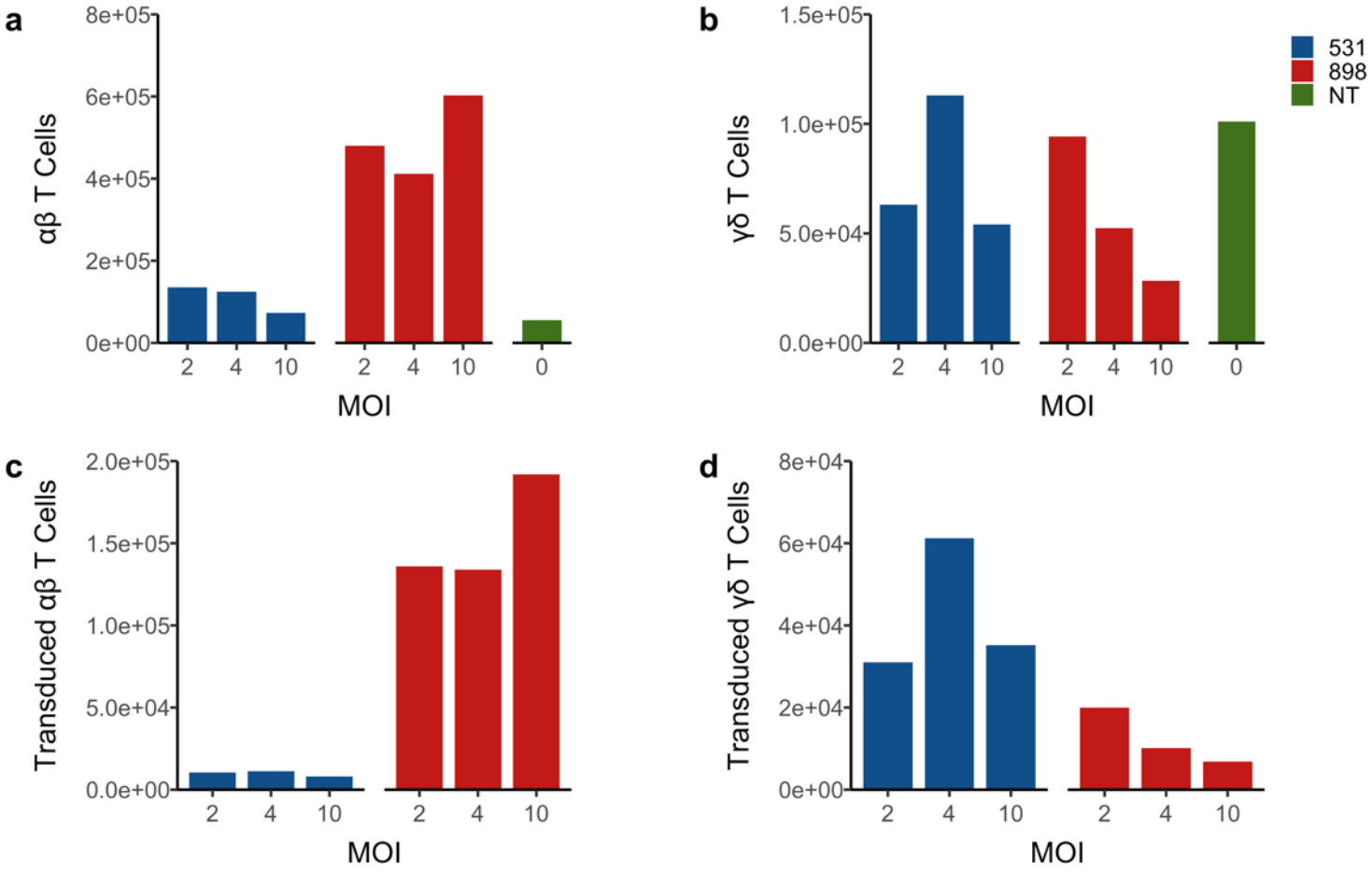

Figure 5*: Normalized total and transduced γδ T cell vs. αβ T cell counts demonstrate that BCMA-TAC#898 and LV-NGFR#531 differentially affect γδ/αβ composition of the cell product. Day 9 flow cytometry data was used for calculations (αβ, γδ, and transduction counts). The number of 96-well starting wells and therefore starting PBMC numbers differed between MOIs due to limited virus (NT = 5 starting wells; 1E6 PBMCs, MOI 2 and MOI 4 = 3 starting wells; 6E5 PBMCs, MOI 10 = 1 starting well; 2E5 PBMCs).* ***A & B)*** *Absolute αβ and γδ counts were first determined by multiplying the cell count for the culture by the percent αβ+ or %γδ+. Counts were then normalized by the number of starting wells.* ***C & D)*** *Transduced αβ and γδ counts were first calculated by multiplying αβ and γδ cell counts calculated in A and B, by the sum of the percent of BCMA+, NGFR+, and double-positive NGFR+BCMA+ αβ or γδ T cells. Counts were then normalized based on number of starting wells.*

Notably, actual γδ T cell counts do not substantially differ between LV-NGFR#531 and BCMA-TAC#898. However, there does appear to be an inverse relationship between BCMA-TAC#898 MOI and γδ T cell counts that doesn't exist for the LV-NGFR#531 culture (Fig 5B). A similar relationship between γδ T cells counts and lentivirus MOI is observed in BCMA-TAC#898 and BCMA-TAC#1072 in Fig 2B. Despite this, transduced γδ T cell counts are similar between LV-NGFR#531 and LV-BCMA-TAC#898 (Fig 5B). In contrast, LV-BCMA-TAC#898 has an outgrowth of αβ T cells and transduced αβ T cells (Fig 5A, 4C). Comparatively, the numbers of transduced αβ are low in the control LV-NGFR#531 (Fig 5D). Notably, transduction of the LV-NGFR#531 culture at MOI 4 has the highest transduced γδ T cell count (Fig 5D), however this is a product of higher ratio of γδ T cells in culture (Fig 4), rather that increased in % transduced. Increased αβ T cells in the LV-BCMA-TAC#898 culture and not in LV-NGFR#531 may indicate that TAC-encoding lentiviruses generate immunologically active mediators in the lentiviral preparation that either induces proliferation or improves survival of αβ T cells in zoledronate + Il-2 culture, leading to a γδ/αβ ratio skewed towards αβ T cells. This effect appears to be a feature of the BCMA-TAC lentivirus construct, as later experiments show that αβ/γδ ratios are not substantially different when γδ T cells are transduced with a γ-retrovirus encoding the equivalent BCMA-TAC transgene as LV-BCMA-TAC#898 (Fig 9 and Fig 11).

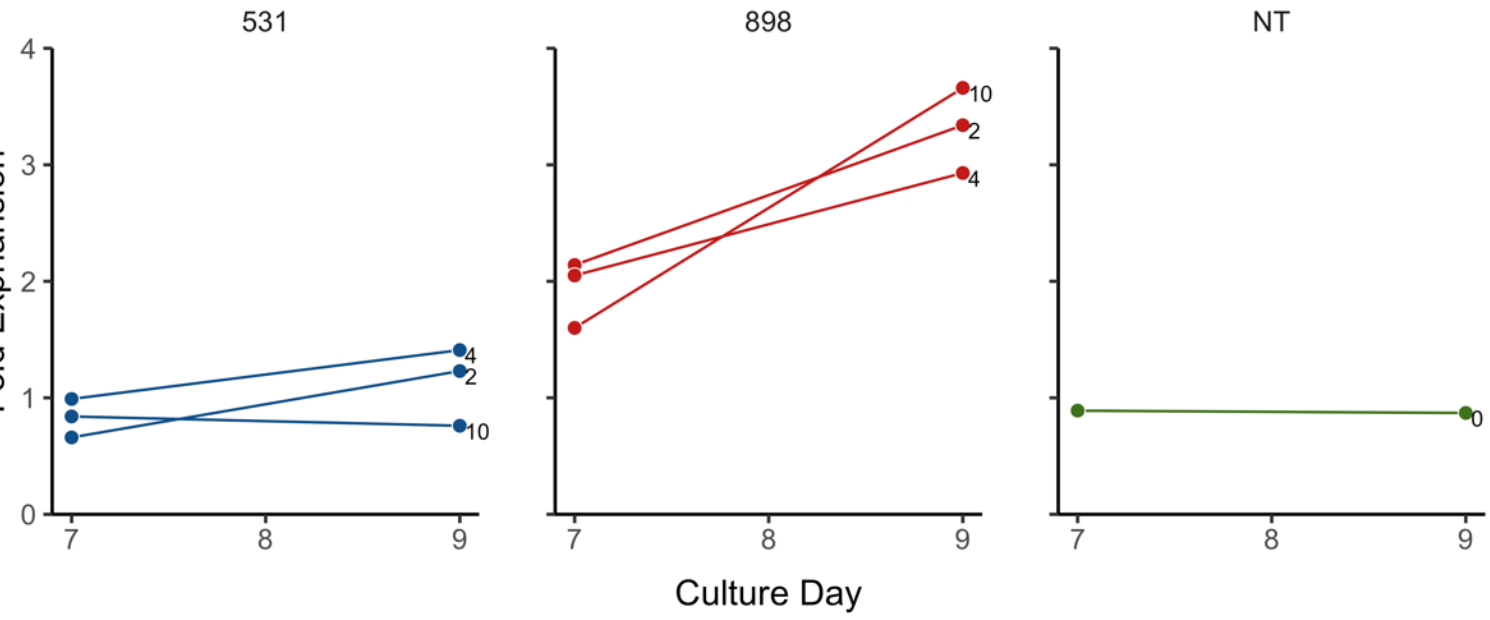

***Figure 6**: LV-BCMA-TAC#898 transduction enhances total cell expansion compared to NT or LV-NGFR-TAC#531 transduced cultures. Fold expansion was calculated relative to PBMC seed number at D0.*

Lentivirus encoding a BCMA-specific TAC (BCMA-TAC#898) leads to increased culture expansion (Fig 6). As demonstrated in Fig 6, the γδ T cell counts are slightly reduced in BCMA-TAC#898, but there are substantial differences between αβ T cell counts compared to LV-NGFR#531. The BCMA-TAC-encoding lentivirus culture has increased cell counts driven by αβ T cell expansion, which does not occur with the LV-NGFR#531 (Fig 6). LV-BCMA-TAC#898 αβ expansion dilutes γδ T cells in culture leading to lower %γδ (Fig 4), in conjunction with viral transduction reducing γδ T cell expansion (Fig 5B, Fig 7B).

Effect of Viral Transduction on γδ Culture Purity and Expansion

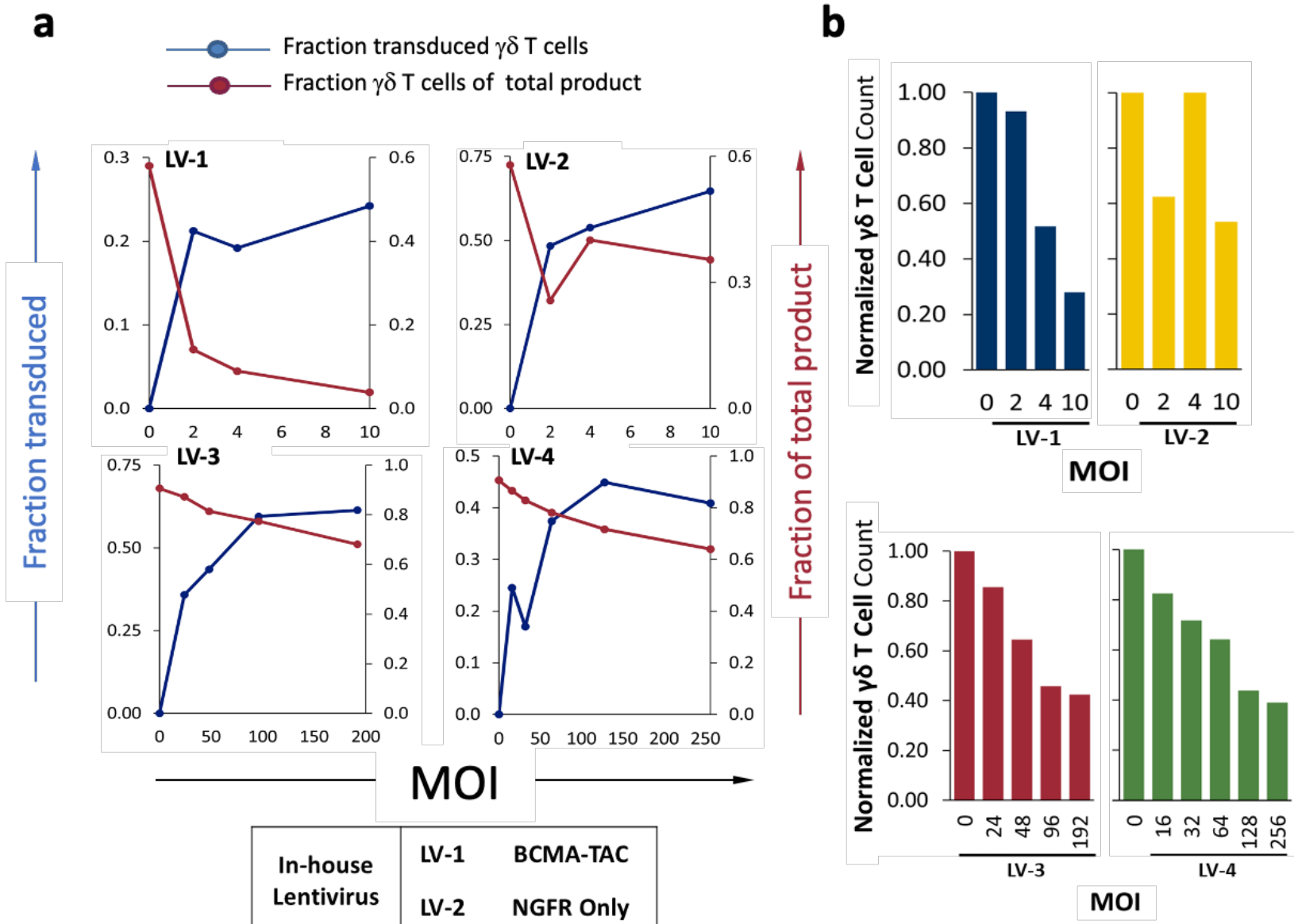

In-house Lentivirus	LV-1	BCMA-TAC
	LV-2	NGFR Only
Lentigen Lentivirus	LV-3	CD19-TAC
	LV-4	HER2-TAC

***Figure 7**: In-house lentivirus has a greater impact on γδ T cell purity and lower transduction than Lentigen LV. Both in-house and lentigen LV reduce γδ T cell expansion in zoledronate and IL-2 stimulated cultures. LV-1 and LV-2 data collected on Day 9, LV-3 and LV-4 data collected on Day 7.* ***a)** Flow cytometry results analyzing the relationship between proportion of γδ T cell in culture and γδ T cell transduction* ***b)** Flow cytometry results for %gd were used to calculate γδ T cell counts, which were then normalized to the γδ T cell counts of NT samples from the same manufacturing run.*

In-house LV transduction (BCMA-TAC#898, BCMA-TAC#1072, and BCMA-TAC#1040) results in a trade-off between γδ T cell transduction and γδ purity (Fig. 7A, Fig. 3). Similarly, commercially available Lentigen LV has a trade-off between γδ T cell transduction and γδ purity, but the trade-off is substantially smaller – whereby higher transduction is associated with a smaller reduction in γδ purity (Fig 7A). Analysis of culture γδ T counts demonstrates that LV transduction results in reduced γδ T cell expansion, in addition to the outgrowth of αβ observed in the in-house BCMA-TAC LV vector. There appears to be a negative relationship between LV MOI and γδ T cell expansion. This data suggests that even under the ideal transduction conditions using the Lentigen LV vector, viral co-incubation and/or transduction hampers γδ T cell expansion.

BCMA-TAC Transduction of γδ T cells using γ-retrovirus

Next, we wanted to test transduction of γδ T cells using in-house γ-retrovirus. The protocol currently used in our lab, which was designed for αβ T cells, recommends transduction on Day 2 post-activation. However, engineered γδ T cell literature traditionally uses Day 5 for retroviral transduction. Consequently, we wanted to assess Day 2 γδ T cell transduction timepoint, in addition to testing a later time point – Day 4.

γδ T cells were successively transduced on either Day 2 or Day 4 using gamma retrovirus (gRV) gRV-BCMA-TAC#1195, which has an equivalent TAC construct as the lentivirus construct LV-BCMA-TAC#898(Fig 8). However, γδ transduction was unexpectedly higher when transduced with the retrovirus on Day 2 (Fig 8). Using gRV to transduce γδ T cells appears to preferentially transduce γδ T cells rather than αβ T cells in culture (Fig 8). This is likely because gRV transduces actively proliferating cells. Proliferation is likely biased towards γδ T cells because of

zoledronate-induced γδ activation, although IL-2 supplement in culture likely stimulates some αβ T cell proliferation as well leading to the small subset of transduced αβ T cells.

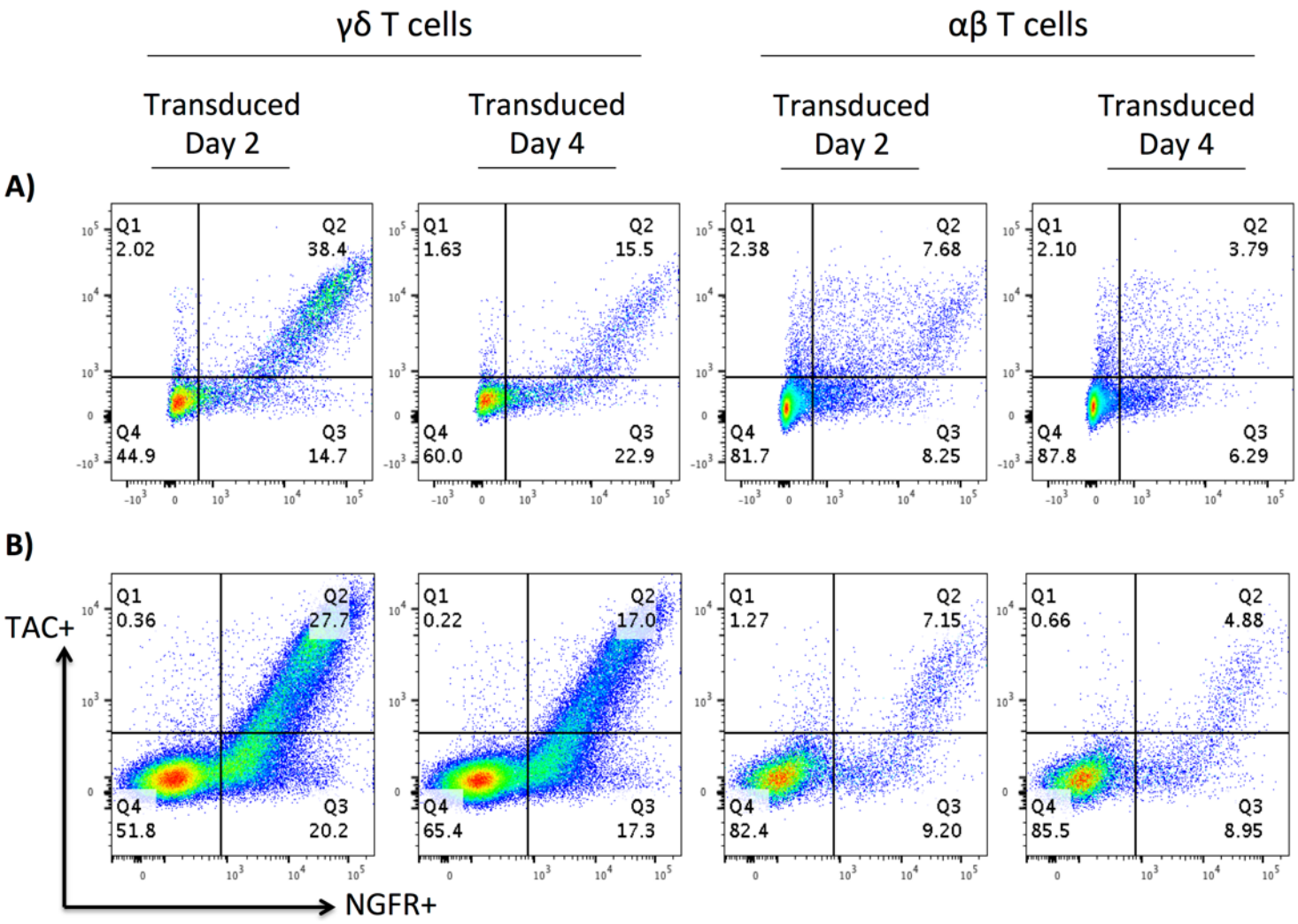

***Figure 8**: Transduction of αβ and γδ T cells with gRV-BCMA-TAC#1195 in* zoledronate *+ Il-2 cultures compared by flow cytometry on Day 7 or Day 14. NGFR is a transduction marker for gRV-BCMA-TAC#1195. TAC+ cells were determined by determining BCMA expression. **A)** Day 7 transduction **B)** Day 14 transduction*

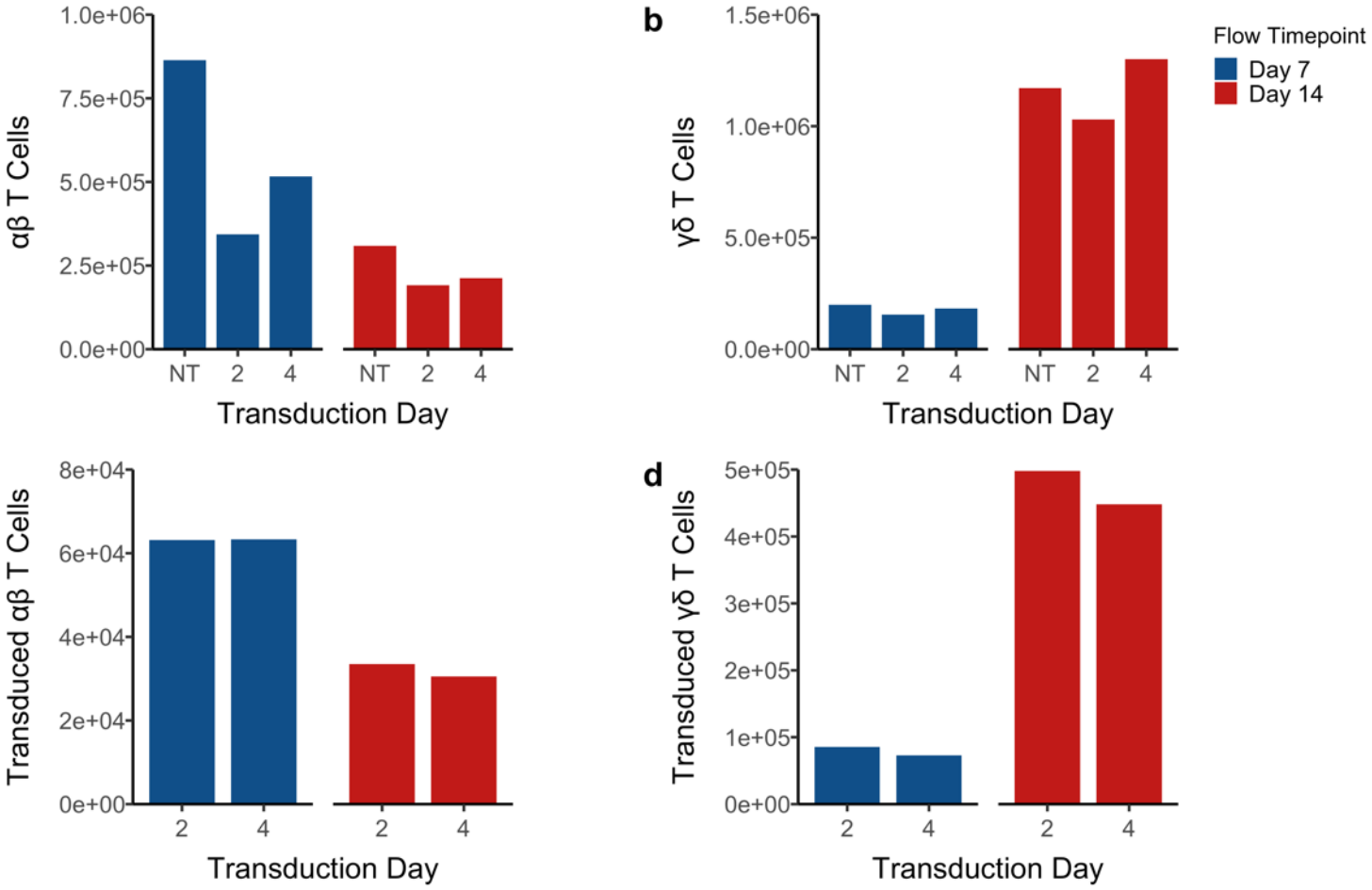

Figure 9*: Total and transduced γδ T cell vs. αβ T cell counts demonstrate that the culture composition of both gRV-BCMA-TAC#1195 and non-transduced (NT) cultures differs between Day 7 and Day 14 culture. Day 7 or Day 14 flow cytometry data was used for calculations (αβ, γδ, and transduction counts).* ***A & B)*** *Absolute αβ and γδ counts were determined by multiplying the cell count for the culture by the percent αβ+ or %γδ+.* ***C & D)*** *Transduced αβ and γδ counts were calculated by multiplying αβ and γδ cell counts calculated in A and B, by the sum of the percent of BCMA+, NGFR+, and double-positive NGFR+BCMA+ αβ or γδ T cells.*

In addition to having lower αβ T cells transduction (Fig 8) than lentivirus transduced cultures (data not shown), gRV-BCMA-TAC#1195 transduction does not support the survival of a αβ T cell population. The number of αβ T cells in both 1195 cultures is lower than the NT culture at Day 7, and the aβ T cell population further restricts in NT and 1195 cultures between Day 7 and Day 14 (Fig 9A). On the contrary, the γδ population expands between Day 7 and Day

14 to similar total γδ counts in both the 1195 transduced and NT cultures (Fig 9B). In accordance with total γδ T cell expansion, the number of transduced γδ T cells continues to expand between Day 7 and Day 14 (Fig 9C).

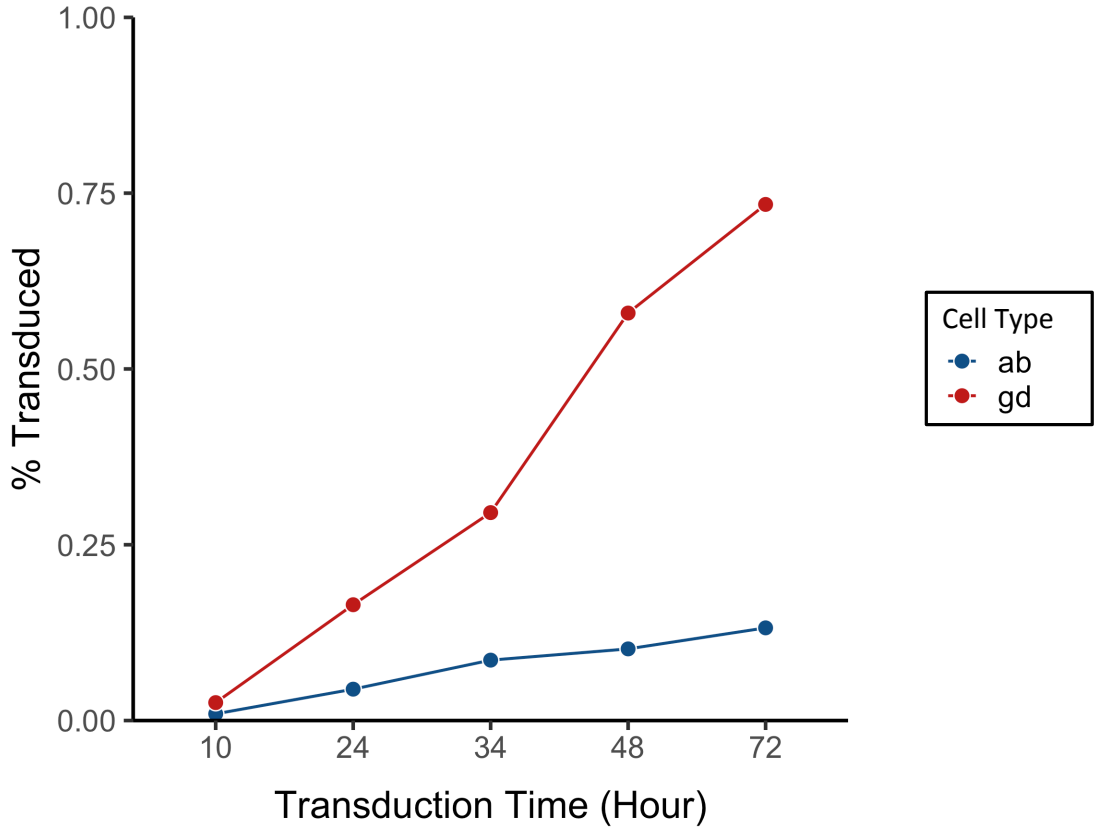

Figure 10*: Transduction of percentage γδ and αβ T cells in zoledronate + IL-2 in gRV-BCMA-TAC#1195 transduced cultures at multiple time points. Flow cytometry was run on day 9. Percent transduced was calculating by summing the percentage of BCMA+, NGFR+ and BCMA+NGFR+ cells for each subset.*

Given the unexpected success of retroviral transduction of γδ T cells at Day 2 –an earlier timepoint than the conventional Day 5 timepoint in the literature – we wanted to test other early timepoints for retroviral transduction. Timepoints from 10h to 72 were tested. The 72-hour timepoint had the highest overall transduction of γδ T cells (Fig 10). Retrovirus transduction timepoints earlier than 48h did not lead to improved γδ transduction (Fig 10).

One concern was that at later timepoints, although γδ T cell transduction would be improved, αβ T cell transduction would also proportionally increase. Although αβ T cell transduction does increase at later timepoints, the rate at αβ T cell transduction increases is lower than γδ T cell transduction (Fig 10). Consequently, later timepoints – such as 72 hours – have a higher percentage of transduced γδ than transduced αβ T cells (Fig 10).

For unknown reasons, the γδ T cell culture transduced at 34 hours had higher cell counts than other cultures (Fig 11A). For this reason, the 34h culture has higher calculated absolute γδ counts (Fig 11C), despite all cultures having a similar percentage of γδ T cell in cultures (data not shown). Overall, the culture expansion is not substantially different between cultures (Fig 11C). Unlike observations made from LV-BCMA-TAC#898 lentivirus transductions, gRV-BCMA-TAC#1195 retrovirus transduction did not lead to increased expansion or maintenance of the αβ T cell population compared to the NT culture (Fig 11B). This may be due to differences in the lentivirus and retrovirus construct, or because of lower αβ T cell transduction – or a combination of both factors. Regardless, the absolute transduced γδ count is highest at 72h (Fig 12E). Going forward, γδ T cells were transduced with γ-retrovirus at 72 hours.

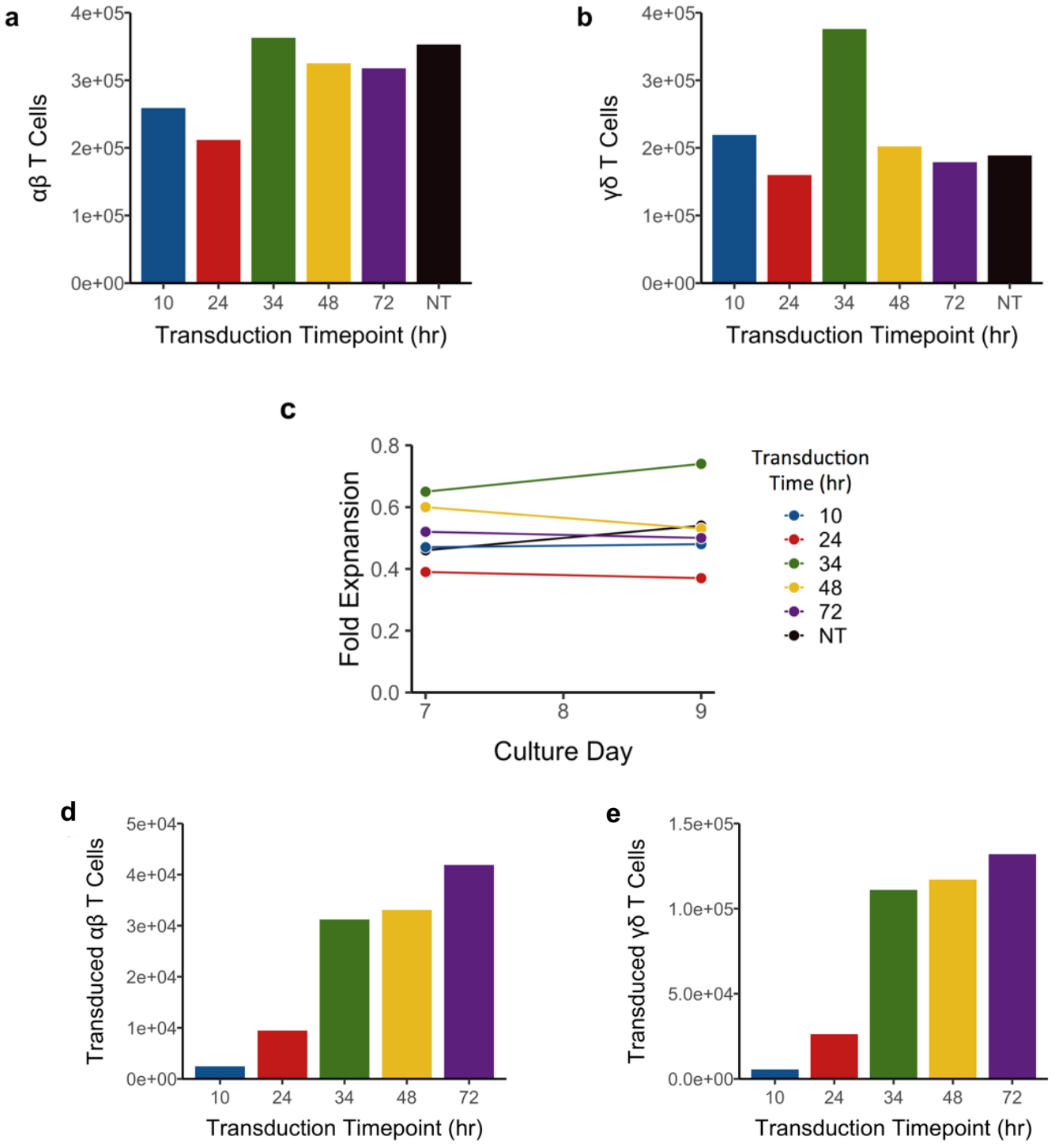

***Figure 11**: Zoledronate + IL-2 culture composition (γδ/αβ) is similar regardless of gRV (gRV-BCMA-TAC#1195) transduction timepoints. Differences in absolute γδ T cell count are due to higher overall cell counts. Transduced αβ and γδ T cells based on Day 9 flow cytometry differ depending on transduction time. **A and B)** Absolute αβ and γδ T cell counts were determined by multiplying the culture cell count by the % αβ or γδ in culture from flow cytometry data collected on Day 9. **C)** Fold expansion of zoledronate + IL-2 gRV-BCMA-TAC#1195 cultures **D and E)** Transduced αβ and γδ T cell counts were first calculated by multiplying αβ and γδ counts by the sum of the percent of BCMA+, NGFR+, and NGFR+BCMA+ αβ or γδ T cells. Counts were then normalized based on number of starting wells.*

Optimization of BCMA-TAC gRV γδ Culture Density

The density of γδ T cell cultures was optimized for the activation and transduction stages of the γδ T cell manufacturing protocol. Given that PBMC γδ T cells are activated by zoledronate via cell-to-cell interactions with monocytes that have accumulated pAgs[109], it was hypothesized that increasing cell density would improve γδ T cell expansion. High-density conditions were assessed at early timepoints (D0 and D3), as early timepoints are likely when most γδ T cells are activated via trans-cellular interactions. High activation density (conditions #1 and #2) generally resulted in higher γδ T cell expansion (Fig 12A) and higher counts of transduced γδ T cell compared to donor-matched controls (Fig 12B). Cell density at the time of transduction did not appear to affect γδ T cell or transduced γδ T cell counts (Fig 12A, 12B), as evidenced by no apparent improvement in density condition 1 compared to condition 2, nor density condition 3 compared to condition 4.

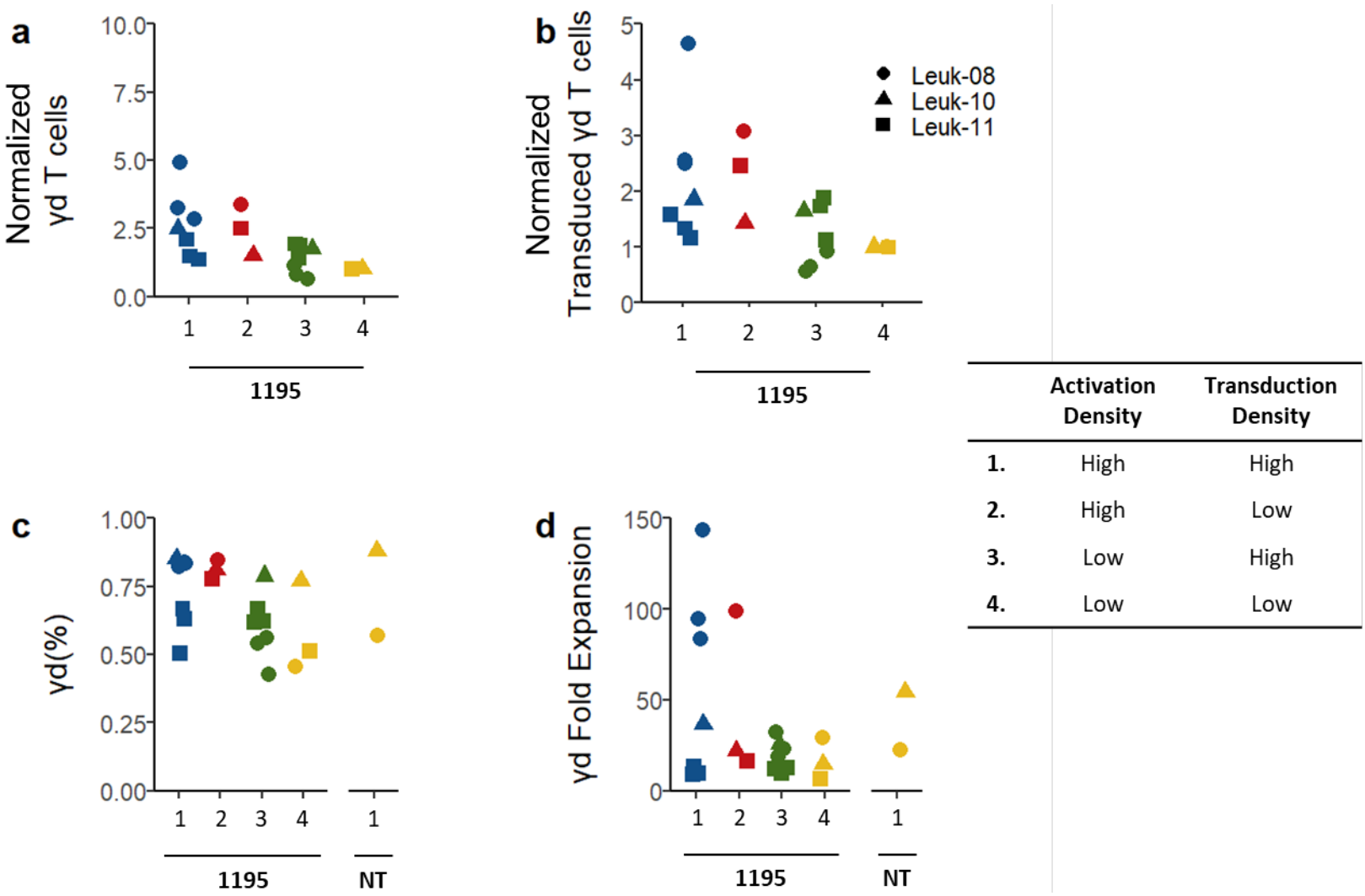

	Activation Density	Transduction Density
1.	High	High
2.	High	Low
3.	Low	High
4.	Low	Low

Figure 12*: Cell density optimization for activation (D0) and transduction (D3) stages of gRV-BCMA-TAC#1195 transduced γδ T cell cultures in multiple donors. Results are calculated from flow data analysis from D10 cultures.* ***A & B)*** *Normalized cell counts were determined by multiplying proportion of γδ T cells, or transduced γδ T cells by cell counts. The counts were then normalized to the donor-matched standard manufacturing (condition #4).* ***C)*** *Proportion of γδ T cells in culture.* ***D)*** *γδ fold expansion was calculated by comparing the number of γδ T cell seeded on D0, versus the γδ T cells in the culture when flow cytometry was performed.*

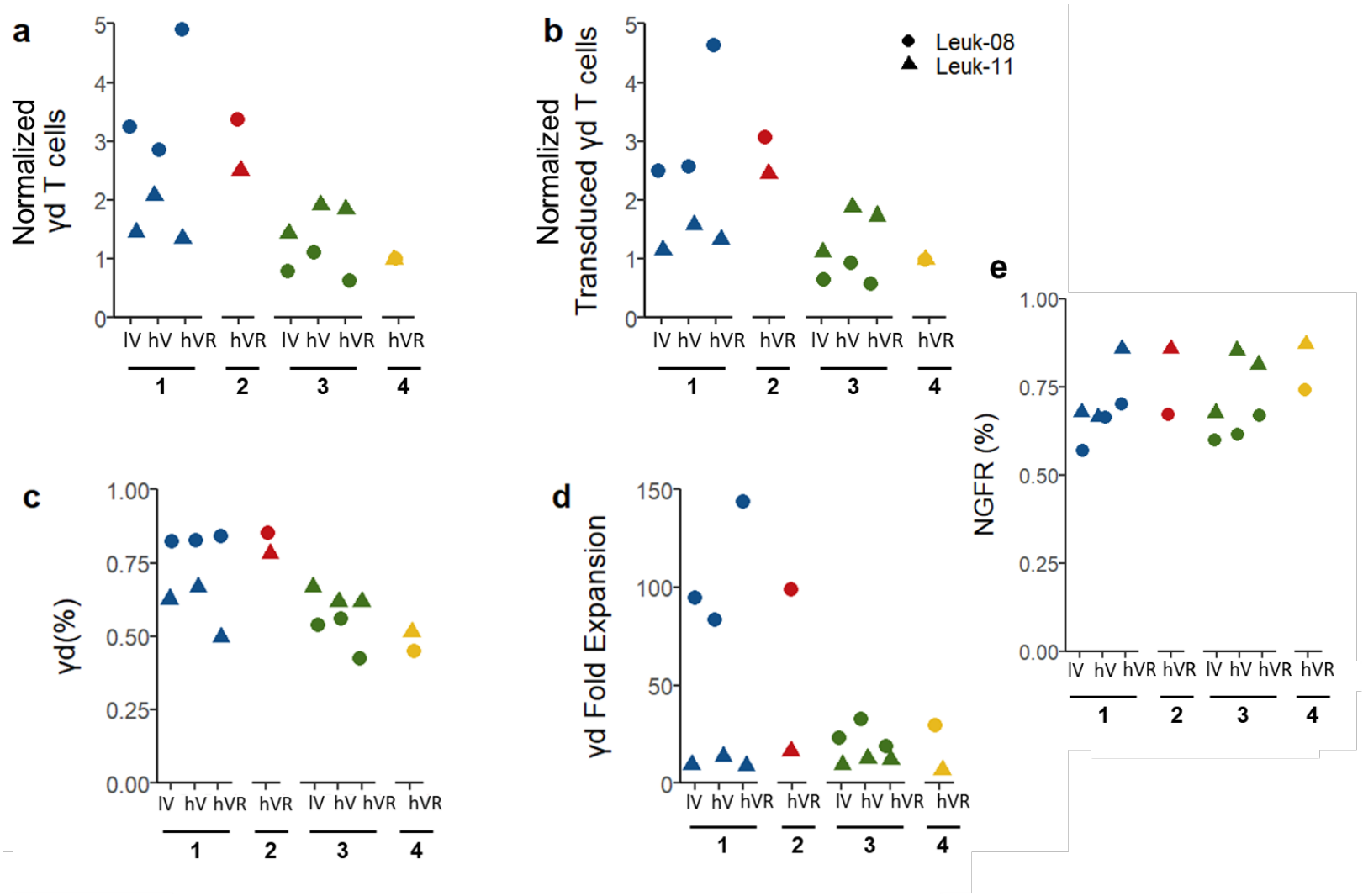

Figure 13*: Optimization of viral supernatant and retronectin volumes for gRV-BCMA-TAC#1195 γδ T cell manufacturing in tandem with culture density conditions; lV = low viral supernatant, hV = high viral supernatant, hVR = high viral supernatant and retronectin. Conditions #1 – 4 reflect activation and transduction densities; 1 = High activation, transduction density, 2 = High activation, low transduction density, 3 = Low activation, high transduction density, 4 = Low transduction, high activation density. Results are calculated from flow data analysis from D10 cultures.* ***A & B)*** *Normalized cell counts were determined by multiplying proportion of γδ T cells, or transduced γδ T cells by cell counts. The counts were then normalized to the donor-matched standard manufacturing conditions (density condition #4).* ***C)*** *Proportion of γδ T cells in culture.* ***D****) γδ fold expansion was calculated by comparing the number of γδ T cell seeded on D0, versus the γδ T cells in the culture when flow cytometry was performed.* ***E)*** *Proportion of γδ T cells that are NGFR+.*

During culture density condition optimization, the volume of gRV-BCMA-TAC#1195 viral supernatant and retronectin added to the transduction well was optimized in high transduction density conditions (conditions #1 and #3). Doubling the number of cells present in the high transduction density conditions halves the ratio of gRV-BCMA-TAC#1195 supernatant: γδ T cell, or retronectin: γδ T cells. Consequently, we wanted to ensure that we were not achieving sub-optimal transduction due to inadequate volume of viral supernatant or retronectin added for the increased number of cells by increasing retronectin and retroviral supernatant volumes. The high viral supernatant and retronectin conditions (hV and hVR) led to either no effect or a deleterious effect on γδ purity (Fig 13C). Despite reductions in purity, the high viral supernatant and retronectin conditions (hV and hVR) either increased the total yield of transduced γδ T cells or had no effect depending on donor (Fig 13B). In accordance with higher yield of engineered γδ T cells, hV and hVR conditions increased the proportion of transduced γδ T cells in culture (Fig 13E). Overall, the conditions with high cell density at transduction benefit from using higher volumes of viral supernatant and retronectin for gRV-BCMA-TAC#1195 γδ T cell cultures, as indicated by higher yield of transduced γδ T cell. For the remainder of the work, we used the high cell density conditions for both activation (4E5 cells) and transduction (2E6 cells), alongside high retronectin (600µL; 50µg/mL) and high viral supernatant (3mL harvested from confluent T75).

Manufacturing BCMA-TAC gRV γδ Cultures Using IL-15

IL-15 has been reported to improve γδ T cell proliferation and reduce cell death in response to phosphoantigen stimulation (Table 1). A head-to-head comparison of standard 660IU/mL IL-2 manufacturing conditions was compared to IL-15 at varying concentrations or with IL-2 and IL-15 combination regimens. While most IL-15 conditions did not generate pronounced effects on γδ T cell cultures, low IL-15 (5ng/mL) either improved or did not affect the yield of transduced (Fig 14B) and overall γδ T cells (Fig 14A).

High levels of IL-15 or combination regimens of IL-2 and IL-15 decreased γδ purity (Fig 14C). Transduction levels remained high regardless of cytokine conditions, albeit slightly lower in high IL-15 or IL-2 and IL-15 combination regimens (Fig 14E). Overall, low IL-15 (5ng/mL) may improve transduced γδ T cell yield without affecting γδ purity (Fig 14D), however the improvement in transduced γδ T cell yields is marginal for most donors.

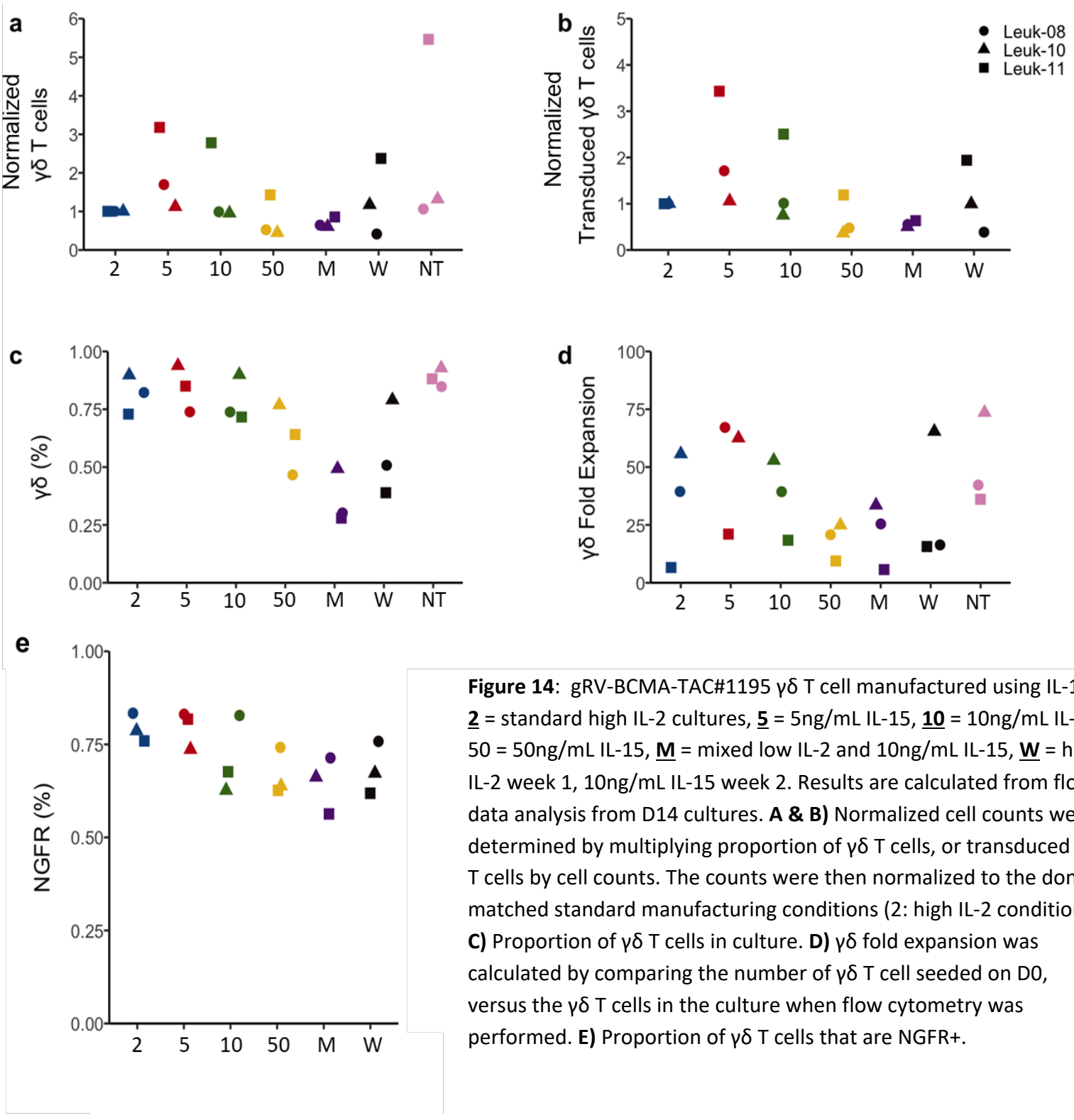

Figure 14: gRV-BCMA-TAC#1195 γδ T cell manufactured using IL-15; **2** = standard high IL-2 cultures, **5** = 5ng/mL IL-15, **10** = 10ng/mL IL-15, 50 = 50ng/mL IL-15, **M** = mixed low IL-2 and 10ng/mL IL-15, **W** = high IL-2 week 1, 10ng/mL IL-15 week 2. Results are calculated from flow data analysis from D14 cultures. **A & B)** Normalized cell counts were determined by multiplying proportion of γδ T cells, or transduced γδ T cells by cell counts. The counts were then normalized to the donor-matched standard manufacturing conditions (2: high IL-2 condition). **C)** Proportion of γδ T cells in culture. **D)** γδ fold expansion was calculated by comparing the number of γδ T cell seeded on D0, versus the γδ T cells in the culture when flow cytometry was performed. **E)** Proportion of γδ T cells that are NGFR+.

The NKR, FcgR and CD27 phenotype of γδ T cells were assessed in the IL-15 and IL-2 cultures and observed differences in phenotype were primarily driven by donor (Fig 15). We did not find that the cytokine conditions had a marked effect on phenotype (Fig 15). CD27 expression was low in all γδ T cell cultures, indicative of effector memory or terminal effector memory differentiation of γδ T cells (Fig 15A). Low CD27 expression suggests that the engineered γδ T cells will have low proliferative capacity upon antigen re-stimulation, which may limit *in vivo* efficacy of engineered γδ T cell therapy. Notably, CD27 expression is highest in Leuk-10 (Fig 15A). CD56 is a marker γδ T cell cytotoxicity and has been associated with NKR-related cytotoxic effector functions[110,111]. Generally, donor effects drove CD56 expression, except for Leuk08 where CD56 is also influenced by cytokine conditions (Fig 15B). In Leuk08, CD56 expression is highest in IL-15 cytokine conditions, and lowest in low IL-15 or IL-2 only conditions (conditions: 2, 5, NT) (Fig 15B). Interestingly, IL-15 has been associated with potentiating CD56 and γδ T cell cytotoxic potential in γδ T cells from AML patients – which generally represent an exhausted subset of γδ T cells[84]. This may suggest that Leuk-08 γδ T cells are similarly exhausted in some capacity. NKR expression does not appear to be influenced by donors. Nearly all γδ T cells express NKG2D, and a small proportion of γδ T cells also express NKp44 (Fig 15C, 15D), suggesting these cells will respond to stress ligands on target cells. Finally, CD16 expression showed distinct variation depending on donor, being highest in Leuk11 and nominal in Leuk08.

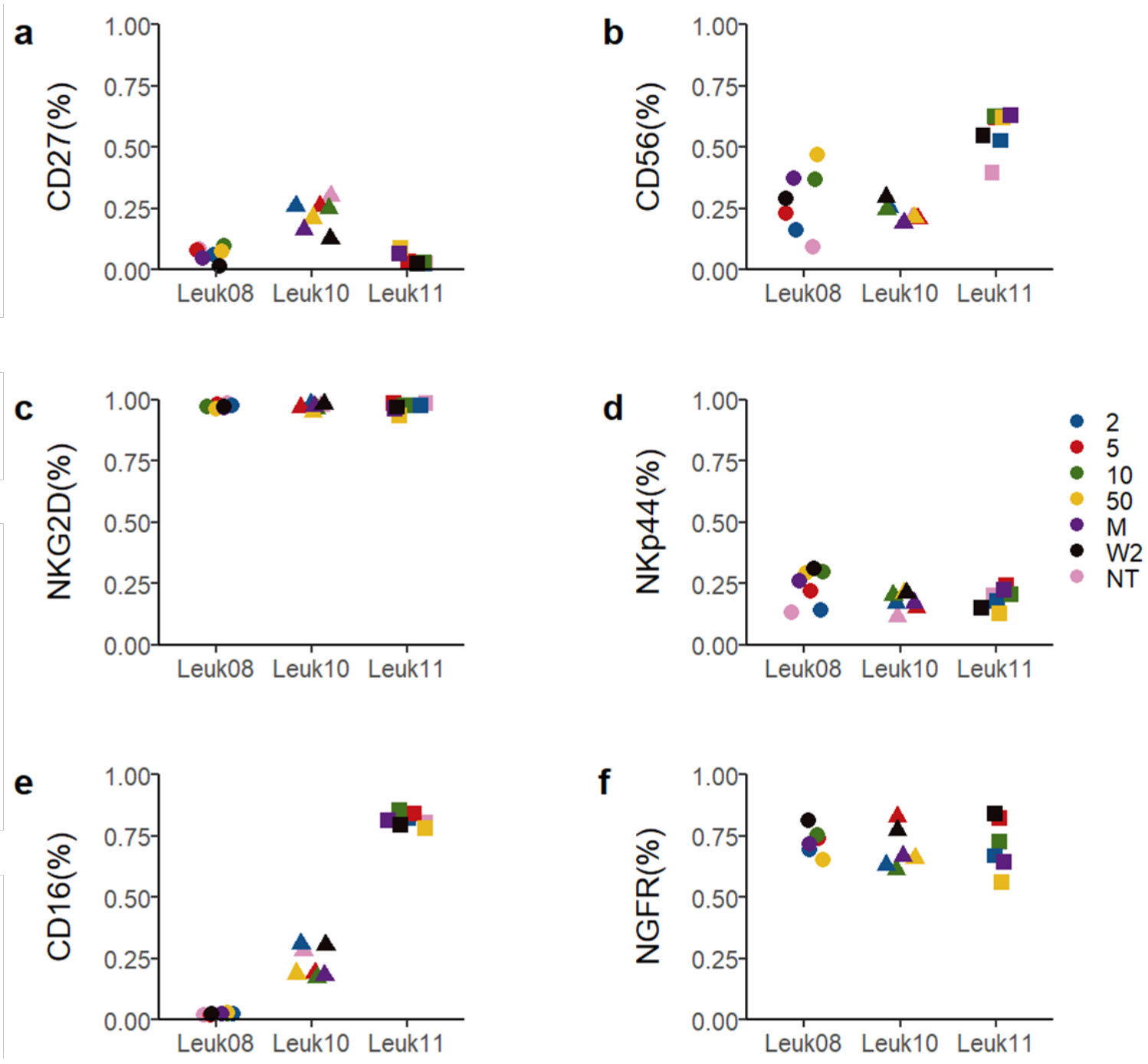

***Figure 15**: NKR, FcγR, CD56, and CD27 phenotype of γδ T cells manufactured with IL-2 or IL-15 in 3 donors. Flow cytometry was stained and collected by Ying Wu on D14 of γδ T cell culture. **2** = standard high IL-2 cultures, **5** = 5ng/mL IL-15, **10** = 10ng/mL IL-15, **50** = 50ng/mL IL-15, **M** = mixed low IL-2 and 10ng/mL IL-15, **W** = high IL-2 week 1, 10ng/mL IL-15 week 2.*

Optimizing KIR-TAC-DAP12 PG13 gRV Seeding Density

In efforts to maximize the efficacy of TAC-transduced γδ T cells, we designed a TAC with an intracellular KIR2DS2 domain that is co-expressed with intracellular signalling adaptor protein DAP12, targeting HER-2 (gRV#1240). Construct variations were cloned to test synthetic antigen receptor functionality without the HER2 binding domain (gRV#1241), DAP12 ITAM signalling domain (gRV#1242), or lacking both (gRV#1243) (Fig 16C). A stable gRV PG13 cell line was generated for each construct, and gRV#1240-1243 γδ T cells were manufactured using the standard high activation and high-density gRV transduction protocol. However, PG13s are typically seeded at 2E6 cells and cultured for 3 days prior to harvesting viral supernatant. Here, PG13s were seeded between 1E6 – 2E6 seeding density to vary the amount of KIRTAC gRV added to the γδ T cell cultures. KIRTAC γδ T cells only have a modest reduction in γδ purity, but poor surface expression of the TAC receptor (Fig 16A, 16B). γδ purity increases between culture day 10 and day 14, suggesting continued expansion of γδ T cells, however TAC surface expression drops below 10% for most conditions (Fig 16B). This suggests either downregulation of TAC in late cultures, or that KIRTAC transduced γδ T cells are not proliferating or dying. TAC surface expression is highest cultures transduced with viral supernatant from gRV PG13s with higher seed counts, and like the transduction-purity trade-off in LV (Fig 7), these cultures have the lowest γδ purity (Fig 16B). Even when using high gRV#1240 PG13 density for retroviral harvest, the HER2-KIR-TAC-DAP12 constructs have poor transduction in γδ T cells. The KIR-TAC-DAP12 γ-retrovirus γδ T cell cultures reproduce the purity-to-transduction trade-off observed with BCMA-TAC lentiviruses and reinforces the need to develop a γδ T cell manufacturing strategy that prevents αβ T cell outgrowth when co-cultured with TAC-encoding viruses.

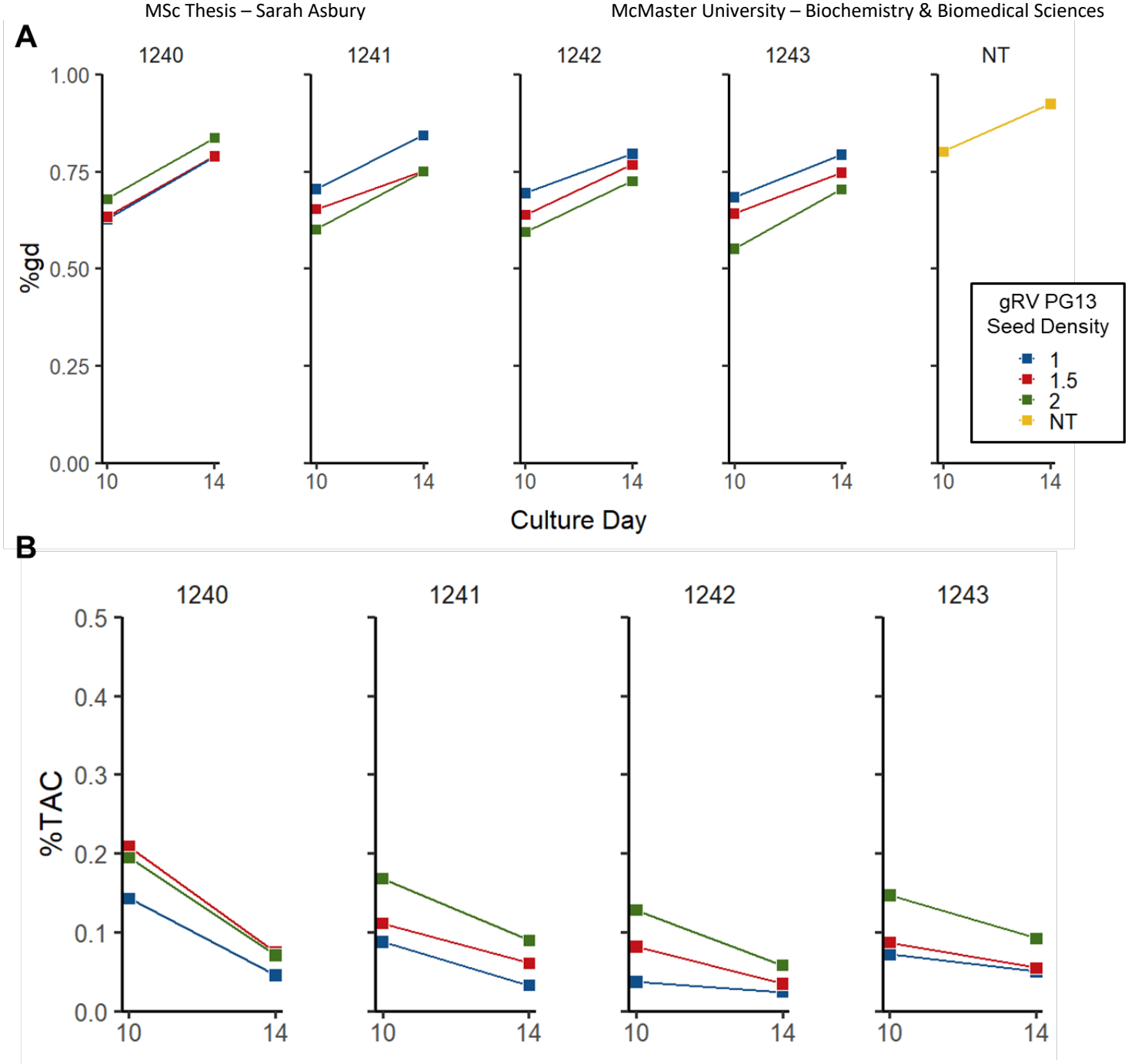

***Figure 16**: HER2-KIR2DS2-TAC-DAP12 engineered γδ T cell cultures achieve relatively high γδ purity but have low TAC expression, which reduces over time. Cultures were transduced with D3 gRV PG13 viral supernatant, which were seeded with 1E6 (1), 1.5E6 (1.5) or 2E6 (2) PG13 cells. **A)** D10 and D14 γδ purity of KIR-TAC constructs at varying PG13 seeding density **B)** D10 and D14 γδ transduction of KIR-TAC constructs at varying PG13 seeding density **C)** 1240 – 1243 KIR-TAC construct design*

αβ T Cell Depleted Manufacturing

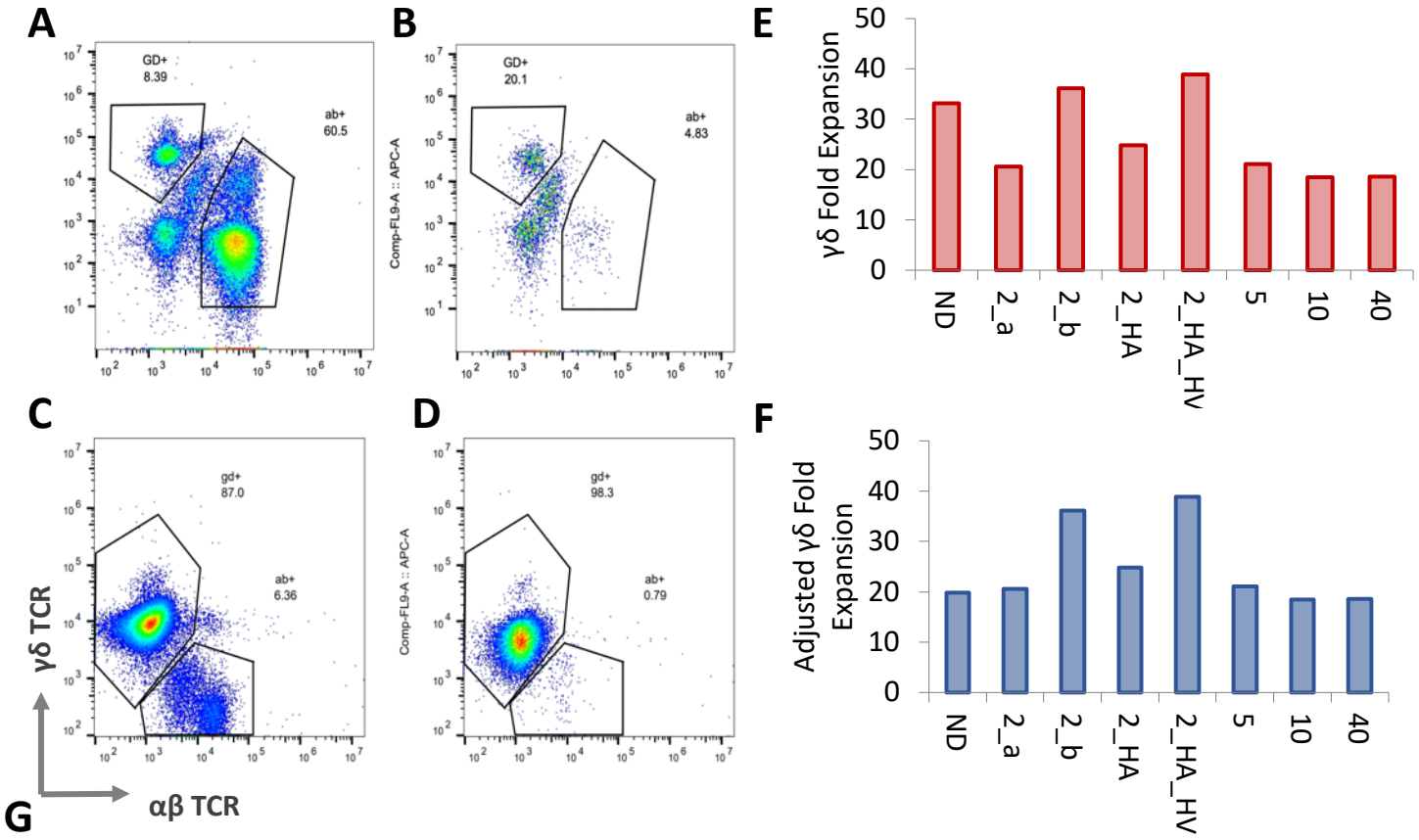

Sample	Purified	Cells Seeded/Well	Well V (µL)	D0 Density (Cells/mL)	[Zoledronate] and [Il-2]	D0 Zoledronate (µg)	Zoledronate: Cells (10E6)	Notes
ND	No	4.00E+05	200	2.00E+06	1	0.2	5	
2_a	Yes	2.50E+04	100	2.50E+05	0.5	0.05	20	Technical Duplicates
2_b			100	2.50E+05	0.5	0.05	20	
2_HA			100	2.50E+05	1	0.1	40	
2_HA_HV			200	1.25E+05	0.5	0.2	80	
5	Yes	5.00E+04	100	5.00E+05	1	0.1	20	
10		1.00E+05	200	5.00E+05	1	0.2	20	
40		4.00E+05	200	2.00E+06	1	0.2	5	

***Figure 17**: Depletion of αβ T cells on D0 PBMCs is a feasible γδ T cell manufacturing strategy. D0 purified cultures are predicted to yield similar amounts of γδ T cells as non-depleted cultures post-D14 purification.* ***A-D)** Flow cytometry measuring γδ T cells (y-axis) and αβ T cells (x-axis) in culture.* ***A)** D0 pre-purified PBMC culture gated on singlets.* ***B)** D0 post-purified PBMC culture gated on singlets. C) D10 non-depleted PBMC culture gated on CD3+* ***D)** D10 representative αβ-depleted cultures (Sample 2_a) gated on singlets* ***E)** Fold expansion of D10 γδ T cell cultures compared to non-depleted samples.* ***F)** Fold expansion of D10 γδ T cell cultures adjusted to accommodate for expected 40% loss of non-depleted cells post-purification on D14.* ***G)** Table describing D0 culture conditions for each sample listed in Figure 16E and Figure 16F.*

TAC γδ T cell manufacturing efforts have been limited by outgrowth of αβ T cells in culture upon transduction with lentiviral or γ-retrovirus vectors. We previously established that the degree of αβ T cell outgrowth was dependent on the type of viral vector, TAC construct, and amount of viral vector added. To circumvent αβ outgrowth, we assessed whether γδ T cells could be expanded *ex vivo* in the absence of αβ T cells. PBMC cultures were depleted using a CD4/CD8 αβ MACS depletion strategy prior to seeding and activating of the γδ T cell populations. The starting PBMC culture had 61% αβ T cells in culture (Fig 17A), which was depleted to 4.8% αβ T cells in the D0 post-depletion culture (Fig 17B). The depleted PBMCs were seeded with varying number of cells per well, densities per well, and amounts of zoledronate and IL-2 (Fig 17G). 2.5E4 cells per well was chosen as the baseline number of cells per well for the αβ T cell depleted cultures because this represents the approximate number of γδ T cells in the non-depleted 4E5 cells/well culture. Zoledronate and IL-2 were added at either 1ng/µL (1x) or 0.5ng/µL (0.5x) concentration (Fig 17G). However, reduced number of cells in each well reduces the ratio of zoledronate or IL-2 molecules to number of cells in each well (Fig 17G). Fold expansion of γδ T cells was calculated using Day 0 and Day 10 cell counts, and the percentage of γδTCR+ singlets from flow cytometry on Day 0 and Day 10.

Fold expansion of γδ T cells for some depleted conditions starting with 2.5E4 cells was comparable to expansion of non-depleted γδ T cell cultures (Fig 17F). However, the non-depleted cultures are not directly comparable to the depleted cultures. Given the high purity of the depleted cultures on D10 (Fig 17D), the αβ-depleted cultures would not need to be re-purified. However, the non-depleted control culture would require a γδ T cell purification at the end of culture for adoptive T cell therapy. On average, 40% of the culture is lost during the

purification process (Table 2) due to both the removal of αβ T cells in culture and technical steps, (e.g centrifugation and washes). The adjusted fold expansion metric accounts for a 40% loss of yield in the non-depleted culture and is a more accurate comparison for the expected final yield of γδ T cells in culture (Fig 17F). The adjusted fold expansion suggests that the yield of γδ T cells in all αβ-depleted cultures is superior or comparable to non-depleted cultures, indicating that an αβ-depleted manufacturing strategy may be viable for preventing αβ outgrowth in TAC γδ T cell cultures, but this remains to be tested.

Table 2: Average proportion of cells lost in the αβ-depletion purification process on Day 14.

Sample	Pre-puri	Puri	Proportion Lost
1195 Leuk08 Sample 1	6.00E+06	2.16E+06	0.64
1195 LeuK08 Sample 2	5.66E+07	3.70E+07	0.35
1195 Leuk11 Sample 1	9.38E+06	4.11E+06	0.56
1195 Leuk11 Sample 2	8.70E+07	4.33E+07	0.50
NT Leuk08 Sample 1	5.94E+06	2.59E+06	0.56
NT LeuK08 Sample 2	2.55E+07	2.28E+07	0.11
NT Leuk11 Sample 1	9.56E+06	5.71E+06	0.40
NT Leuk11 Sample 2	4.48E+07	3.12E+07	0.30
NT Leuk10 Sample 1	2.71E+07	1.56E+07	0.42
NT Leuk10 Sample 2	1.43E+08	8.42E+07	0.41
		Mean	**0.43**
		SD	**0.15**

BCMA-TAC Functionality

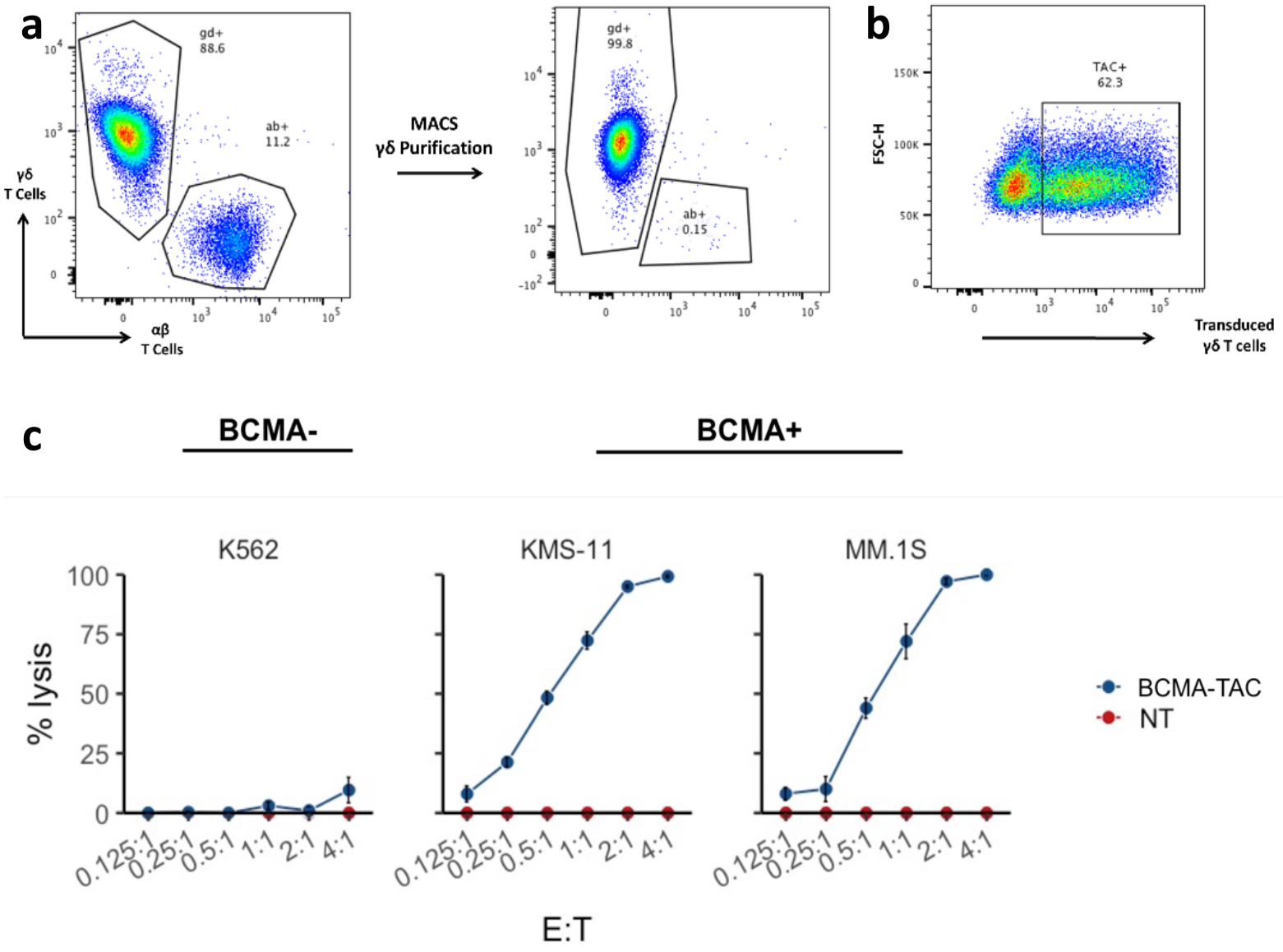

***Figure 18**: Purified BCMA-TAC γδ T cell cultures rapidly and specifically kill BCMA+ MM tumour in vitro. **a)** Example of gRV-BCMA-TAC#1195 TAC γδ T cells purified to >99% γδ T cell purity on D14. **b)** Example of transduction efficiency of gRV-BCMA-TAC#1195 in γδ T cells on D10. **c)** Leuk-10 donor gRV-BCMA-TAC#1195 TAC γδ T cells were co-cultured with MM tumour cell lines for 24 hours.*

BCMA-TAC γδ T cells can be purified to >99% purity on D14 using MACS purification column (Fig 18A). γδ T cells can also be transduced with high efficiency using the supernatant of a gRV-BCMA-TAC#1195 expressing PG13 cell line cultured for 3 days and seeded at 2E6 PG13 cell density (Fig 18B). Furthermore, BCMA-TAC γδ T cells specifically and rapidly clear Multiple Myeloma tumor cells at low E:T *in vitro* (Fig 18C). The absence of BCMA-TAC γδ T cell killing in the BCMA- MM cell line target (K562), indicates specificity of engineered γδ T cell cytotoxicity. Non-transduced γδ T cells do not display cytotoxic activity against Multiple Myeloma tumour cells at these E:T ratios. The results demonstrate that BCMA-TAC potentiates the anti-tumour function of γδ T cells in a target-specific manner.

We assessed the cytokine response of gRV#1195 BCMA-TAC and non-transduced γδ T cells to Multiple Myeloma tumour cells *in vitro*. A Th1-like cytokine response predominates in BCMA-TAC γδ T cells co-cultured with MM tumour cells *in vitro*, demonstrated by elevated levels of IFNγ and TNFα in the supernatant after 4 hours (Fig 19A). The cytokine response of TAC γδ T cells is target-specific, as BCMA-TAC γδ T cells do not generate IFNγ and TNFα when cultured alone (Fig 19A). BCMA-TAC γδ T cells produce very low levels of IL-10 and IL-17 cytokines in response to MM tumour cells. The concentrations of these cytokines are marginal, reflecting a present, but very weak pro-tumour Th17-like response to MM tumour cell stimulation, as compared to the predominant anti-tumour Th1-like cytotoxic response (Fig 19C).

Comparatively, NT γδ T cells are non-responsive to MM tumour cells at these low E:T, producing neither Th1 nor Th17 associated cytokines in response to stimulation (Fig 19A, 19C). IL-2 cytokine production was also assessed. γδ T cells are known to produce IL-2 in response to

stimulation, generating an autocrine proliferation signal[110]. Accordingly, IL-2 spikes approximately 6x upon tumour co-cultures (Fig 19B).

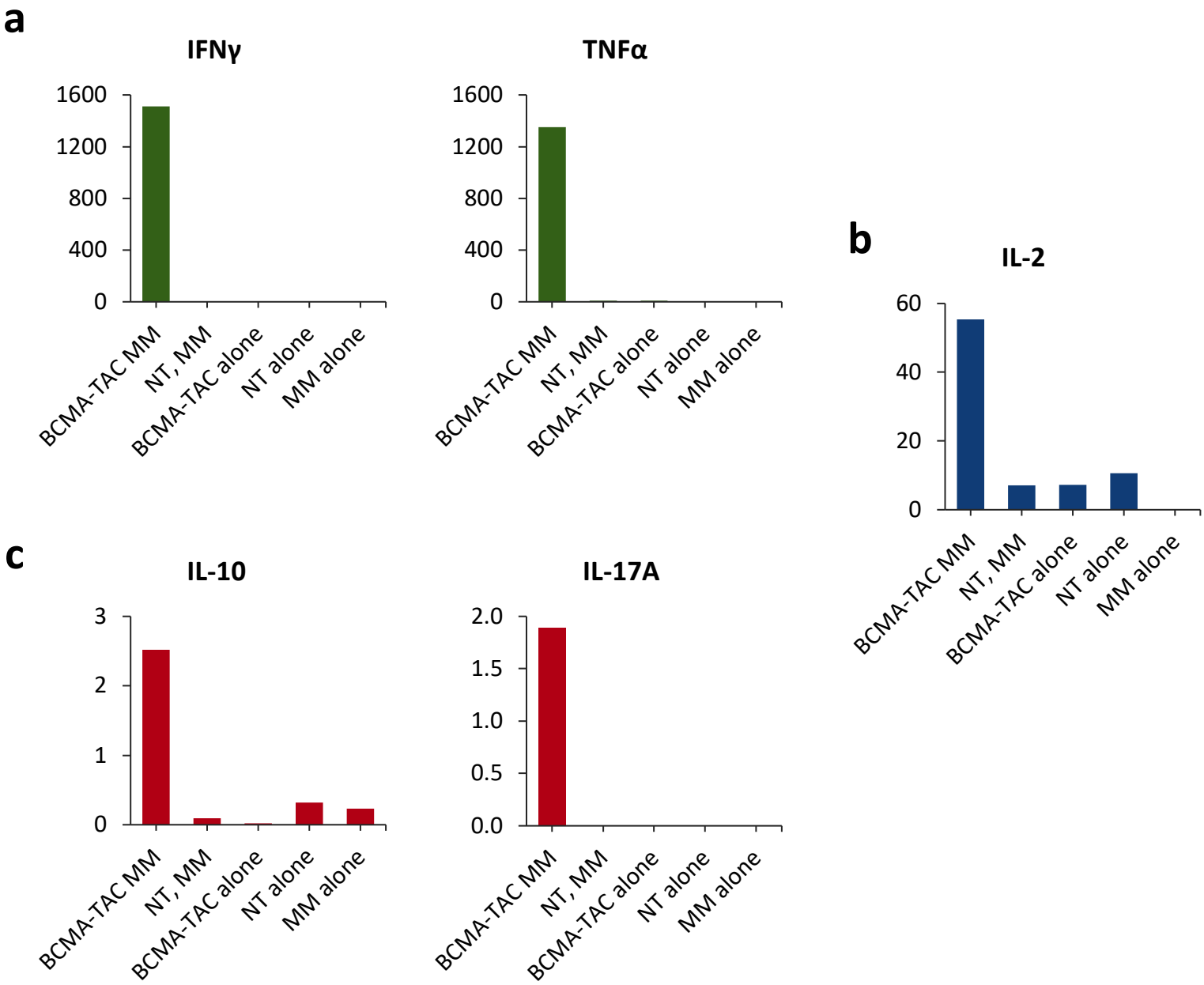

***Figure 19**: BCMA-TAC γδ T cells transduced with gRV-BCMA-TAC#1195 produce cytokines indicative of Th1-like cytotoxic phenotype when co-cultured with MM tumour cell line. γδ T cells (gRV-BCMA-TAC#1195 engineered or non-transduced) were co-cultured alone or with MM.1S at a 1:1 E:T for 4 hours. Cytokine concentrations in the supernatant were measured by Eve technologies. **a)** Cytokines indicating Th1-like antitumor cytotoxic phenotype in γδ T cells **b)** IL-2 cytokine production, which reflects neither phenotype **c)** Cytokines indicating Th17-like pro-tumour phenotype in γδ T cells.*

CD16-based BCMA-TAC γδ T Cells Combination Therapy

BCMA-TAC γδ T Cell FcγR Expression and ADCC

Given that FcγR has been shown in the literature to enhance γδ T cell activation-related signalling and cytotoxicity, we wanted to assess CD16, CD32, and CD64 expression on γδ T cells, and the binding of daratumumab to γδ T cell, an anti-CD38 IgGk mAb clinically approved for the treatment of MM patients.

A manufactured γδ T cell culture (donor: Leuk-11) demonstrated expression of CD16, but not CD32 and CD64 (Fig 20A). CD16 expression was also demonstrated in γδ T cell from other donors in our IL-15 cytokine condition manufacturing experiments (Fig 14). A flow-based binding assay assessing daratumumab bound to γδ T cells, indicates that a subset of γδ T cells can bind daratumumab at similar proportions to the frequency of CD16 expression (Fig 20B). However, given that other γδ T cell donors have been shown to express CD38 (Fig 20C, 20D), it cannot be ruled out that some or all the Streptadivin-PE signal is daratumumab binding to CD38, rather than FcγRIII. Furthermore, despite γδ T cell CD16-expression (Fig 20A), our luciferase-based *in vitro* cytotoxicity killing assay suggests that daratumumab does not improve killing of MM.1S cells by gRV-BCMA-TAC#1195 TAC T cells at 1:10 or 1:100 dilutions (Fig 21).

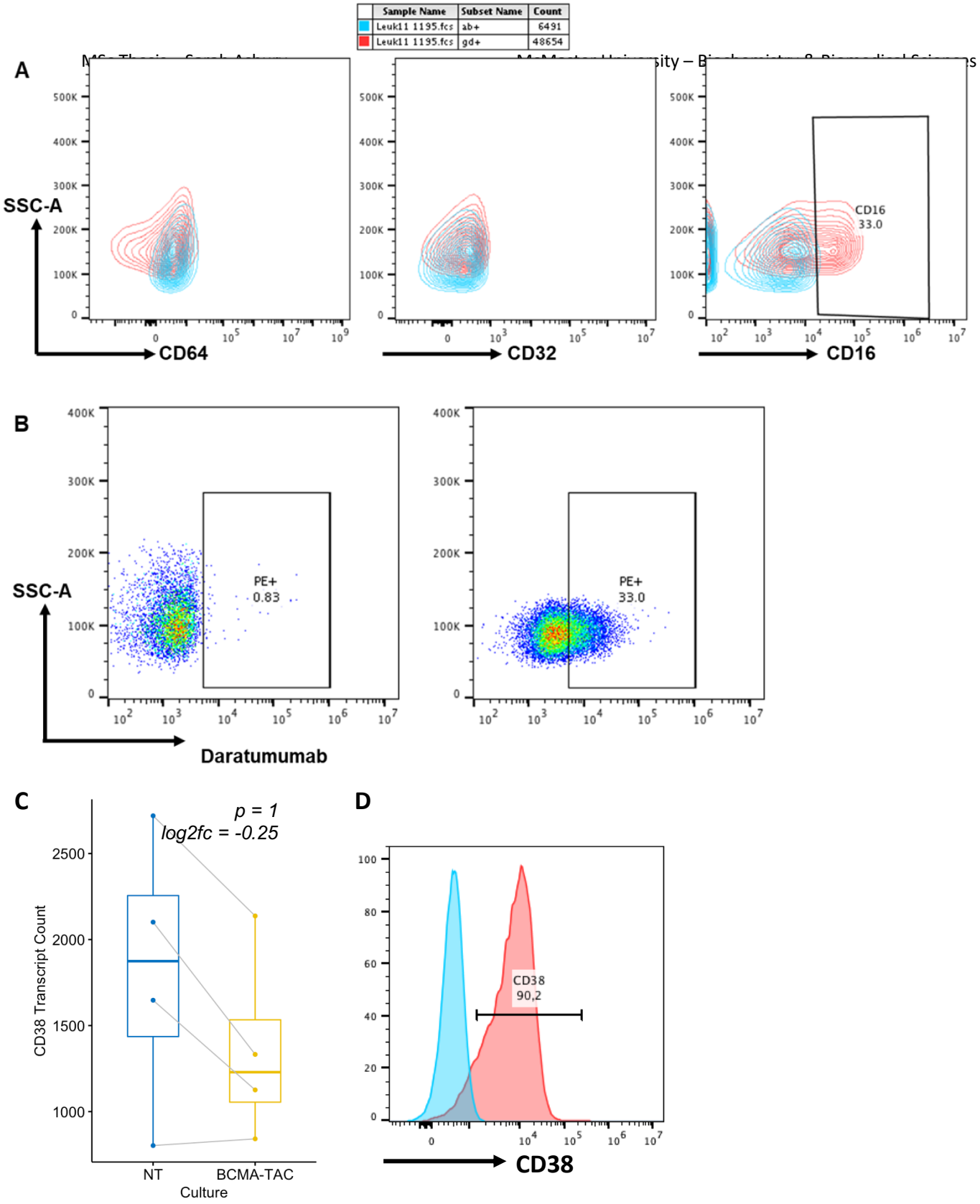

***Figure 20**: γδ T cells express FcγR CD16 and bind Daratumumab – an anti-CD38 antibody that binds MM tumour cells, including MM.1S. However, γδ T cells also express CD38. **A)** Example of CD16 expression in D10 Leuk-11 NT and gRV-BCMA-TAC#1195 γδ T cells. CD32 and CD64 were not expressed in our γδ T cell cultures.**B)** NT purified γδ T cells are capable of binding 1:10 diluted daratumumab. **Left**: NT stained γδ T cells. **Right**: NT γδ T cells stained with Daratumumab, Protein L, and Streptavidin-PE. **C)** Normalized transcript counts of CD38 in RNA-seq of NT and BCMA-TAC cultures. **D)** Surface expression of CD38 on Vδ2+ cells from donor MAC-028 BCMA-TAC γδ T cell culture.*

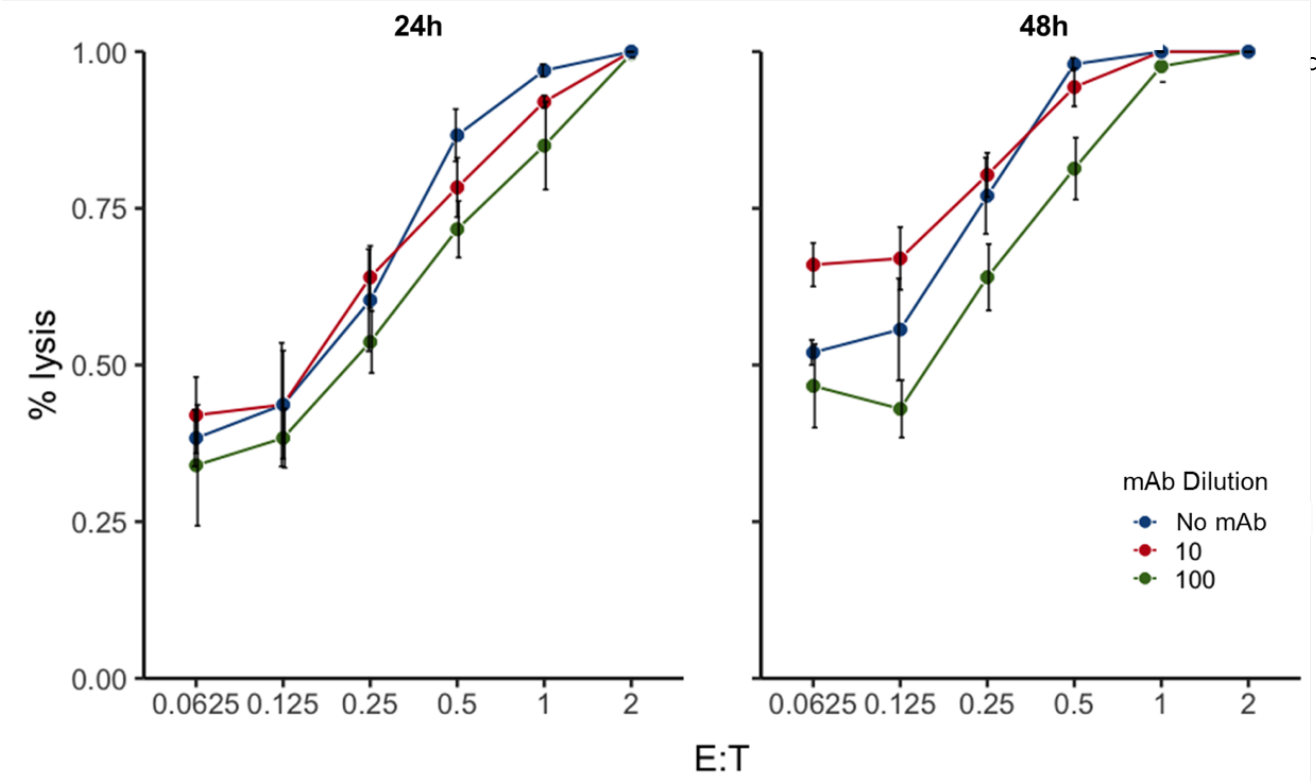

***Figure 21**: Daratumumab does not potentiate BCMA-TAC γδ T cells in vitro. BCMA-TAC γδ T cells were co-cultured with MM.1S and Daratumumab (anti-CD38 mAb) at 1:10 or 1:100 dilutions for luciferase-based in vitro cytotoxicity assay. Luminescence was recorded after 24 hours (**right**) and 48 hours (**left**).*

CD16 and TAC Stimulation

While our *ex vivo* non-transduced and BCMA-TAC γδ T cells express CD16, the functionality of surface expressed CD16 was unclear. We wanted to ensure that CD16 expressed on our manufactured γδ T cells was indeed functional. We performed a 4-hour plate-bound stimulation with an agonistic CD16 monoclonal antibody and assessed the dose-response of CD107a mobilization and TNFα expression to stimulation (Fig 22). We observed a dose-dependent response of the γδ T cell culture to CD16 stimulation for both CD107a mobilization and TNFα expression (Fig 22A). The highest CD16 stimulation had similar proportions of CD107a+ and TNFα+ γδ T cells as the proportion of CD16+ γδ T cells in the non-stimulated culture (Fig 22B), suggesting this CD16 concentration likely stimulates all CD16+ γδ T cells in culture.

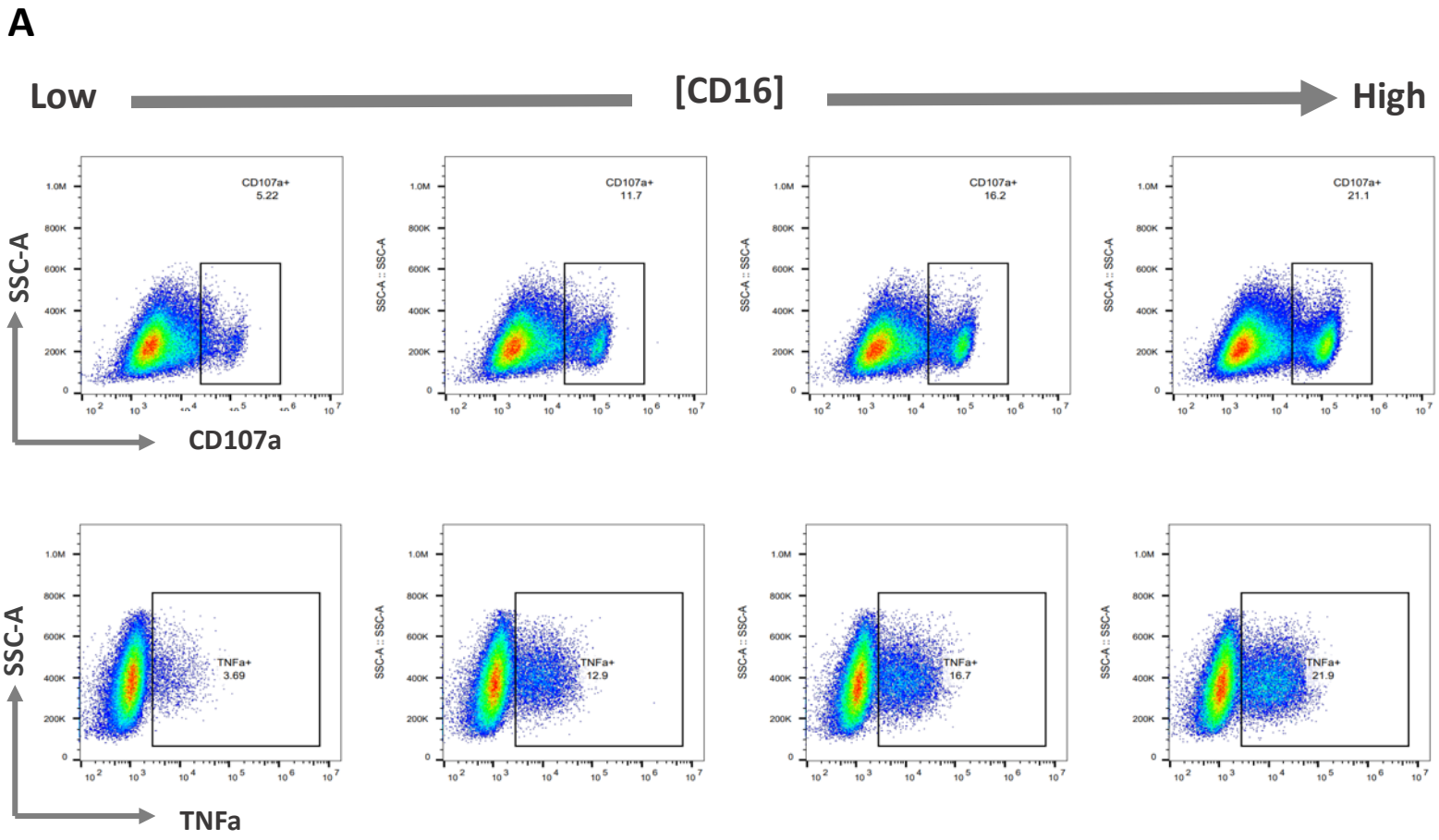

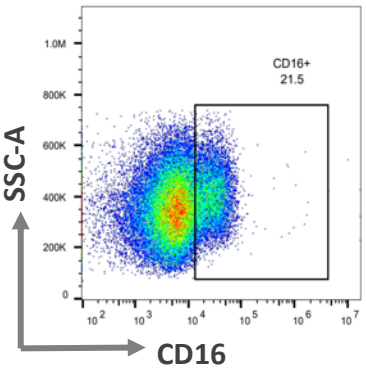

Figure 22: *Ex vivo manufactured γδ T cells can respond to CD16 stimulation.* ***A)*** *γδ T cell CD107a or TNFα expression 4h post-stimulation of non-transduced γδ T cells with plate-bound agonistic CD16 mAb bound at 10, 25, 50, or 100 ng/μL concentrations.* ***B)*** *CD16 expression in the unstimulated non-transduced γδ T cell culture.*

A

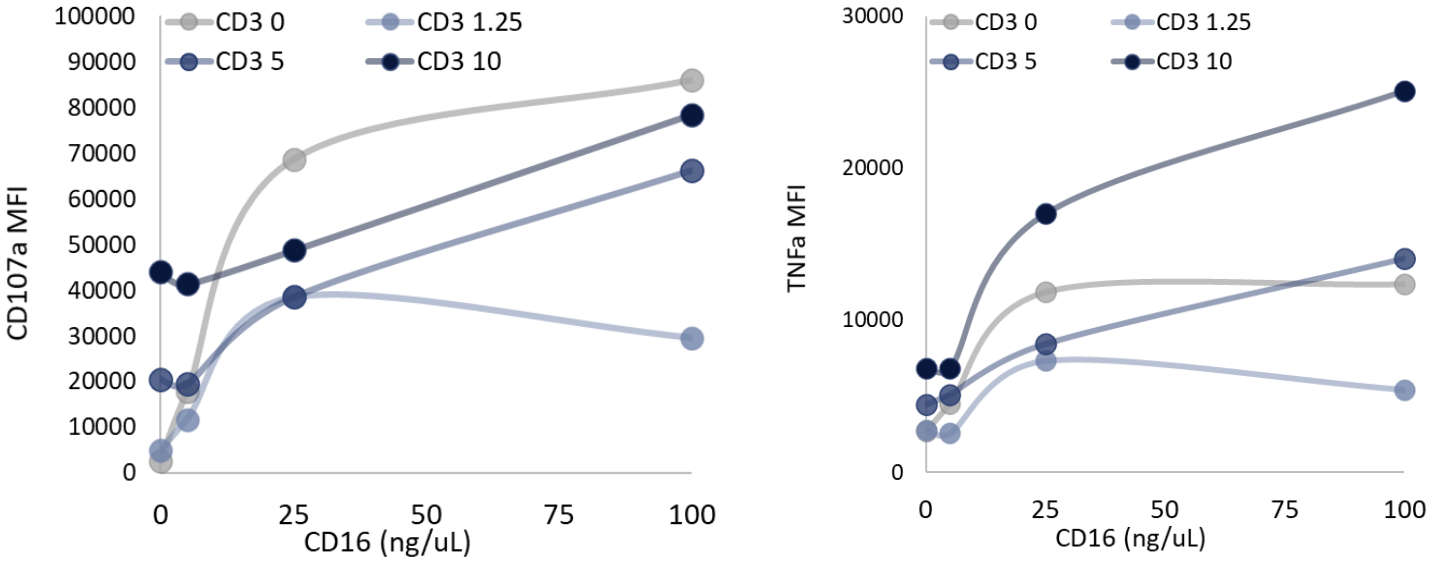

B

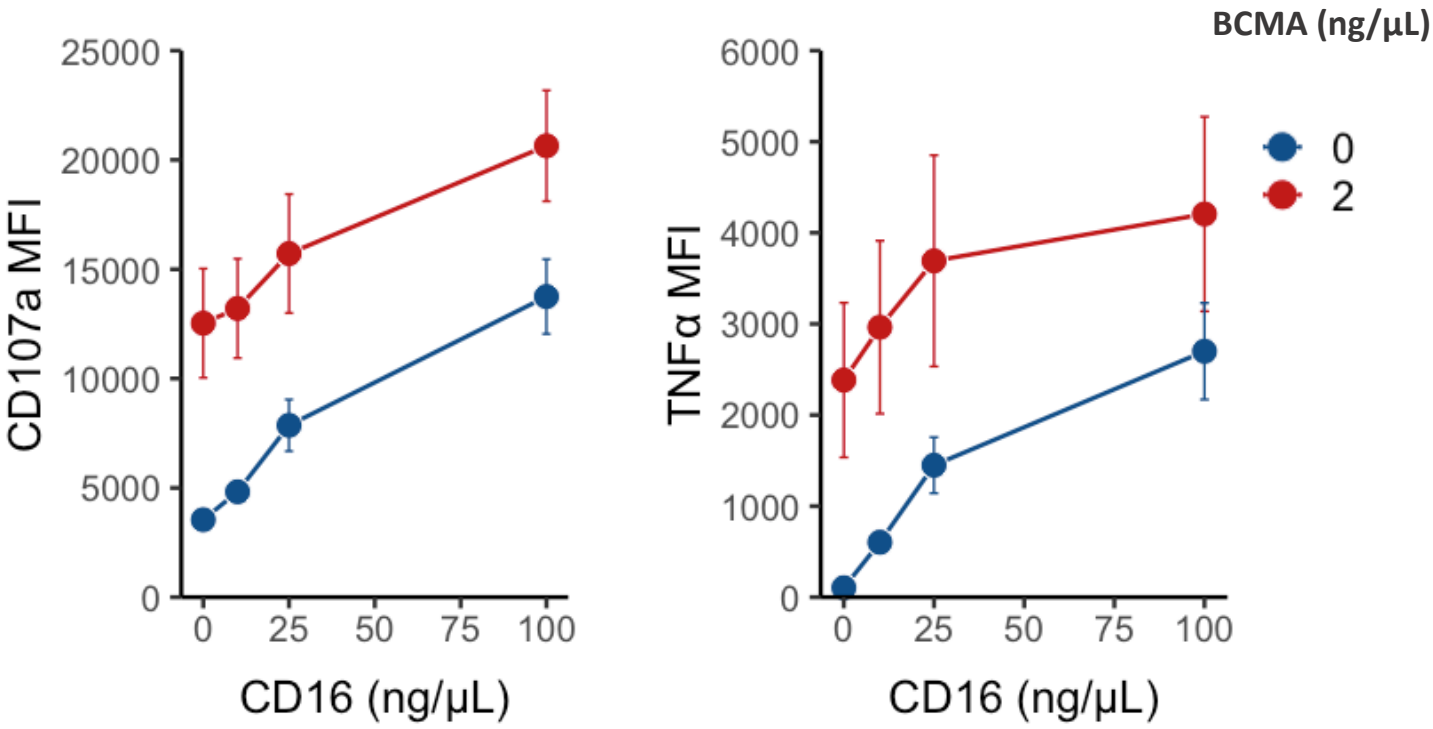

***Figure 23**: Effector functions of TAC or CD3 stimulated γδ T cells can be enhanced by CD16 stimulation. **A)** CD107a and TNFα mean fluorescence intensity (MFI) in Vδ2+ cells from a non-transduced γδ T cell culture stimulated for 4 hours with plate-bound UCHT-1 mAb bound at 0, 1.25, 5, or 10 ng/µL concentrations and CD16 mAb bound at 0, 10, 25, or 100 ng/µL concentrations. **B)** CD107a and TNFα MFI in Vδ2+ NGFR+ cells from a BCMA-TAC γδ T cell culture stimulated for 4 hours with plate-bound BCMA-Fc bound at 0 or 2 ng/µL concentrations, and CD16 bound at 0, 5, 25, or 100 ng/µL concentrations. Mean CD107a and TNFα were calculated from the performance of 6 donors' BCMA-TAC γδ T cell cultures.*

Next, we assessed the dual stimulation of non-transduced ex vivo manufactured γδ T cells with CD3 mAb (UCHT-1 clone) and agonistic CD16 mAb. UCHT-1 is the same clone used for the TAC anti-CD3 scFv. CD16 stimulation enhanced CD107a mobilization and TNFα expression in UCHT-1 stimulated cells in most cases (Fig 23.A). Despite benefit of CD16 agonism in most stimulations, low levels of CD16 stimulation (5ng/μL) have minimal impact or may be slightly inhibitory to γδ T cells exposed to higher concentrations of UCHT-1 stimulation (Fig 23.A). However, low levels of CD16 stimulation with low levels (1.25ng/μL) or no CD3 stimulation still boosts CD107a MFI in Vδ2+ γδ T cells. Furthermore, high CD16 stimulation (100ng/μL), in the presence of low CD3 stimulation (1.25 ng/μL) appears to be inhibitory to CD107a mobilization compared to moderate levels of CD16 stimulation (25ng/μL). However, high CD16 stimulation in low CD3 (1.25ng/μL) stimulations still improves CD107a mobilization compared to stimulations without CD16 (Fig 23A). These results demonstrate that CD16 can increase degranulation and TNFα cytokine production of CD3-stimulated γδ T cells, but dual stimulation with mixed high and low levels of CD16 or CD3 may dim CD107a and TNFα expression.

We also wanted to determine whether effector functions from TAC stimulation could be boosted by CD16 stimulation. FcγR affinity affected by polymorphisms, leading to reported donor differences in *in vitro* ADCC assays, as well as patient response to monoclonal antibody therapy[112]. Therefore, we attempted to maximize the number of CD16+ γδ T cell donors used in our *in* vitro functional assays. We screened 10 donors for CD16+ γδ T cell population and selected 7 CD16+ donors for large-scale γδ T cell manufacturing for functional assays. We first assessed whether TAC stimulation via plate-bound BCMA antigen could be enhanced by direct stimulation of CD16 using an agonistic CD16 mAb in a plate-bound assay repeated across 6

donors (Fig 23.B). There appears to be a dose-dependent response of CD16 in BCMA-TAC γδ T cells whether dual stimulated with BCMA and CD16 or stimulated with CD16 alone. The dose-response of CD16 on degranulation of γδ T cells is more pronounced in BCMA-TAC γδ T cells stimulated with CD16 alone, as demonstrated by significant differences between all CD16 stimulation conditions in the absence of BCMA stimulation (Table 3). While BCMA stimulated BCMA-TAC γδ T cells following a similar dose-response trend to CD16 stimulation, there is only a significant difference in degranulation between BCMA-TAC γδ T cells stimulated with BCMA alone and dual stimulated with the highest CD16 concentration (100 ng/µL) (Table 3). However, these results confirm that CD16 can enhance BCMA-TAC γδ T cell degranulation in the presence of robust CD16 signal. Similarly, there is a dose-dependent response of TNFα expression in response to CD16 stimulation in BCMA-TAC γδ T cells (Fig 23B). Dual stimulation of BCMA-TAC γδ T cells and CD16 also follow a similar dose-dependent response trend, albeit there is higher variance in response. Furthermore, CD16 boosting of TNFα expression appears to plateau between 25ng/µL and 100ng/µL in BCMA stimulated cells (Fig 23B). However, none of the CD16 agonism conditions comparisons reach statistical significance for TNFα production in BCMA stimulated cells (Table 4), likely in part due to high variation in TNFα response following dual stimulation. Overall, the results demonstrate that BCMA-TAC γδ T cells can have increased degranulation when dual stimulated via CD16 and the TAC receptor, but that robust differences in engineered γδ T cell response requires high level of CD16 stimulation.

Table 3: T-test results comparing NGFR+ CD107a MFI in samples stimulated with differing concentrations of plate-bound CD16.

BCMA (ng/µL)	y	CD16 (ng/µL) group1	CD16 (ng/µL) group2	n1	n2	df	p	p.signif
0	NGFR+ CD107a MFI	0	10	6	6	7.10	0.004	**
		0	25	6	6	5.12	0.014	*
		0	100	6	6	5.06	0.002	**
		10	25	6	6	5.54	0.05	*
		10	100	6	6	5.26	0.003	**
		25	100	6	6	8.90	0.02	*
2	NGFR+ CD107a MFI	0	10	6	6	9.91	0.846	ns
		0	25	6	6	9.93	0.409	ns
		0	100	6	6	10.00	0.046	*
		10	25	6	6	9.69	0.495	ns
		10	100	6	6	9.88	0.054	ns
		25	100	6	6	9.95	0.215	ns

Table 4: T-test results comparing NGFR+ TNFα MFI in samples stimulated with differing concentrations of plate-bound CD16.

BCMA (ng/µL)	y	CD16 (ng/µL) group1	CD16 (ng/µL) group2	n1	n2	df	p	p.signif
0	NGFR+ TNFa MFI	0	10	6	6	9.98	0.011	*
		0	25	6	6	6.26	0.006	**
		0	100	6	6	5.43	0.004	**
		10	25	6	6	6.38	0.04	*
		10	100	6	6	5.47	0.01	**
		25	100	6	6	8.03	0.075	ns
2	NGFR+ TNFa MFI	0	10	6	6	9.88	0.659	ns
		0	25	6	6	9.16	0.386	ns
		0	100	6	6	9.51	0.212	ns
		10	25	6	6	9.63	0.638	ns
		10	100	6	6	9.86	0.405	ns
		25	100	6	6	9.93	0.751	ns

BCMA-TAC γδ T cells and Tumour Cell Co-Culture with Daratumumab

Given that dual CD16 and TAC stimulation enhanced degranulation in BCMA-TAC γδ T cells, we wanted to determine whether Daratumumab opsonized BCMA+ tumour targets would enhance BCMA-TAC γδ T cell effector functions. We selected 7 tumour cell lines for investigation with varying expression levels of CD38 and BCMA (Fig 24). The K562 tumour cell line is a negative control, lacking both CD38 and BCMA expression. KMS-11 is a negative control

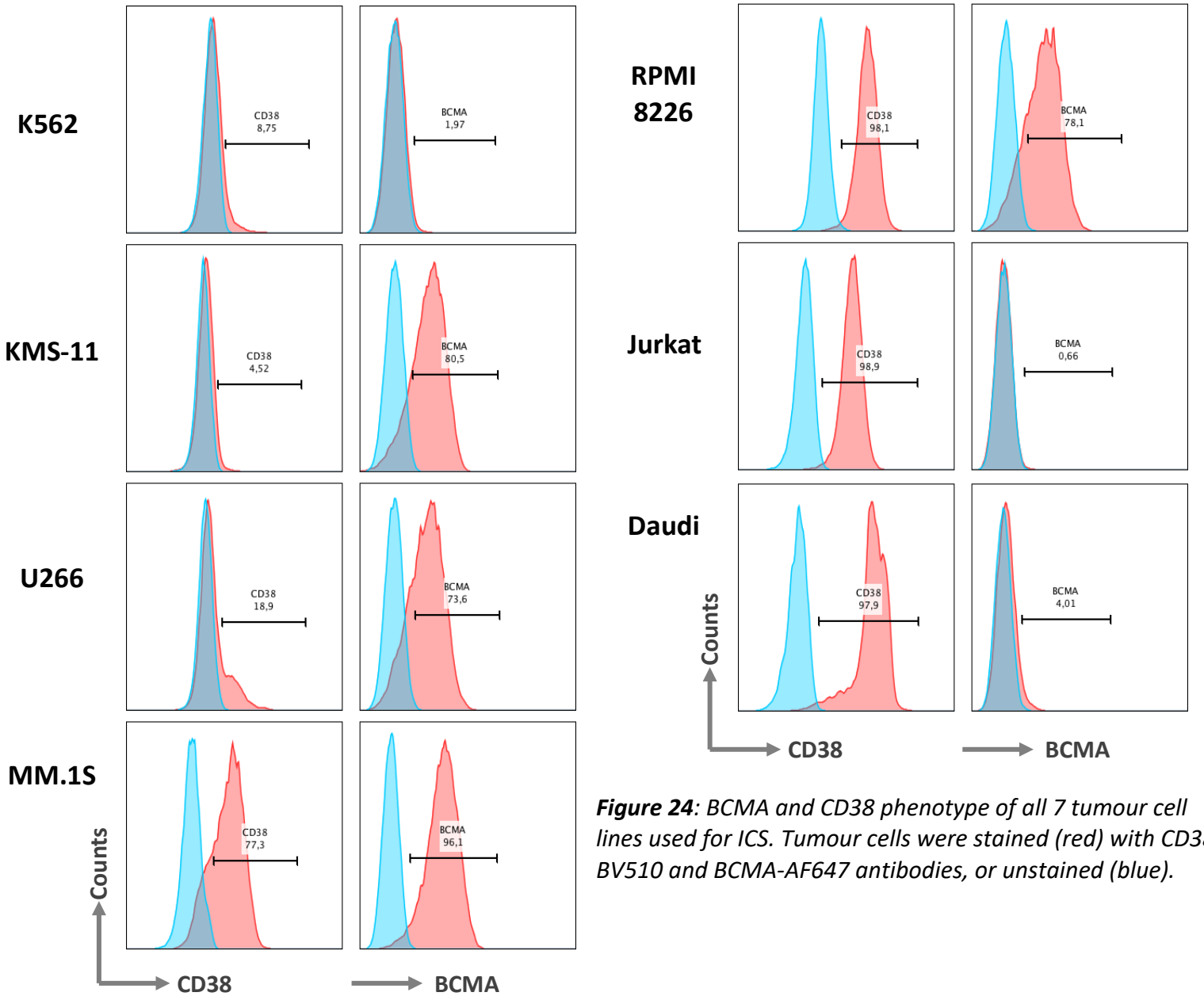

***Figure 24**: BCMA and CD38 phenotype of all 7 tumour cell lines used for ICS. Tumour cells were stained (red) with CD38-BV510 and BCMA-AF647 antibodies, or unstained (blue).*

for daratumumab in TAC stimulated γδ T cells because it lacks CD38 but expresses BCMA. Jurkat is a positive control for daratumumab stimulation alone because it expresses CD38 and lacks BCMA. Daudi cells were BCMA- in our phenotype assay, however, have been reported as BCMA low in the literature [113,114]. RPMI-8226, MM.1S and U266 all represent tumour cell lines with variable expression of CD38 and BCMA (Fig 24).

The Daratumumab tumour ICS was initially tested using non-transduced γδ T cells. Daratumumab was added to MM.1S tumour cells 30 minutes prior to the addition of γδ T cells for 4 hours and remained in the co-culture for the duration of the entire 4-hour stimulation. Daratumumab was added to MM.1S tumour cells at concentration between 20 – 400µg (Fig 25A), or without Daratumumab (Fig 25A, right). Opsonization of tumour targets with Daratumumab led to up to 20% of NT γδ T cells mobilize CD107a to their surface membrane, however there was an unexpected inverse relationship where higher Daratumumab concentrations led to lower degranulation (Fig 25A). Daratumumab tumour ICS was also performed for gRV-BCMA-TAC#1195 γδ T cells in the pilot experiment with a single amount of Daratumumab – 200µg (Fig 22B). There appeared to be a modest 1.5% increase in degranulation of BCMA-TAC γδ T cells in response to Daratumumab opsonized MM.1S tumour cells, however this increase could be the result of random variation (Fig 25B).

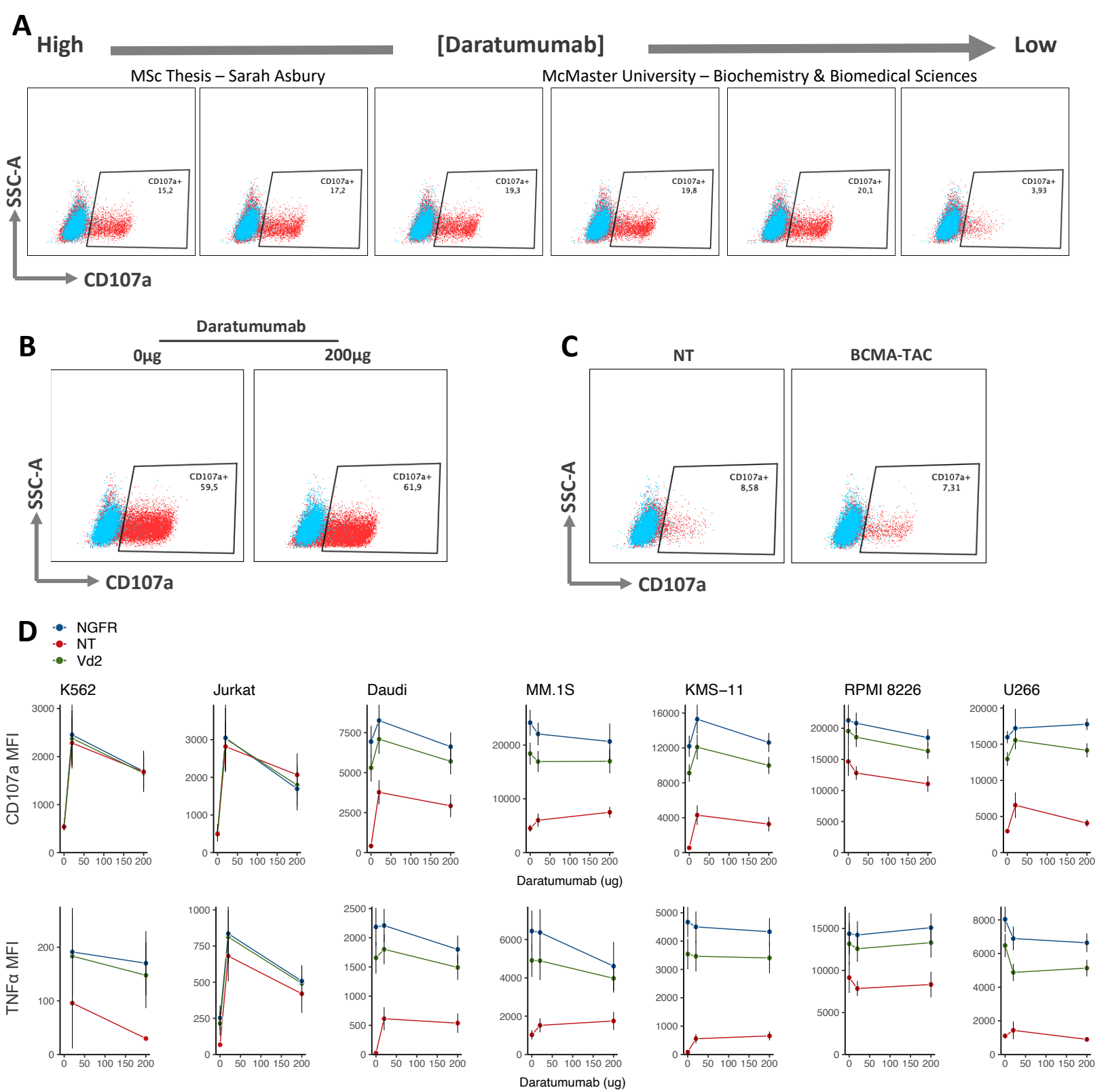

***Figure 25**: Daratumumab has an unexpected or no effect on non-transduced and BCMA-TAC γδ T cells effector functions when co-cultured with several hematological tumour cell lines. **A)** CD107a mobilization in Vδ2+ cells from NT γδ T cell cultures stimulated with MM.1S and Daratumumab for 4 hours. Daratumumab was added at 400, 200, 80, 40, 20, or 0 µg per well (left to right). γδ T cells and tumour cells were co-cultured at a 1:1 ratio. **B)** CD107a mobilization in Vδ2+ cells from BCMA-TAC γδ T cultures stimulated with MM.1S and Daratumumab for 4 hours. 200µg (left) or 0 µg (right) Daratumumab was added to each well. Cells were co-cultured at a 1:1 ratio. **C)** Non-specific CD107a mobilization from NT or BCMA-TAC γδ T cells incubated for 4 hours with Daratumumab alone. **D)** CD107a mobilization in NGFR+ Vδ2+ cells from BCMA-TAC γδ T cells co-cultured with 7 tumour cell lines for 4 hours. γδ T cells and tumour cells were co-cultured at a 1:1 ratio, except Daudi cells which were co-cultured at a 1:0.5 E:T ratio. Mean CD107a and TNFα were calculated from the performance of 6 – 7 donors' BCMA-TAC γδ T cell cultures.*

BCMA-TAC and NT γδ T cells were also incubated in the presence of Daratumumab alone for 4 hours to assess the effect of excess soluble Daratumumab on degranulation. Daratumumab alone leads to 7 – 8% of γδ T cells degranulating (Fig 25C). While Daratumumab tumour opsonization appeared to lead to robust degranulation in NT γδ T cells, the effect in BCMA-TAC γδ T cells was modest. However, degranulation of BCMA-TAC γδ T cells is substantially higher in response to tumour-derived BCMA (59.5%) (Fig 25B), than from plate-bound BCMA stimulation (20 – 30%) (data not shown). Consequently, it could be possible that any benefit of CD16 signalling via Daratumumab is superseded by exceptionally robust TAC signalling.

Next, we assessed the effect of Daratumumab in tumour co-cultures using several donors and tumours with varying expression of BCMA and CD38 to further understand whether Daratumumab could benefit the BCMA-TAC γδ T cell tumour response. Tumour cells were pre-incubated with 0, 20 or 200μg of Daratumumab for 30 minutes, and then BCMA-TAC γδ T cells were added for 4 hours. Daratumumab was left in the tumour co-culture for the duration of the entire 4-hour stimulation. Each tumour co-culture condition was repeated for BCMA-TAC γδ T cells derived from 6 – 7 donors. The results of the Daratumumab tumour ICS suggests that there is a minimal or no impact of Daratumumab on degranulation and cytokine production for BCMA-TAC γδ T cells co-cultured with several BCMA+ CD38+ tumours (Fig 25.D). We also observed non-specific enhancement of degranulation in Daratumumab cultures in CD38- tumours (Fig 25D). In BCMA+ CD38+ tumours MM.1S and RPMI-8226 co-cultures, Daratumumab appears to result in a modest decrease in BCMA-TAC γδ T cell degranulation and

cytokine production. BCMA-TAC γδ T cells co-cultured with KMS-11 appears to benefit from the addition of Daratumumab in culture, despite being a CD38- tumour cell line (Fig. 25D). Daudi cells and U226 are both CD38+ cell lines where BCMA-TAC γδ T cells degranulation is enhanced by addition of low concentration Daratumumab to the co-culture, although TNFα cytokine production in response to U266 co-culture is diminished by the addition of Daratumumab. While BCMA-TAC γδ T cells had enhanced degranulation and TNFα cytokine production in response to Jurkat cells – the positive control for Daratumumab stimulation – there was a similar degranulation response as in K562 tumour cells – the negative control for both BCMA-TAC and Daratumumab stimulation (Fig 25D). Given these conflicting results, we were concerned the concentration of Daratumumab was too high, leading to high concentrations of excess unbound Daratumumab causing degranulation. This is based on our previous observation that γδ T cell cultures incubated with Daratumumab alone have CD107a mobilization (Fig 25.C). This could explain why we observed increased degranulation in K562 and KMS-11 co-cultures with Daratumumab. Overall, the effect of Daratumumab is difficult to interpret from the Daratumumab tumour ICS in Fig 25 because the experimental setup did not account for the effects of excess Daratumumab.

We attempted to improve the experimental setup of the tumour ICS by using pre-loading Daratumumab and assessing the binding at each concentration for each tumour cell line. We assessed the amount of antibody bound when tumour cells were incubated for 30 minutes with several amounts of Daratumumab between 0.3 – 200µg (Fig 26). Daratumumab binding was detected using anti-huIgG-PE.

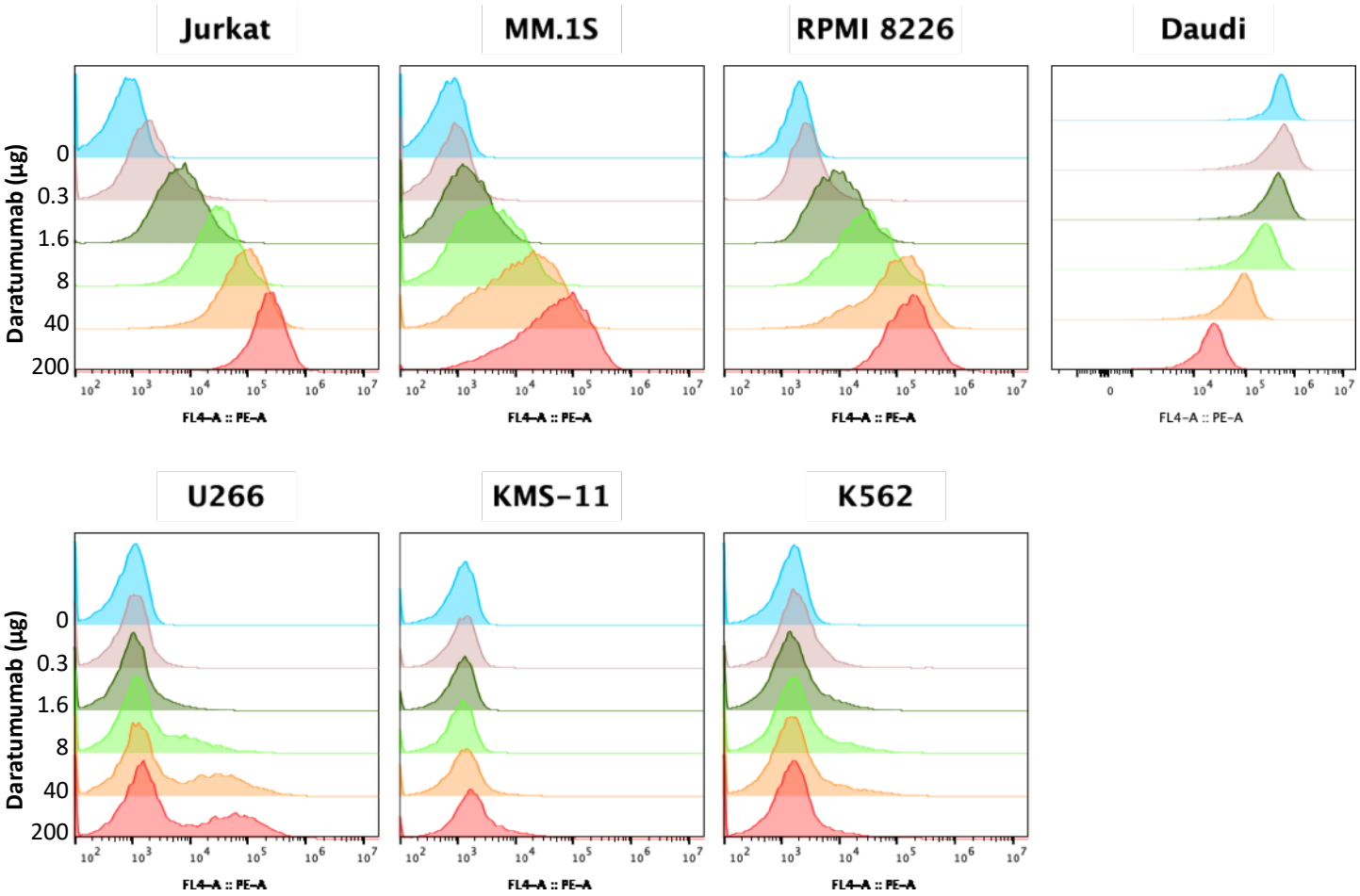

Figure 26*: Daratumumab binding to each tumour cell lines used for ICS. Tumour cells were incubated for 30 minutes in Multiple Myeloma media with Daratumumab added at varying concentrations. Daratumumab binding was detected using an anti-human IgG-PE antibody.*

Jurkat, MM.1S, and RPMI 8226 all demonstrate high level of Daratumumab binding (Fig 26). U266 has Daratumumab binding in a subset of the tumour cells (Fig 26), as CD38 is only expressed in a subset of U266 cells (Fig 24). A small amount of PE signal is present in all K562 samples. Given that the signal is present even at low levels of Daratumumab, it is unlikely to be non-specific Daratumumab binding (Fig 26). KMS-11 also has a minimal shift in PE at the highest level of Daratumumab, which may be non-specific Daratumumab binding at high concentrations (Fig 26). Finally, Daudi cells have an unusual PE signal pattern. The huIgG-PE antibody appears to be binding to Daudi cells in the absence of Daratumumab, and this signal

decreases with the addition of Daratumumab. Daudi cells are not considered surface IgG+, but they are surface IgM+ and IgD+[115]; the unexpected PE signal may be a result of cross-reactivity of the hu-IgG antibody with surface immunoglobulin expressed by Daudi cells. A pilot experiment Daratumumab tumour ICS experiment was run using Daratumumab pre-loaded for 30 minutes, and then washed with PBS to remove unbound excess antibody. The same Daratumumab binding conditions and concentrations used in the binding assay (Fig 26) were used in the tumour ICS (Fig 27). As previously observed in MM.1S (Fig 25B), the effect of Daratumumab on TAC stimulated γδ T cell degranulation was modest in CD38+ tumour cells, MM.1S and RPMI 8226. However, there did not appear to be a dose-dependent effect of Daratumumab. BCMA-TAC γδ T cell degranulation from CD16 alone was also observed in Jurkat cells. The difference of Daratumumab presence and absence on BCMA-TAC γδ T cell degranulation in co-cultures is more pronounced in Jurkats than the BCMA+ tumour cell lines, with 7 – 9% higher degranulation in Daratumumab conditions (Fig 27). This may suggest that robust TAC signalling signal supersedes the benefits provided by CD16 agonism, causing CD16 signalling to become redundant. Despite pre-loading Daratumumab, we observed similar levels of degranulation in the K562 CD38- control and Jurkat CD38+ control, indicating there was no CD38-specific effect of Daratumumab. This result was unexpected and makes it difficult to accurately interpret the results of the tumour ICS. It is possible that Daratumumab is binding to the plate during the 30-minute incubation with tumour cells – as the incubation is performed at 37°C. Plate-bound daratumumab may stimulate CD16 and induce degranulation of BCMA-TAC γδ T cells irrespective of interaction with tumour cells.

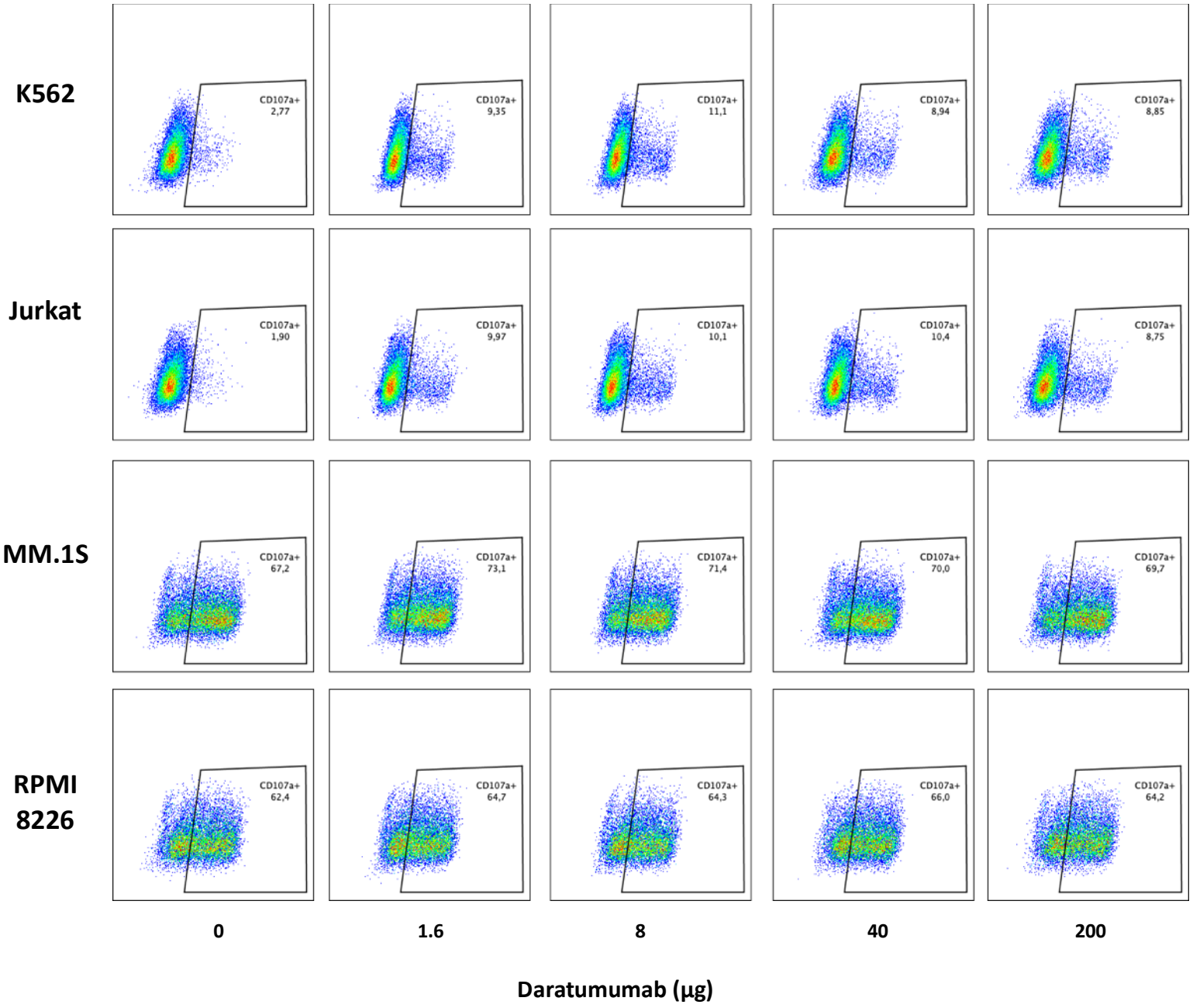

***Figure 27**: CD107a mobilization from daratumumab BCMA-TAC γδ T cell tumour ICS using pre-loaded Daratumumab. Tumour cells were incubated with Daratumumab for 30 minutes in Multiple Myeloma media. Excess soluble Daratumumab was removed by PBS wash. Daratumumab-bound tumour cells were co-cultured with BCMA-TAC γδ T cells at a 1:1 ratio for 4 hours. CD107a mobilization of NGFR+ Vδ2+ cell is shown here.*

CD16+ γδ T Cell Model Feature Prediction

We collected extensive phenotyping data of δ T cell cultures from the CD16 Donor screening manufacturing experiment – and the subsequent 7 donor Large-scale NT and gRV-BCMA-TAC#1195 manufacturing for CD16+ γδ T cell donors. 6 out of 7 donors in the Large-scale manufacturing experiment (Experiment 2; Fig 25A) were also analyzed in the CD16 Donor screening experiment (Experiment 1; Fig 25A). Using the data from the donor screening and large-scale manufacturing experiments, we wanted to analyze the determinants of CD16+ γδ T cell expression across donors. The large-scale donor manufacturing run included both NT and BCMA-TAC γδ T cell cultures for each donor. There was high correspondence between donor CD16 expression in the donor screening manufacturing run and the large-scale manufacturing run, regardless of whether cultures were NT (Fig 28A; $R = 0.86$, $p = 0.027$) or transduced (Fig 28A; $R = 0.86$, $p = 0.029$). Within the same manufacturing experiment, the correspondence of CD16 expression was even higher between NT and transduced cultures from the same donor (Fig 28A; $R = 0.99$, $p < 0.001$). These results indicate that CD16 expression is primarily donor-dependent feature but can vary between manufacturing runs.

We performed extensive phenotyping of cultures from the donor screening experiment. PBMCs from D0 were phenotyped for percentage of: αβ T cell, γδ T cells, γδ T cell CD16 expression, NK cells, and monocytes. Day 14 γδ T cell cultures in the Donor Screening experiment were also phenotyped for: αβ T cells, Vδ2 T cells, CD16 expression, CD56 expression, CD27 expression, and DAP12 expression. D14 culture fold expansion was also calculated for these cultures. To determine whether any PBMC (D0) variables could be used as biomarkers to predict CD16 expression, and to assess the nature of the D14 γδ T cell

phenotype, we used Spearman correlation analyses, Stepwise Forward Regression (Gaussian), and Generalized Linear Models (Beta regression). Stepwise Forward Regression is a feature selection algorithm for linear models which systematically adds predictor variables to an initially null linear model, and assesses which variables have the largest impact on model accuracy at each step[116]. The top performing models are returned from the algorithm. From these, the best model was selected using the Mallow's Cp statistic, which is calculated using the Residual Sum of Squares and a variable that penalizes large numbers of predictor variables, ensuring only impactful features are maintained in the model (Fig 25C)[116]. The significance of features selected during stepwise linear regression were validated using a linear model (Fig 25C). Linear models are limited to only detecting linear relationships. Given that our response variable (% D14 CD16+) is bounded by a range of 0 to 1, also used a Generalized Linear Model with a beta distribution – beta regression – to determine whether any predictor variables contribute significantly to the model (Table 6).

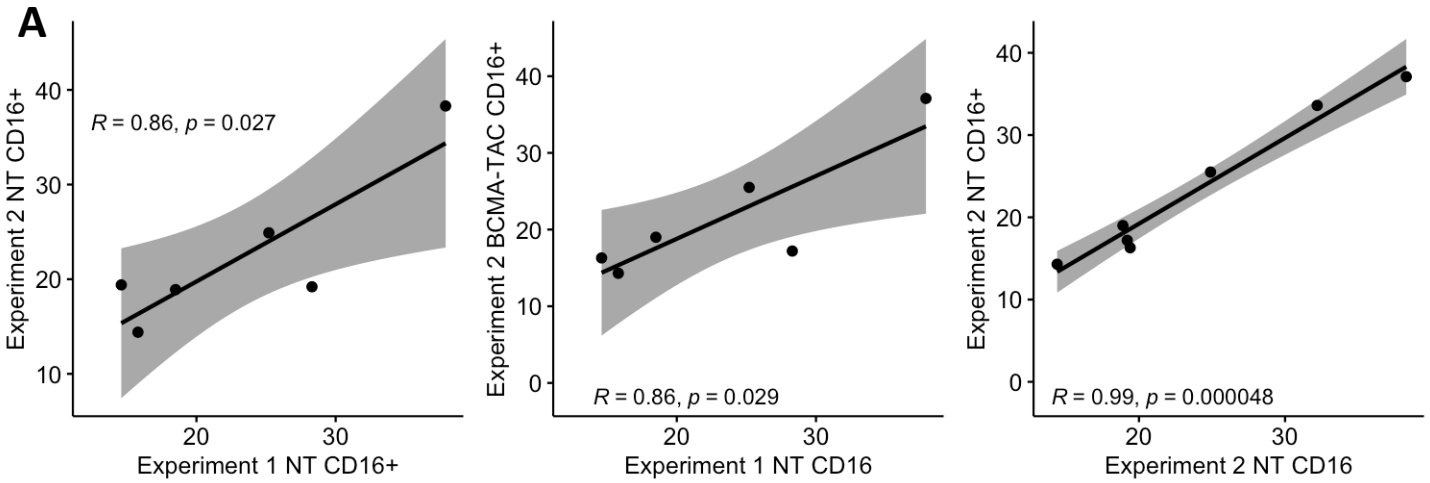

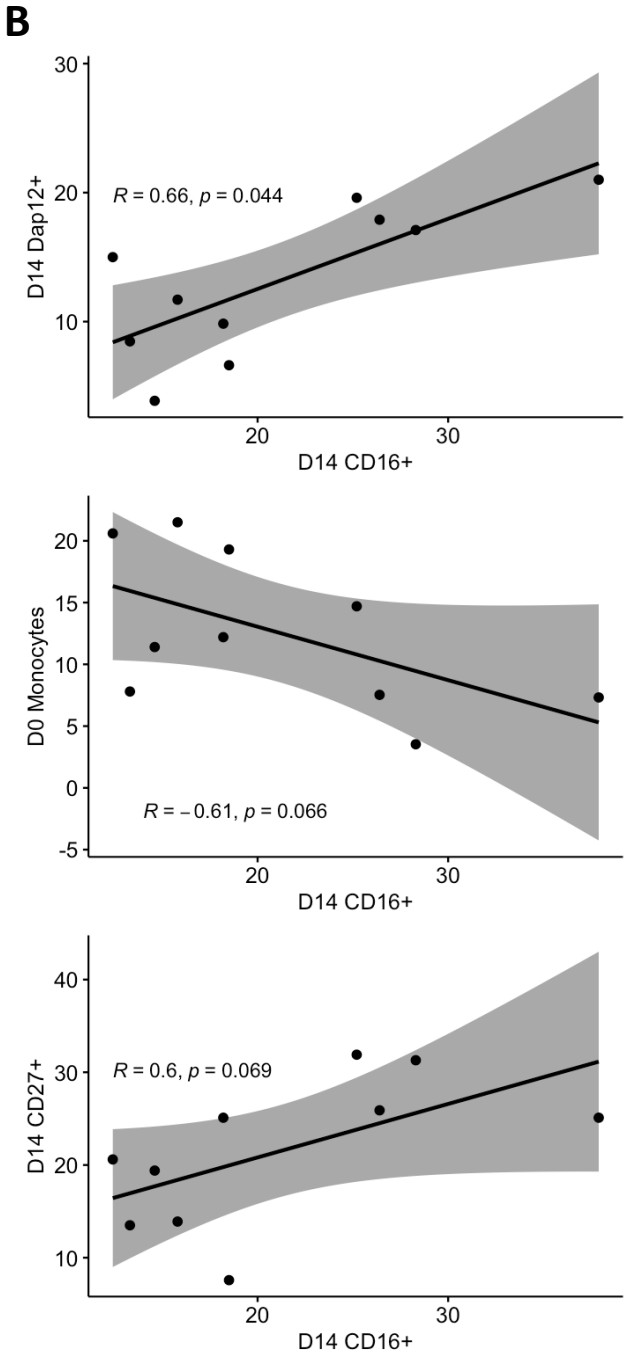

C

Step-wise Forward Regression

Characteristic	Beta	95% CI[1]	p-value
D14.vd2.Dap12_pos.nt	1.1	0.32, 1.8	0.011

[1]CI = Confidence Interval

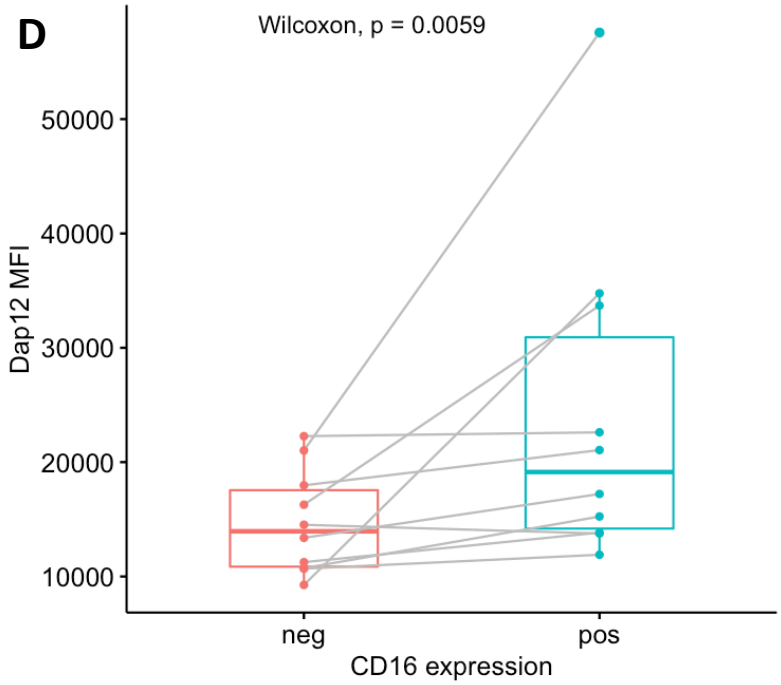

***Figure 28**: CD16 expression is a feature of donor expression. CD16+ γδ T cells have higher DAP12 expression compared to CD16- γδ T cells. CD16+, Monocytes, and CD27+ metrics are % of singlets from Flow Cytometry data. **A)** Day 14 Vδ2 CD16+ expression is a donor-dependent feature, with high correlation (Pearson) of donor CD16 expression between independent donor screening and large-scale manufacturing experiments and transduced or NT cultures. **B)** Culture Day 14 CD16 expression was correlated (Spearman) with several predictor variable (Table 5). Highest p-values variables are reported. No correlations survived Benjamini-Hochberg (BH) correction (Table 5). **C)** Feature selection predicting D14 Vδ2 CD16+ (%) using Stepwise Forward Regression. Full variable set before feature selection equivalent to those used in General Linear Modelling (Table 6) **D)** Pairwise comparison by donor of DAP12 expression in CD16+ and CD16- Vδ2 cells from Day 14 γδ T cell culture using Wilcoxon test.*

None of the Spearman correlations between D0 or D14 culture features and CD16 expression survived multiple comparisons correction (Table 5), however top correlations (non-significant) included D14 DAP12 expression, D14 CD27 expression, and a negative relationship with the proportion of D0 monocytes. Stepwise Forward Regression confirmed that D14 Vδ2 DAP12 expression was the most important predictor variable and was the only predictor variable included in the best model (Fig 28C). The results of the stepwise forward regression were validated by generating a linear model predicting D14 CD16 expression using only D14 DAP12 expression, which confirmed a positive relationship between CD16 and DAP12 expression ($p = 0.011$) (Fig 28C). Beta regression using only 1 predictor variable in each model also confirmed that D14 Vδ2 DAP12 has a significant positive relationship to D14 Vδ2 CD16 expression. None of the PBMC (D0) culture feature predictor variables were present in the best Stepwise Forward Regression model (Fig 28C) or significant in the beta regression models (Table 6). A greater number of observations may improve the statistical detection of observed trends, particularly for D0 monocytes. However, it also may not be possible to predict D14 CD16 expression from PBMC composition alone. Other biological metrics, such as gene expression of γδ T cells in starting PBMCs, may provide better biomarkers for predicting CD16 expression at the end of culture.

Given that the percentage of D14 Vδ2 DAP12 cells was associated with CD16+ Vδ2 T cells, we wanted to further investigate DAP12 expression in D14 γδ T cell cultures. The MFI of DAP12 was compared within CD16+ and CD16- γδ T cells from D14 culture. We found that DAP12 has higher expression in CD16+ γδ T cells compared to CD16- cells of the same culture (Fig 28D; $p = 0.006$).

Correlation Pair		R	p.adj
D14 Vδ2 CD16+ (%)	D14 Vδ2 Dap12+ (%)	0.66	0.48864891
	D0 Monocytes (%)	-0.61	0.77963785
	CD14 Vδ2 CD27+ (%)	0.60	0.89902597
	D0 γδ+ (%)	0.44	1
	D0 NK Cells (%)	-0.43	1
	D0 CD16 MFI (%)	-0.33	1
	D0 CD3+ (%)	0.18	1
	D14 Vδ2 CD56+ (%)	-0.12	1
	Culture Fold Expansion	-0.09	1
	D14 Vδ2+ (%)	-0.08	1
	D0 αβ+ (%)	-0.05	1
	D14 αβ+ (%)	-0.03	1
	D14 CD3+ (%)	0.02	1

Table 5: Pearson correlation between %D14 Vδ2 CD16+ and D0 or D14 culture features. Percentages are measured as % of singlets.

Culture Feature	Estimate	Std. Error	p
D14 Vδ2 Dap12+	0.064	0.017	0.003 *
D14 Vδ2 CD27+	0.037	0.015	0.093
D0 Monocytes	-0.041	0.020	0.177
D0 γδ+	0.101	0.056	0.230
D0 NK Cells	-0.042	0.033	0.557
D0 Vδ2 CD16 MFI	0.000	0.000	0.643
D0 CD3+	0.012	0.013	0.646
Culture Fold Expansion	0.030	0.040	0.736
D0 αβ+	0.008	0.013	0.758
D14 αβ+	0.020	0.041	0.758
D14 Vδ2+	-0.008	0.017	0.758
D14 CD3+	-0.004	0.023	0.858
D14 Vδ2 CD56+	-0.004	0.014	0.858

Table 6: Generalized Linear Models (Beta Regression) of D0 or D14 cultures features predicting D14 Vδ2 CD16+. Expression with BH correction. Percentages are measured as % of singlets.

Bulk RNA-Sequencing of CD16+ and CD16- γδ T Cell Fractions

While the effector functions and memory phenotype of CD16+ γδ T cells have been previously described, there has not yet been RNA sequencing analysis investigating the gene expression signature of CD16+ Vδ2 T cells. We performed bulk RNA-sequencing on CD16+ and CD16- fractions of Day 14 Vδ2 T cells from 4 distinct CD16+ donors in BCMA-TAC Zoledronate/IL-2 cultures. Cell fractions were generated by flow-sorting Vδ2+ CD16+/- cells. RNA was extracted immediately post-flow sort.

Principal Component Analysis (PCA) plot of PC1 and PC2 demonstrate that primary contribution to variation in γδ T cell CD16+ and CD16- transcriptomes is donor (Fig 29A). Donor differences were corrected for PCA visualization using the limma batch correction function to visualize the contribution of treatment condition alone to variation (Fig 29B). CD16+ and CD16- conditions cluster by condition when plotted on PC1 and PC2 (Fig 29B), indicating that treatment effects on gene expression is likely.

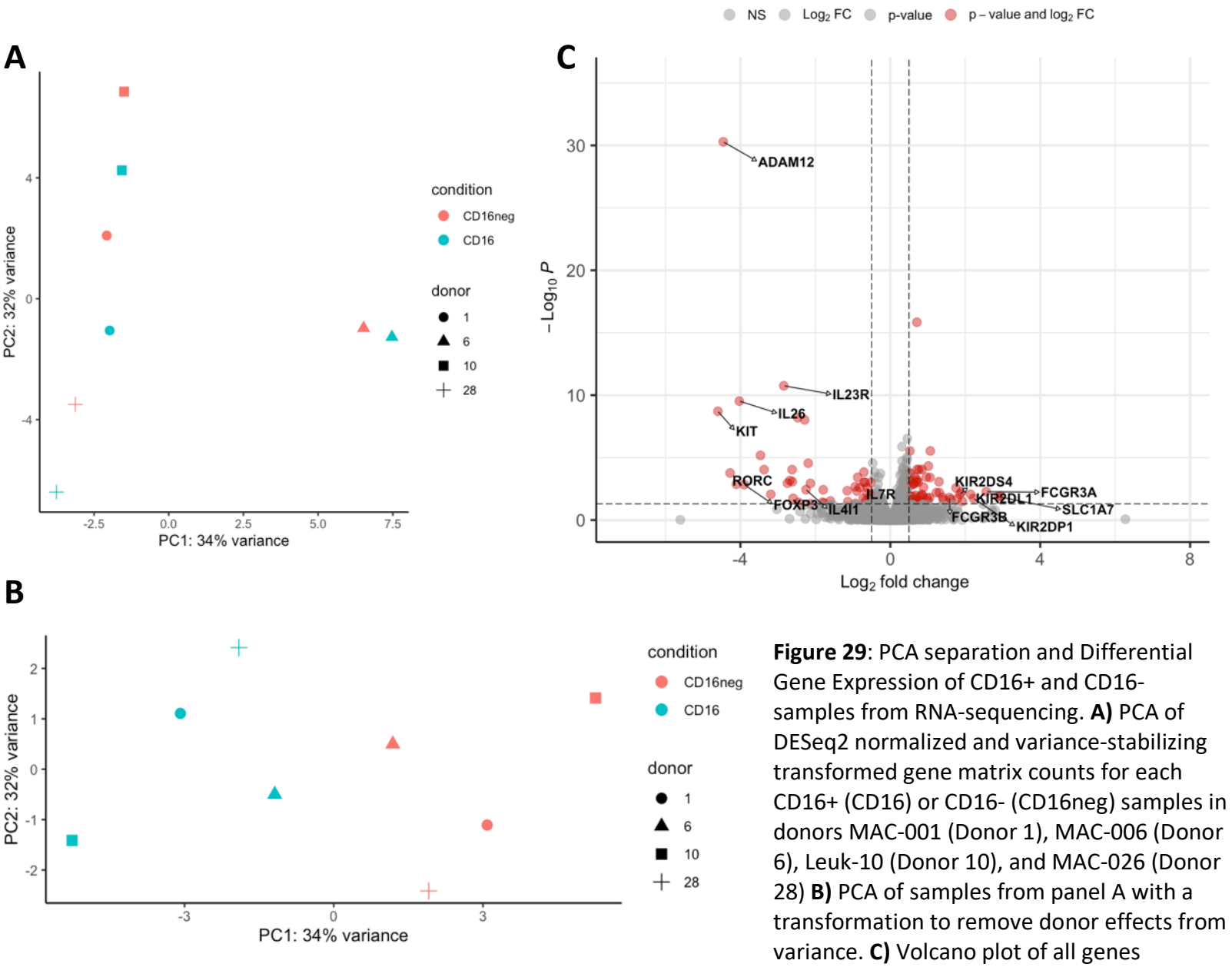

Figure 29: PCA separation and Differential Gene Expression of CD16+ and CD16- samples from RNA-sequencing. **A)** PCA of DESeq2 normalized and variance-stabilizing transformed gene matrix counts for each CD16+ (CD16) or CD16- (CD16neg) samples in donors MAC-001 (Donor 1), MAC-006 (Donor 6), Leuk-10 (Donor 10), and MAC-026 (Donor 28) **B)** PCA of samples from panel A with a transformation to remove donor effects from variance. **C)** Volcano plot of all genes detected via RNA-seq. DEG Cut-off: Benjamini-Hochberg adjusted p-value < 0.05 and |LFC| > 0.5.

Differentially expressed genes (DEGs) were identified using DESeq2 Likelihood Ratio Models with donor as a covariate. There were 100 DEGs (adjusted p-value < 0.05, |log2 Fold Change (LFC)| > 0.5) between the CD16+ and CD16- Vδ2 fractions (Fig 29C). Genes of immunological interest are labelled on the volcano plot; the full list of DEG is also available (Supplementary Table 1A/B). Both CD16 isoforms are upregulated in the CD16+ fraction, providing a proxy validation of the flow-sort and sequencing methods. In accordance with previous literature describing KIR expression on CD16+ Vδ2 T cell subsets[66], activating KIR2DS4, inhibitory KIR2DL1, pseudogene KIR2DP1, and KIR signalling adapter DAP12 (TYROBP) are upregulated in the CD16+ Vδ2 subset. The most highly upregulated gene is pseudogene NDUFA4P1 (Supplementary Table 1A). The second most highly upregulated gene in CD16+ Vδ2 sodium-independent glutamate transporter SLC1A7 (Supplementary table A)[117]. Glutamate metabolism is associated with both Th1 and Th17 differentiation of conventional CD4+ T cells upon stimulation[118]. However, the downregulation of several Th17 associated genes in conventional or γδ T cells – including RORC[119], IL-23R, IL-26[120], IL-7R[121], ADAM-12[122], and IL-4I1[123] – indicates that SLC1A7 may be upregulated in relation to changing metabolic demands related to Th1 differentiation (Fig 29A)[118]. Th17 γδ T cells are rare in humans, however they can be found in highly immunosuppressed environments, including tumours and granulomas[25,39,40]. The Th17 γδ T cell phenotype has properties of pro-tumour regulatory T cells, thereby contributing to the development and maintenance of human cancers[25]. Given that human γδ T cells differentiate in the periphery and maintain plasticity between Th1 and Th17 differentiation in the periphery[25], further polarization of immunotherapeutic γδ T cells towards cytotoxic anti-cancer Th1 phenotype may be therapeutically beneficial. In accordance with downregulation of

Th17-related genes in the CD16+ subset, T regulatory transcription factor Foxp3 is also supressed, and other Treg associated genes that overlap with Th17 differentiation (RORC[124] and IL4I[125]). Upregulated expression of Th17 and Treg-associated genes in CD16- γδ T cells was unexpected given that Leuk-10 BCMA-TAC γδ T cells, which are predominantly CD16- (Fig 15), release very low levels of IL-17 and IL-10 relative to Th1 cytokines when co-cultured with Multiple Myeloma tumour cells *in vitro* (Fig 19). This prompted us to investigate the normalized transcription count of Th17 and Treg associated transcription factors Foxp3 and RORC, along with Th1-associated transcription factor T-bet for reference, to ensure LFC of Th17 and Treg associated transcription factors (TFs) is not a consequence of low transcript counts slightly decreasing in CD16+ γδ T cells (Fig 30). Foxp3 normalized transcript counts – between 10^1 and 10^2 magnitudes, indicate that the transcript is lowly expressed, but not exceedingly rare. While RORC transcripts are between 10^2 and 10^3 (Fig 30) – indicating there may be substantial protein expression of the Th17-associated RORγ TF in a subset of γδ T cell cultures. Protein expression

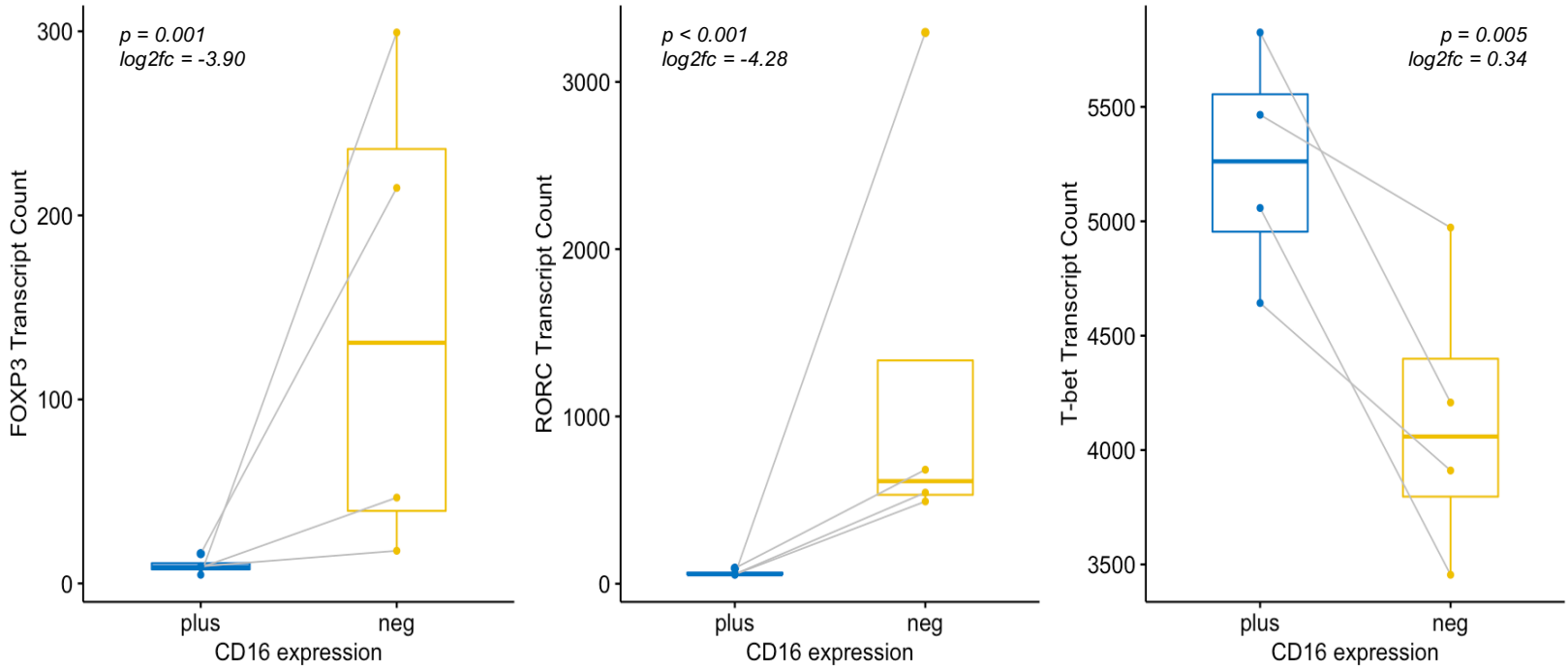

Figure 30: *Normalized transcript counts (DESeq2 normalization method) for FoxP3, RORC, and T-bet (TBX21). Log-fold change and DESeq2 LRT p-value of CD16+ vs. CD16- comparison are reported for each gene.*

of RORγ and Foxp3 should be experimentally validated to assess the magnitude of regulatory or Th17 γδ T cell subset in culture, as these subsets could negatively impact cancer immunotherapy applications.

Based on the list of 100 DEGs, there were 5 predicted transcription factors when analyzed using the Dorothea database (Supplementary Fig 1). The genes associated with dorothea predicted TFs do not have unidirectional up/downregulated LFCs (Supplementary Fig 1B – C). Despite this, genes associated with downregulated TF STAT1 – a Th17-associated TF[126] – appear to be mostly downregulated, especially Foxp3 (Supplementary Fig 1A). However, the DEG list was also analyzed with another transcription factor prediction method – TFEA.ChIp – which uses a GSEA algorithm and a transcription factor database curated from ChIp experiments annotated by cell types. TFEA.CHIP did not return any significantly enriched TFs after multiple comparisons correction (data not shown). The inconsistency of LFC directionality and lack of reproducibility between prediction tools likely indicates our DEG list is too short (n = 100) for meaningful TF predictions.

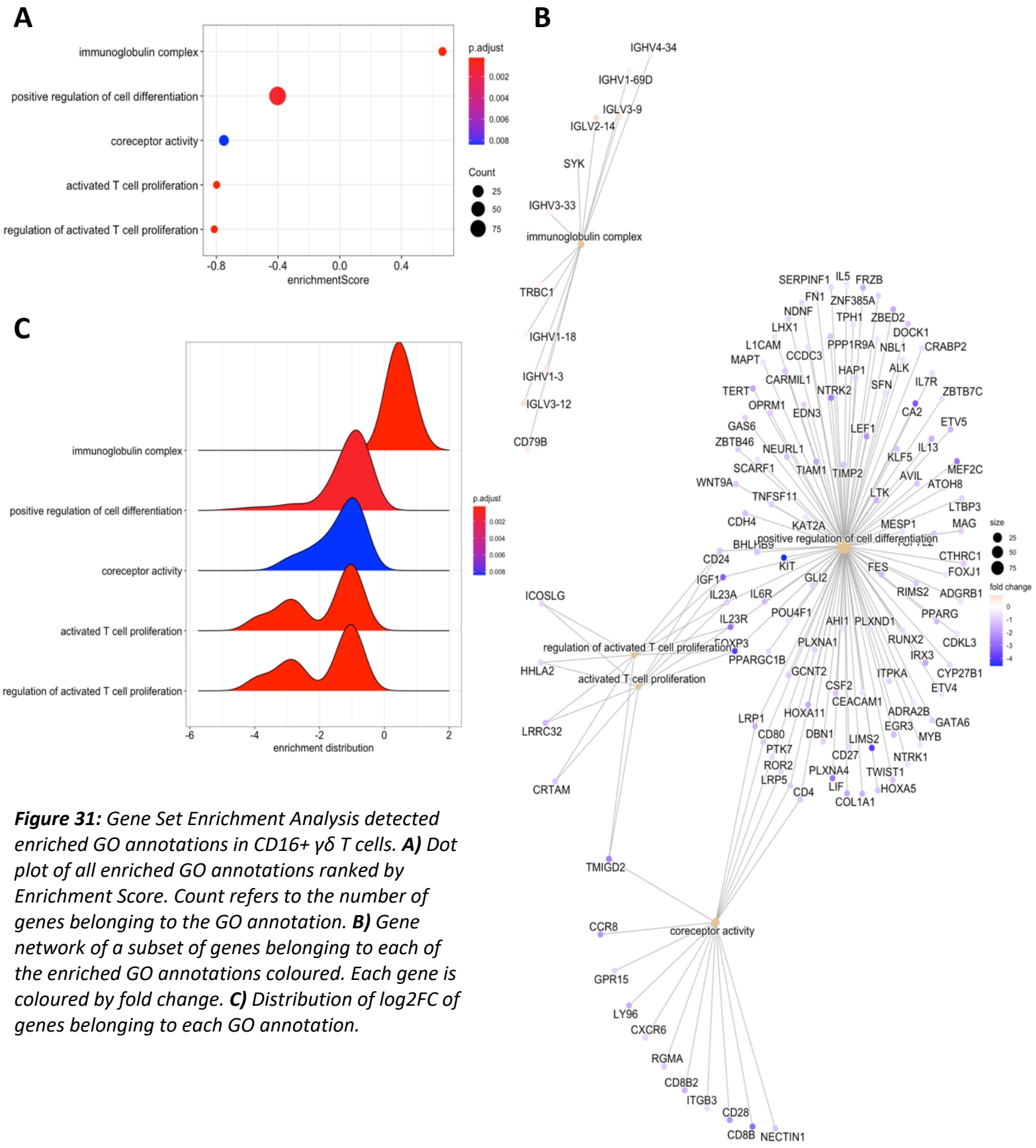

Figure 31: *Gene Set Enrichment Analysis detected enriched GO annotations in CD16+ γδ T cells.* ***A)*** *Dot plot of all enriched GO annotations ranked by Enrichment Score. Count refers to the number of genes belonging to the GO annotation.* ***B)*** *Gene network of a subset of genes belonging to each of the enriched GO annotations coloured. Each gene is coloured by fold change.* ***C)*** *Distribution of log2FC of genes belonging to each GO annotation.*

Gene Set Enrichment Analysis (GSEA) was performed to determine which GO biological processes are upregulated in CD16+ T cells. Although upregulation of genes associated with the immunoglobulin complex process was the most significant, this is an artefact of unfiltered GSEA (Fig 31A, 31C). The normalized counts for most immunoglobulin complex genes are very low (>10 reads) thus their apparent upregulation in the CD16+ γδ T cells may be spurious and reflect minor B-cell contamination (Supplementary Fig 2). Downregulated GO processes include positive regulation of cell differentiation, coreceptor activity, and activated T cell proliferation, which may reflect that CD16+ γδ T cells have a terminally differentiated, low proliferation phenotype characteristic of TEMRA cells. Indeed, c-KIT – shown to be lowly expressed in TEMRA cells[127] – is downregulated in CD16+ γδ T cells (Fig 31B).

While CD16+ γδ T cells can express an intermediate CD27+ memory phenotype, they are primarily associated with TEMRA memory phenotype[26,66,128]. Several downregulated genes assigned to positive regulation of cell differentiation are associated with Th17 γδ T cell differentiation, including: FOXP3, IL-23A, IL-23R, and IL-7R (Fig 31B). A small subset of genes associated with positive regulation of cell differentiation have increased or no change in expression, while most genes have a small decrease in expression, and only a few have large a magnitude of downregulation (Fig 31C). Finally, the two categories associated with activated T cell proliferation – which almost certainly contain mostly overlapping genes based on their enrichment distribution (Fig 31C) – have relatively high count of highly downregulated genes (Fig 31C). This suggests that the CD16+ compartment of γδ T cells would have reduced proliferative capacity.

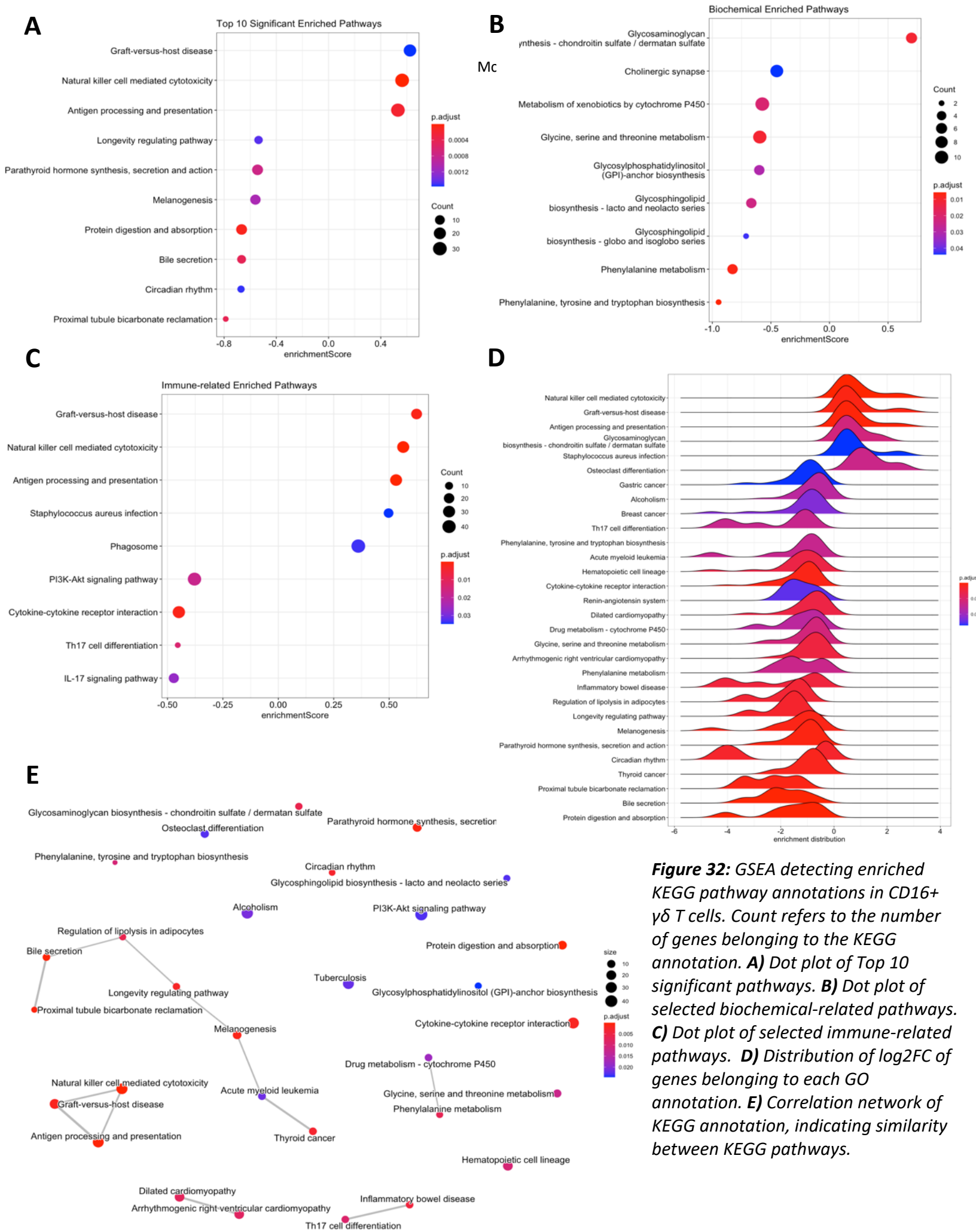

Figure 32: *GSEA detecting enriched KEGG pathway annotations in CD16+ γδ T cells. Count refers to the number of genes belonging to the KEGG annotation.* ***A)*** *Dot plot of Top 10 significant pathways.* ***B)*** *Dot plot of selected biochemical-related pathways.* ***C)*** *Dot plot of selected immune-related pathways.* ***D)*** *Distribution of log2FC of genes belonging to each GO annotation.* ***E)*** *Correlation network of KEGG annotation, indicating similarity between KEGG pathways.*

GSEA was also performed to determine which KEGG pathways are enriched in CD16+ γδ T cells. The top 3 most significant upregulated pathways were Graft-versus-host-disease, Natural killer cell mediate cytotoxicity, and antigen processing and presentation (Fig 32A) – all of which have a high-degree of collinearity (Fig 32E). The most significant down-regulated pathways were unexpected based on CD16+ γδ T cell biology, but likely reflect genes that have broad functions (e.g metabolic) or have different functions in γδ T cells. For example, downregulated TNFSF11 annotated as belonging to a Parathyroid hormone pathway is Receptor Activator of NF-κB ligand (RANKL), which has been shown to be highly expressed in the Th17 subset (Fig 33)[129]. Slightly downregulated Solute Carrier Family (SLC) genes appear frequently in miscellaneous categories including Protein digestion and absorption, Bile Secretion, and the Parathyroid hormone pathway (Fig 33). SLCs are broadly important for activated T cells to intake nutrients from their environment to accommodate high metabolic demands[117]. The downregulation of the SLCs assigned to these miscellaneous categories (Fig 33), and upregulation of other SLCs such as SLC1A7 (Fig 29) may represent a shift in T cell metabolic needs. However, the normalized counts of the SLCs in Figure 32 are rare or non-existent transcripts in the CD16+ and CD16- samples, consequently an accurate interpretation of their expression is limited by the low sequencing depth (data not shown). Overall, these erroneous pathways contain genes that are relevant to T cell biology, despite also belonging to other pathways.

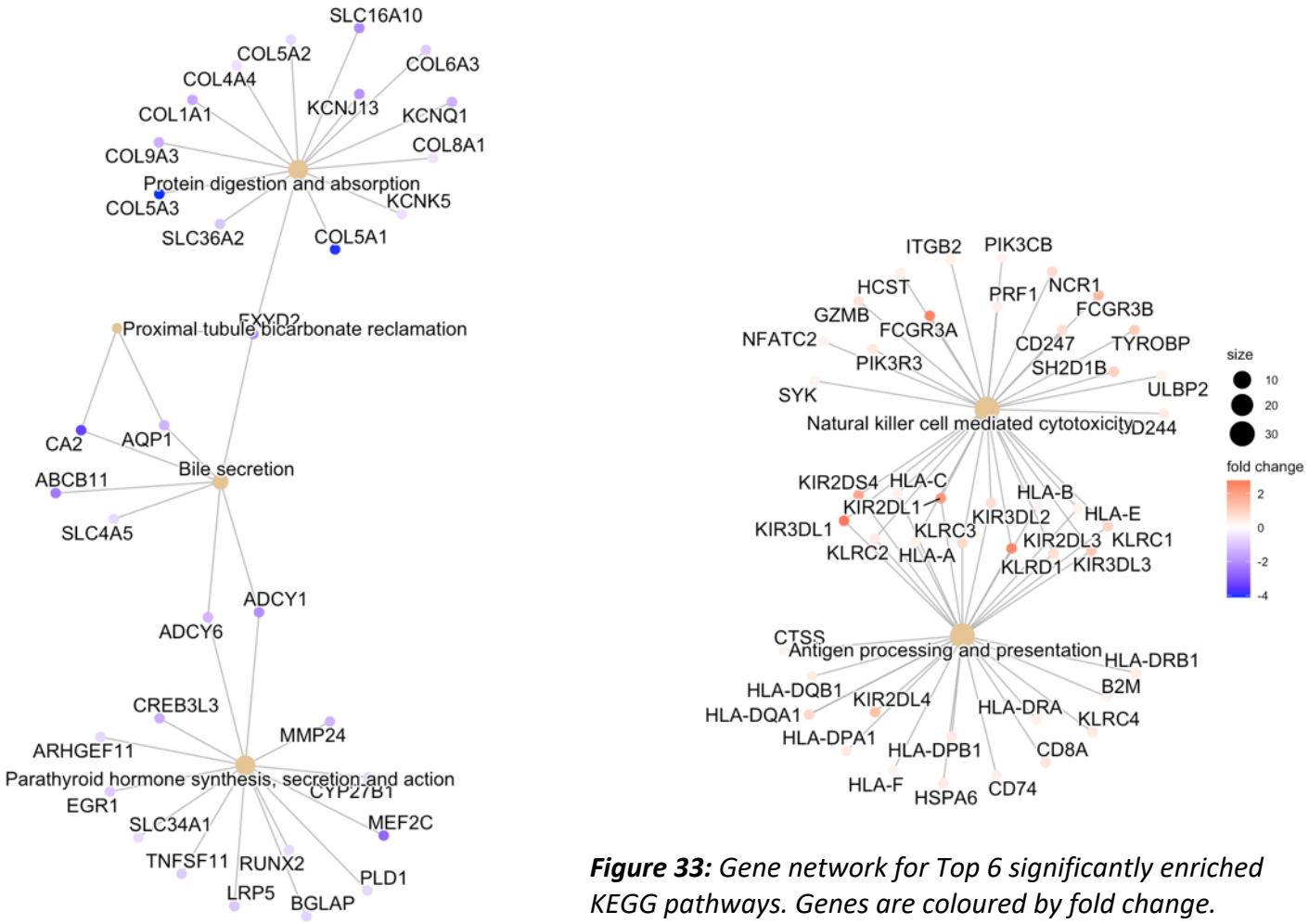

Figure 33: *Gene network for Top 6 significantly enriched KEGG pathways. Genes are coloured by fold change.*

The most significant upregulated biochemical pathway was related to Chrondroitin Sulphate (CS) biosynthesis. CS is a glycosaminoglycan capable of inhibiting the NFκB pathways[130]. CS is primarily described as being expressed on connective cells or deposited in the extracellular matrix[131], thus its relevance to expression in γδ T cells is unclear Fig 32B). The downregulation of amino acid synthesis and metabolism in CD16+ γδ T cells (Glycine, serine, and threonine metabolism, phenylalanine metabolism, and phenylalanine, tyrosine, and tryptophan biosynthesis) (Fig 32B, 34) is likely related to the expected low proliferation TEMRA phenotype of CD16+ γδ T cells, as depletion of phenylalanine and tryptophan both lead to the suppression of T cell proliferation[132].

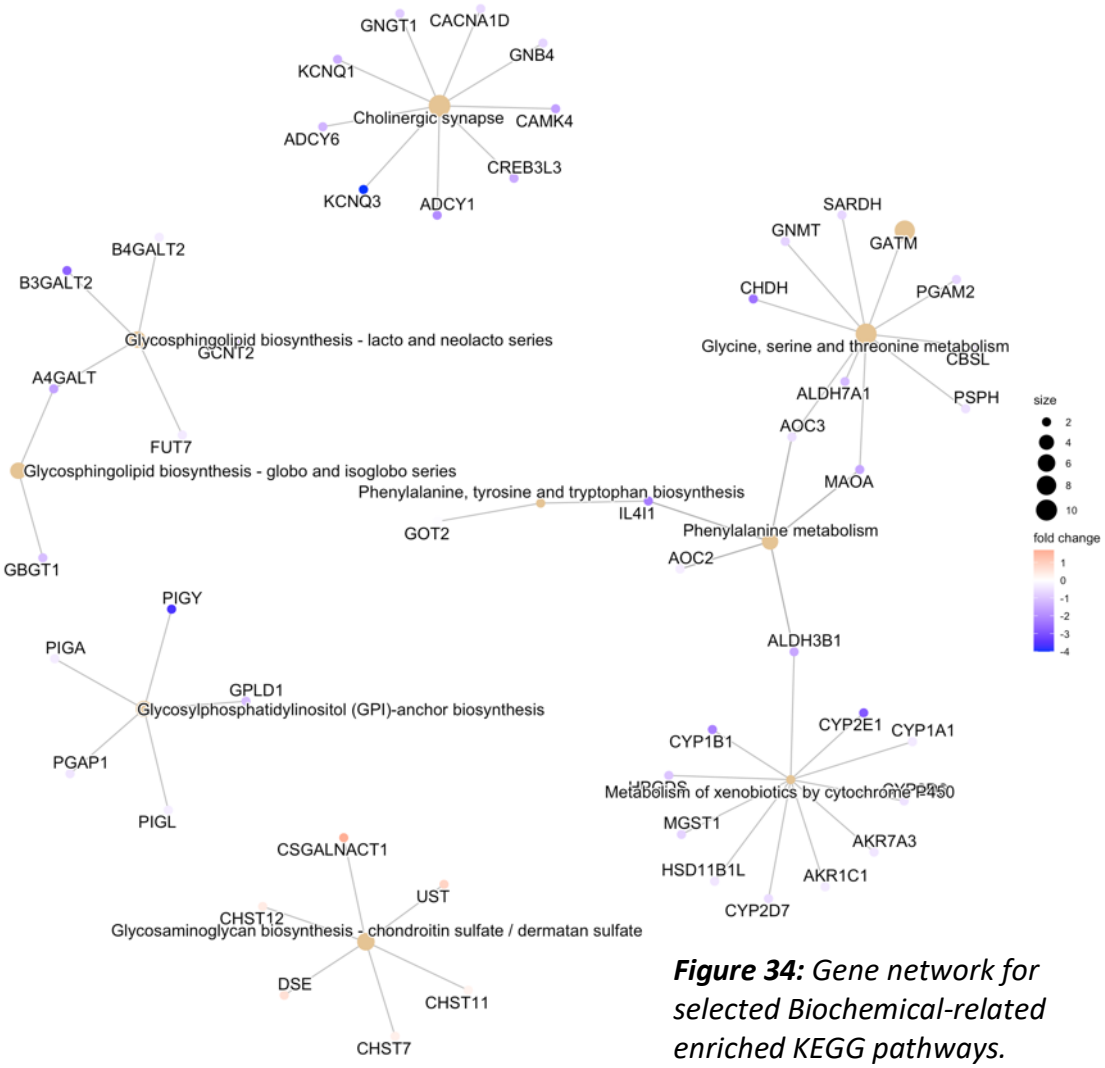

Figure 34: *Gene network for selected Biochemical-related enriched KEGG pathways. Genes are coloured by fold change.*

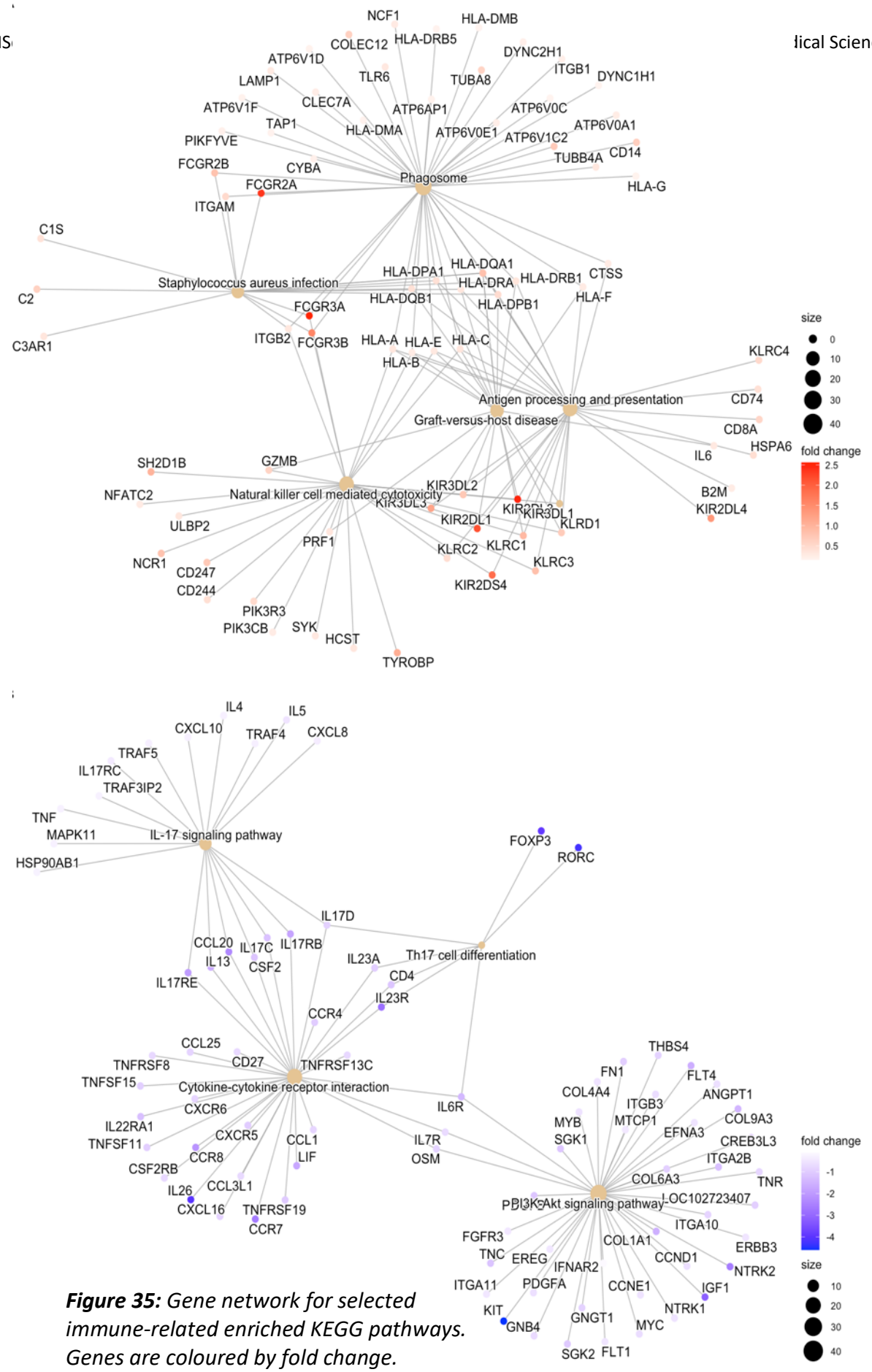

Figure 35: *Gene network for selected immune-related enriched KEGG pathways. Genes are coloured by fold change.*

While CD16+ γδ T cells are typically identified as having the undesirable low-proliferation-associated TEMRA phenotype[66], they benefit from high cytotoxicity against tumour targets[67,133], upregulating NK cytotoxicity receptors and perforin/granzyme[66,133]. Indeed, CD16+ Vδ2 T cells upregulated the Natural Killer cell mediated cytotoxicity KEGG pathways, which includes KIR receptors, DAP12 (TYROBP), Granzyme B (GZMB), NKp46 (NCR1), CD94 (KLRD1), and NKG2 receptors (KLRC1/NKG2A, KLRC2/NKG2C, KLRC3/NKG2E) (Fig 32C, 35, 36). Additionally, CD3ζ is slightly upregulated in CD16+ Vδ2, while the other signalling pathway for FcγRIII activation –

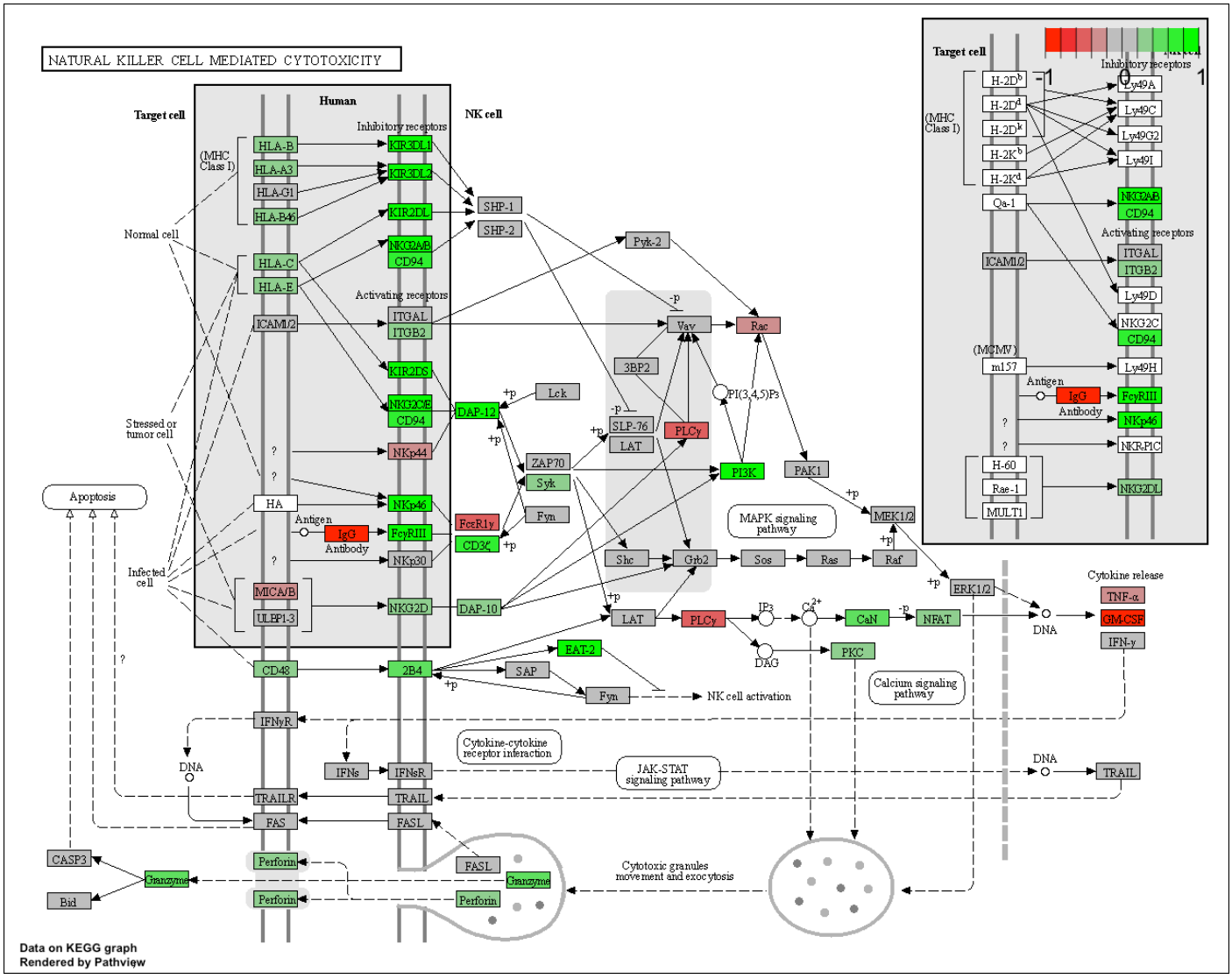

Figure 36: *Detailed analysis of CD16+ Vδ2 gene expression associated with the enriched Natural killer cell mediated cytotoxicity KEGG pathway. Generated using Pathview. Colours represent LFC, to a max/minimum of 1/-1. Values outside these bounds are assigned to the colour at their extreme.*

FcεR1γ – has low normalized counts and is slightly downregulated (non-significant), indicating FcγR activation in CD16+ γδ T cells is likely primarily transduced via CD3 (Fig 36).

The antigen presentation capabilities of CD16+ γδ T cells is of particular interest for γδ T cell immunotherapies because it may provide a unique anti-tumour function to engineered γδ T cells not possible in other commonly engineered immune cells (i.e., T cells, NK cells). ADCP of infectious agents by CD16+ Vγ9Vδ2 T cells is important for γδ T cell response to both *E. Coli*[62] and *Plasmodium falciparum* infection[134]. CD16+ γδ T cells are also capable of phagocytosing

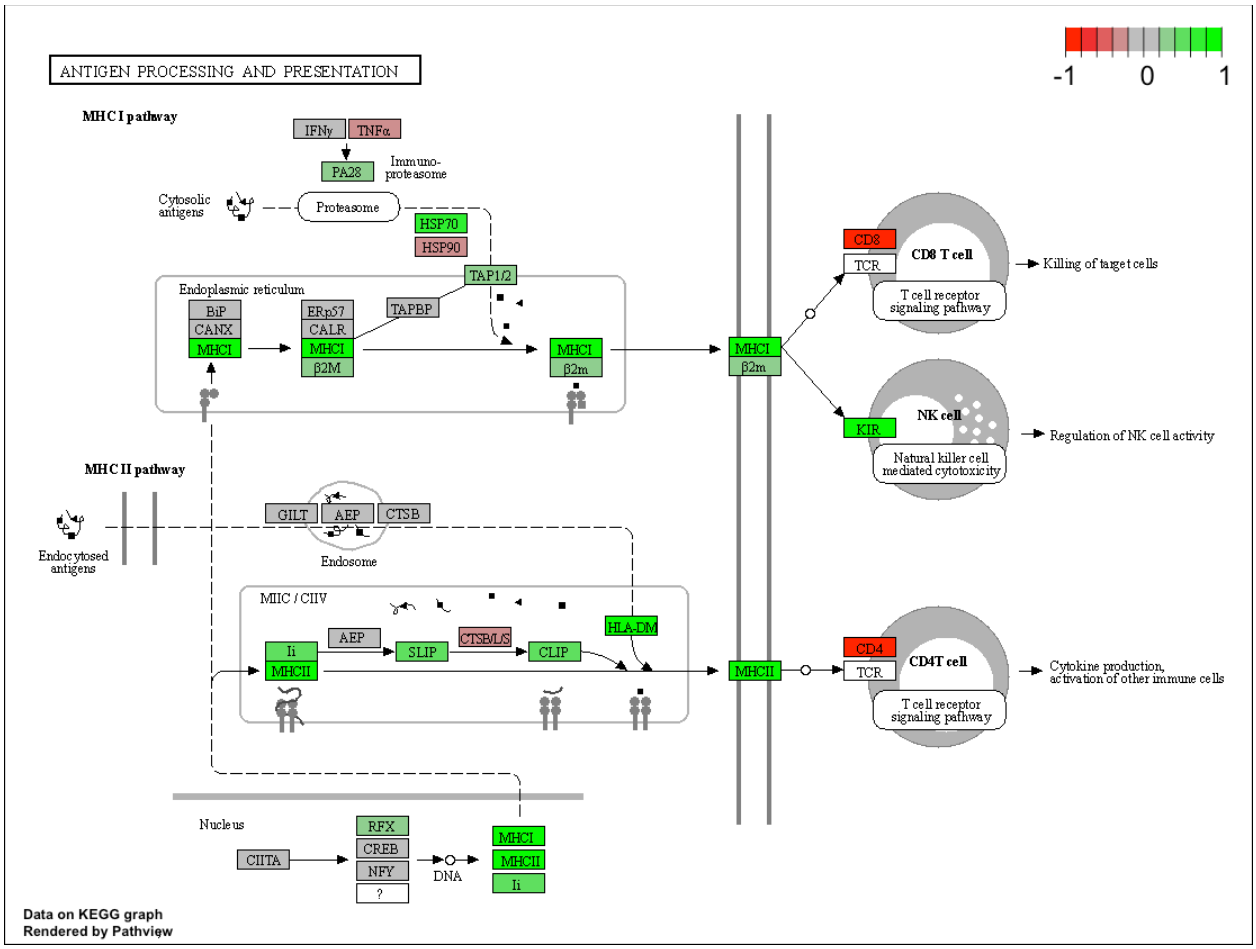

Figure 37: *Detailed analysis of CD16+ Vδ2 gene expression associated with the enriched Antigen processing and presentation KEGG pathway. Generated using Pathview. Colours represent fold-change, to a max/minimum of 1/-1. Values outside these bounds are assigned to the colour at their extreme.*

several antibody-opsonized tumour cell lines and presenting tumour antigen to naïve αβ T cells[61]. In accordance with CD16+ γδ T cells APC potential, CD16+ Vd2 cells upregulate both the phagosome and antigen processing and presentation KEGG pathways (Fig 32C). CD16+ Vδ2 upregulate both MHC-I and MHC-II – which is typically reserved to expression on professional APCs. MHC-II is often loaded within phagosomes to facilitate antigen presentation of extracellular components surveilled by APCs. Ii, CLIP, SLIP, and HLA-DM, which are required for loading peptides onto MHC-II, also have upregulated gene expression (Fig 37). Taken together, the upregulation of MHC-II and phagosome pathways imply that CD16+ BCMA-TAC γδ T cells will be capable of ADCP.

In accordance with analysis of significant DEGs (Fig 29C, 32A) Th17 differentiation and IL-17 signalling are among downregulated immune-related KEGG pathways in CD16+ Vδ2 cells (Fig 32C, 35). Th17 differentiation has many genes with a large negative log2FC (Fig 32D). While IL-17 production by BCMA-TAC γδ T cells in response to Multiple Myeloma tumour targets is nominal, enrichment of Th17 differentiation is CD16- cells suggests low levels of IL-17 production are likely produced by CD16- BCMA-TAC γδ T cells.

The PI3K-AKT signalling pathway is also downregulated in CD16+ Vδ2 (Fig 22C, 35), despite the gene encoding PI3K itself (PIK3CA) being slightly upregulated (non-significant) (Fig 36). Research on the role of PI3K/AKT signalling in γδ T cells is limited. PI3K/AKT signalling is required for expansion of γδ T cells expanded with IL-12 and bacterial phosphoantigen HMBPP, but not for IL-2 and HMBPP expanded γδ T cells[135]. PI3K/AKT signalling is also required for chemokine receptor expression upon TCR stimulation. Yin et al. demonstrate blocking PI3K signalling prevents upregulation of CCR4, CCR7, CCR8, CXCR1, and CXCR3 on Vδ2+ cells from

systemic lupus erythematosus patients[136]. Indeed, reduced expression of chemokine receptors CXCR3, CCR5, and CCR6 have been observed on CD16+ γδ T cells[66]. Accordingly, the fold change for most of these chemokines were downregulated in CD16+ Vδ2 cells, albeit CXCR3 was upregulated in our dataset (Fig. 38). Finally, PI3K/AKT signalling has been shown to play an important role in Vγ9Vδ2 T cell degranulation and IFNγ production in response to TCR stimulation. However, PI3K/AKT signalling is not required for degranulation of TCR stimulated Vγ9Vδ2 T cells co-stimulated with NKG2D, and adding NK2GD signalling partially rescues IFNγ production of TCR-stimulated γδ T cells treated with PI3K/AKT inhibitors[137]. CD16+ γδ T cells have been previously described as hyporesponsive to TCR stimulation with reduced production of IFNγ. However, CD16+ γδ T cells tend to have higher levels of anti-tumour cytotoxicity compared to their CD16- counterparts[66]. Downregulation of PI3K/AKT signalling pathway may be associated with observed TCR signalling hyporesponsiveness and reduced IFNγ production observed in CD16+ γδ T cells in the literature, as well as altered chemokine expression phenotype observed both in our dataset (Fig 31) and in the literature. Given that CD16+ Vδ2 are highly cytotoxic, cytotoxicity may be co-stimulated or entirely activated via non-TCR cytotoxicity receptors (NKG2 family, KIRs, FcγRs, etc.) that doesn't require PI3K/AKT for activation. For example, NKG2D doesn't require PI3K/AKT signalling for degranulation in Vγ9Vδ2 T cells[137]. This may explain the highly cytotoxic phenotype of CD16+ Vδ2 cells described in the literature, while simultaneously having TCR hyporesponsiveness and PI3K/AKT downregulation.

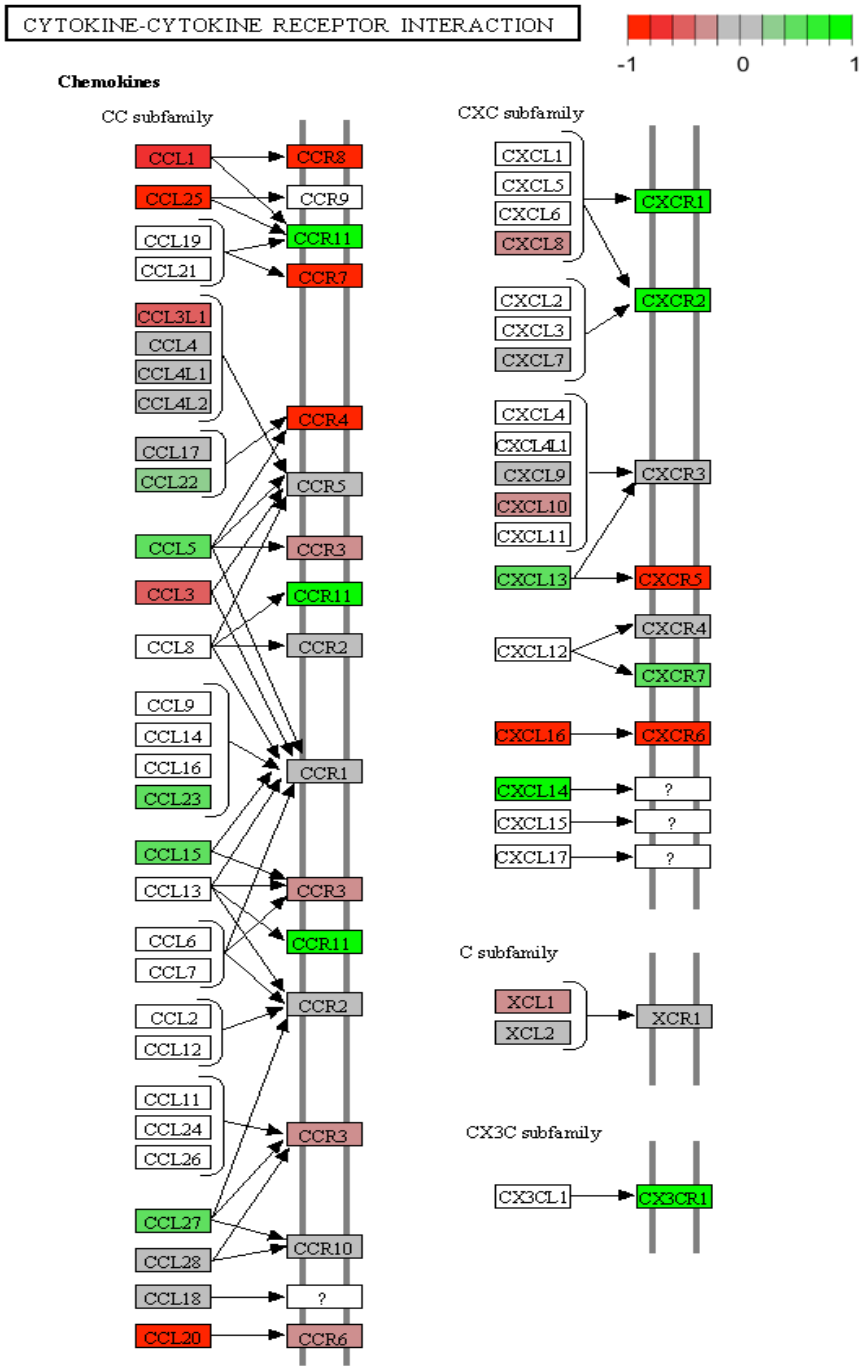

Figure 38: *Detailed analysis of CD16+ Vδ2 gene expression associated with the enriched Cytokine-cytokine receptor interaction KEGG pathway. Generated using Pathview. Colours represent fold-change, to a max/minimum of 1/-1. Values outside these bounds are assigned to the colour at their extreme.*

RNA-sequencing of NT and BCMA-TAC γδ T Cell Cultures

We also wanted to confirm that TAC does not alter the transcriptional program of resting γδ T cells in the absence in the absence of TAC target ligand. To assess the transcriptome of NT and BCMA-TAC.γδ T cells, we first using the CD4/CD8 MACS depletion kit to deplete NT and BCMA-TAC γδ T cell cultures to >99% γδ purity. RNA was extracted from the cultures immediately after purification and sent for bulk RNA sequencing. Only one gene was differentially expressed – HSPA1B (Fig. 39). HSPA1B encodes for Heat Shock Protein 70 (HSP70), an anti-apoptotic chaperone protein, which can be upregulated in response to cellular stress[138]. Upregulated HSP70 may be functioning as a chaperone protein to fold nascent TAC polypeptides, or it may indicate BCMA-TAC γδ T cells have increased cellular stress.

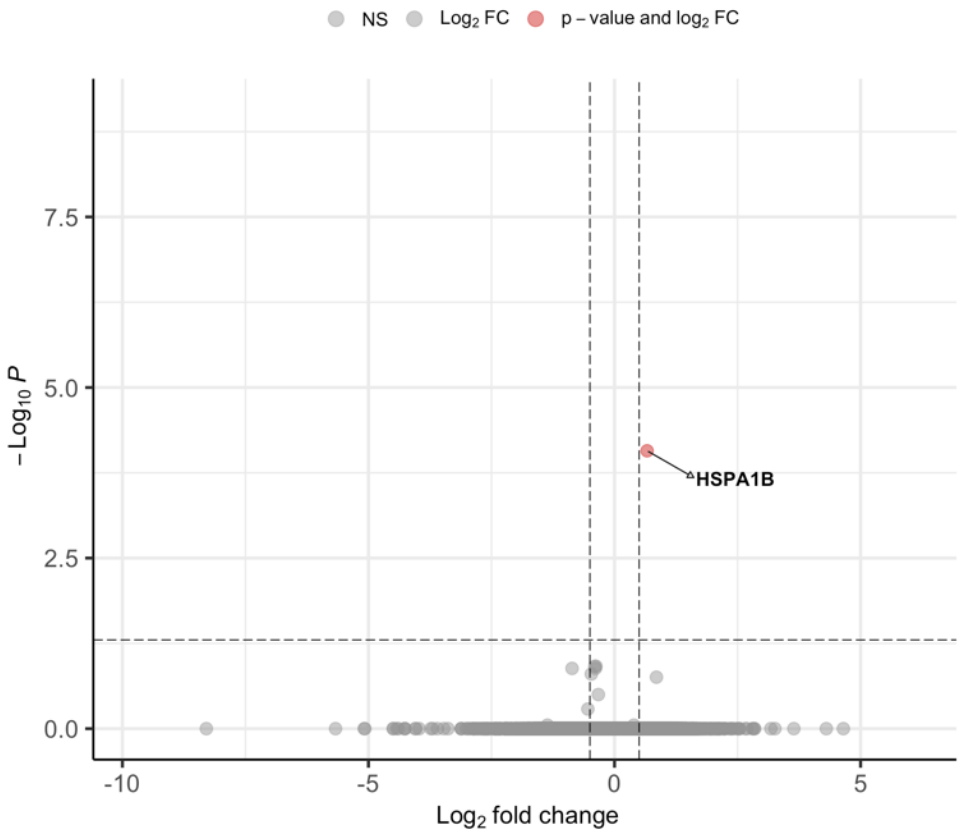

***Figure 39**: Differential gene expression of BCMA-TAC vs. non-transduced γδ T cell cultures. DGE Cut-off: Benjamini-Hochberg adjusted p-value < 0.05 and log2 Fold Change > 0.5.*

Discussion

Engineered γδ T cells are candidates for next-generation allogeneic engineered T cell therapies, which aim to address the unsustainable financial cost of autologous engineered T cell therapies. We engineered γδ T cells with TAC receptors, which is a unique synthetic antigen receptor that uses CD3 monoclonal antibody UCHT-1 and a CD4 cytoplasmic tail to activate engineered T cells in response to antigen receptor recognition[21]. The TAC receptor more closely resembles a conventional αβ T cell receptor and may reduce engineered T cell-related toxicities compared to FDA-approved CAR-T cell therapies[21]. TACs have been developed against Multiple Myeloma[22], as it is an incurable hematological malignancy with a targetable tumour-associated antigen – BCMA. While CAR-T cell therapies have been clinically approved for Multiple Myeloma, these therapies have limited success in generating durable responses clinically [19]. We investigated strategies to engineer BCMA-TAC γδ T cells and further enhance their anti-tumour efficacy using a monoclonal antibody combination therapy.

Manufacturing

Prior to this thesis, our lab had developed a manufacturing protocol for engineering TAC γδ T cells using commercially available Lentigen lentiviruses. The Lentigen viruses are expensive and limit our experiments. To address questions related to the impact of TAC design on functionality in γδ T cells, we sought to engineer γδ T cells with our in-house vector systems. In this thesis, we show that our in-house lentiviral vectors led to αβ T cell outgrowth in γδ T cell

cultures. However, when the equivalent γ-retroviral vector was used, there was minimal αβ outgrowth and exceptional TAC transduction (60 – 80%).

Given the promising results of the γ-retroviral transduction, we further developed the γ-retrovirus manufacturing protocol, optimizing transduction day, early culture cell density, and cytokine conditions. Published γδ CAR-T cell manufacturing protocols typically transduce γδ T cells Day 5 post-activation[78,91,93], however we found that we achieved the highest transduction Day 3 post-activation. Even with increased transduction of γδ T cells with our Day 3 γ-retroviral transduction protocol, we did not observe any additional αβ T cell outgrowth.

We wanted to increase the yield of engineered γδ T cells by enhancing the expansion of our cultures. Zoledronate-treated PBMCs activate γδ T cells because zoledronate inhibits the mevalonate pathway and leads to pAg accumulation in monocytes in culture[109]. Phosphoantigen accumulation causes conformational changes of butyrophilin transmembrane proteins on the monocytes' cell surface, which induces Vγ9Vδ2 TCR activation[36]. We increased the cell density of early culture conditions, with the rationale of increasing the trans-cell interactions of Vγ9Vδ2 and monocytes during the culture activation stage, as both cell types are infrequent cell populations in PBMCs[24,139]. We found that increasing cell density at D0 led to an increased yield of γδ T cells across multiple donors. Increased cell density at D3 had no effect on γδ T cell expansion, however we decided to integrate higher cell densities at D3 into our manufacturing protocol because this reduced the quantity of 24-well plates required for manufacturing. We simultaneously increased the amount of retronectin and viral supernatant added during D3 transduction, as this increased transduction in the high density conditions.

The effects of exogenous IL-15 on γδ T cell expansion in the literature has been mixed, but generally trended towards improving γδ T cell yield and memory phenotype[79,83–87]. We tried several concentrations of IL-15, and simultaneous or temporal combination with IL-2. High concentrations of IL-15 or combination regimens with IL-2 decreased γδ T cell transduction, γδ purity, and consequently the yield of engineered γδ T cells. However, the lowest IL-15 condition improved engineered γδ T cell yield, although this improvement was marginal. While IL-15 has been reported to increase the proportion of central memory T cells in culture[79,87], we found that it had no effect on CD27 expression. Given the minimal improvement of IL-15 on engineered γδ T cell yield, and limited differences in γδ T cell phenotype, we decided to continue using IL-2 for our γδ T cell manufacturing protocol. We used the optimized protocol – high density at early culture timepoints, D3 γ-retroviral transduction, and high IL-2 supplemented cultures – for the functional analyses of BCMA-TAC γδ T cells and CD16-expressing γδ T cells. Using RNA-seq, we also demonstrate that the BCMA-TAC γδ T cells generated with our optimized protocol have limited differential gene expression from NT cells, only upregulating HSP70.

We applied the optimized γδ TAC T cell γ-retroviral engineering protocol to HER-2-TAC-KIR2DS2-Dap12 (KIR-TAC) constructs we developed. However, γδ T cell γ-retroviral transduction with the KIR-TAC constructs was poor and led to decreased γδ purity. While the trade-off between γδ purity and TAC transduction was lower in KIR-TAC γ-retroviruses than in-house BCMA-TAC lentiviral transduction, the continued observation of αβ T cell outgrowth in transduced cultures prompted us to investigate a manufacturing strategy where αβ T cells were depleted prior to manufacturing. Siegers et al. reported that depleting αβ T cells from γδ T cell

cultures manufactured with Concanavalin A reduced expansion[140]. Consequently, it was imperative that we assessed fold expansion of non-engineered γδ T cells manufactured from αβ-depleted PBMCs using our standard manufacturing protocol. We found that after adjusting for cells that would be lost from non-depleted γδ T cell cultures during purification, the yield of γδ T cells in the αβ-depleted PBMC cultures was similar or greater than non-depleted ones, suggesting that αβ T cell-depletion prior to manufacturing may be a viable strategy to circumvent viral transduction induced αβ T cell outgrowth. However, the αβ T cell depletion manufacturing strategy still requires evaluation in transduced cultures to confirm that the residual population of aβ T cells leftover after purification do not expand in response to viral transduction.

BCMA-TAC Functionality

BCMA-TAC γδ T cells were manufactured and purified according to our optimized BCMA-TAC γ-retroviral manufacturing protocol. We used purified γδ T cells to assess the functionality of BCMA-TAC γδ T cells in response to Multiple Myeloma tumour cell lines. BCMA-TAC γδ T cells rapidly and specifically destroy BCMA+ Multiple Myeloma tumour cell lines MM.1S and KMS-11, but not BCMA- tumour cell line K562. While γδ T cells have innate anti-tumour cytotoxicity, NT γδ T cells do not eradicate any of the tumour cell lines at the low E:Ts used, demonstrating that BCMA-TAC enhances sensitivity of γδ T cells to BCMA+ tumour killing. In addition to anti-tumour cytotoxicity, we demonstrate that BCMA-TAC γδ T cells primarily release Th1-like cytokines associated with the anti-tumour γδ T cell phenotype – IFNγ and TNFα – when co-cultured with MM tumour cells. There is a marginal amount of Th17 associated cytokine produced by BCMA-TAC γδ T cells, however the dominant cytokine profile of stimulated BCMA-

TAC γδ T cells are Th1-associated cytokines. Ryan et al. have also identified small subset of Th17 Vδ2+ T cells responding to PMA/Ionomycin stimulation, however these IL-17 producing cells only represent >1% of Vδ2+ cells[67]. Resting BCMA-TAC γδ T cells did not release any cytokines, suggesting that activation of TAC γδ T cells is ligand-dependent.

CD16 Functionality

γδ T cells have been shown to express FcγRs CD16[50–54] and CD32[50], and can respond to antibody-opsonized targets via both ADCC[50] and ADCP[61]. Given that γδ T cells can respond to CD16, and the recent integration of Daratumumab into the front-line therapy for MM, we wanted to investigate the possibility of an engineered γδ T cell and mAb combination therapy. First, we demonstrated that our γδ T cells express CD16, although we did not detect CD32 or CD64 expression. We also demonstrated that Daratumumab binds to γδ T cells at a similar proportion to CD16 expression, however we have also shown that γδ T cells express CD38, thus it can't be ruled out that we were detecting CD38 rather than FcγR binding.

Despite demonstrating that γδ T cell express CD16, co-culturing BCMA-TAC γδ T with luciferase-expressing MM.1S cells and Daratumumab did not improve *in vitro* killing within a 48-hour period. FcγR activation has been shown to improve killing in γδ T cells, especially against tumours that are otherwise resistant to γδ T cell killing[50]. Daratumumab may potentiate TAC γδ T cells and induce long-term anti-tumour cytotoxicity only under circumstances where there is less potent stimulation (e.g compared to CD3 stimulation via TAC). On the contrary, low levels of Daratumumab appeared to decrease γδ T cell cytotoxicity against MM.1S cells. This is also likely to be an artefact of luminescence spill-over. However, it is possible that these low concentrations of daratumumab lead inhibitory monovalent FcγR engagement. Monovalent Fc-

engagement is thought to induce weak phosphorylation of downstream signalling molecules (e.g. ERK), leading to the recruitment of SHP-1 to the cell membrane[55]. SHP-1 phosphatase can dephosphorylate signalling molecules necessary for both FcγR and TAC-TCR-CD3 signalling transduction including CD3, Lck, and Zap70[57]. Consequently, monovalent FcγR interactions could reduce cytotoxic activation of γδ T cells. Daratumumab-induced fraticide of CD38+ γδ T cells may also explain the lack of increased tumour killing of BCMA-TAC γδ T cells co-cultured with Daratumumab.

To confirm that the CD16 receptor on our γδ T cells was indeed functional, we used a plate-bound anti-CD16 stimulation assay, which confirmed that γδ T cells degranulate and produce TNFα in response to CD16 activation in a dose-dependent manner. We then performed a CD16 screening experiment from 10 PBMC donors and selected 7 donors with D14 CD16+ γδ T cells for large-scale manufacturing. We used 6 CD16+ donors to test whether BCMA-TAC γδ T cells can respond to dual stimulation via TAC and CD16. We demonstrated that BCMA-TAC γδ T cell cultures stimulated with both TAC and CD16 have increased degranulation, and a trend towards increased TNFα cytokine production compared to samples stimulated with TAC alone. These results suggest that combination therapy with a monoclonal antibody and engineered T cells therapy may be synergistic.

To further investigate CD16 and TAC dual activation of BCMA-TAC γδ T cells, we assessed degranulation and cytokine production in response to 7 CD16+ donors' BCMA-TAC γδ T cells co-cultured with Daratumumab and 7 different tumour cell lines with several BCMA and CD38 expression phenotypes. We observed that higher Daratumumab concentrations led to decreased degranulation. Due to the high concentration of Daratumumab used, and an inverse

dose-response relationship, we considered that excess soluble Daratumumab may be monovalently binding to FcγR and providing an inhibitory signal via SHP-1 phosphatase recruitment[58]. Inhibition via excess soluble Daratumumab in culture could explain why BCMA-TAC γδ T cell stimulated with higher concentrations of Daratumumab have lower levels of degranulation compared to low Daratumumab concentrations. Consequently, we amended the tumour ICS protocol by pre-incubating tumour cell lines with Daratumumab and washing excess Daratumumab prior to engineered γδ T cell co-culture. However, even with Daratumumab pre-incubation, we observed BCMA-TAC γδ T cell degranulation when co-cultured with Daratumumab-treated BCMA- CD38- tumour cells, and only a modest increase in BCMA-TAC γδ T cell degranulation otherwise. The presence of signal when co-cultured with CD38- tumour cells may be due to plate-bound Daratumumab Fc region providing an FcγR ligand, as Daratumumab was added directly to the stimulation plate and incubated at 37°C for 30 minutes before washing. The modest increase in degranulation in response to Daratumumab culture is challenging to interpret because of the signal in the negative control. However, if these data reflect true CD16 activation, the lack of additive stimulation by CD16 ligation may be due to the high intensity of TAC signalling in response to BCMA on the tumour cells. Stimulation with plate-bound recombinant BCMA only led to CD107a mobilization in approximately 30% of Vδ2+ TAC-T cells. In contrast, stimulation with BCMA-positive tumour cells triggered TAC-dependent CD107a mobilization in >60% Vδ2+ TAC-T cells, indicating a much stronger signal from the tumor cells which likely overcomes the need for additional stimulus through CD16. Consistent with these results. Gertner-Dardenne et al.'s ADCC assays suggest that tumour cells already susceptible to TCR-based γδ T cell killing, do not have increased lysis when monoclonal

antibodies are added[50]. Consequently, BCMA-TAC γδ T cells may not benefit from Daratumumab treatment in an *in vitro* setting because there is already a high level of TAC-mediated activation and degranulation, thus antibody opsonization provides minimal benefit.

Overall, we demonstrate that TAC γδ T cells can degranulate and produce TNFα in response to CD16 stimulation, and that CD16 stimulation can synergize with TAC stimulation to enhance activation of BCMA-TAC γδ T cell cultures. However, the possibly synergy of a BCMA-TAC γδ T cell therapy and Daratumumab combination therapy is unclear; this is in part due to limitations of tumour ICS and cytotoxicity assays, but also due to CD38 expression on engineered γδ T cells. Further investigation of an engineered γδ T cell therapy combined with a mAb that has been well-validated to induce ADCC in γδ T cells, such as Rituximab[50,59] or Trastuzumab[53], may clarify the viability of a combination therapy.

Despite the unclear potential of a combination therapy, the dual responsiveness of γδ T cells to both CD16 and CD3-induced (TAC) stimulation suggests that a TAC with an FcRγ domain may be a plausible strategy to enhance TAC γδ T cell functionality. A FcRγ synthetic antigen receptor γδ T cells may also engage their antigen presentation functions to enhance anti-tumour functionality of engineered γδ T cells. Indeed, a similar strategy has been investigated by γδ T cell ACT company TC Biopharm, who have filed a patent protecting a FcγR-based γδ CAR-T cells[141].

CD16+ γδ T Cell Phenotype

To further investigate the nature of CD16+ γδ T cells, we analyzed phenotype at baseline (D0) and after 14 days of culture (D14) phenotyping results from multiple donors. CD16 expression in our γδ T cell cultures was a donor-dependent feature, being highly correlated

between the same donor across experiments and was not influenced by virus-transduction. We could not identify features in D0 PBMCs that predicted CD16 expression in D14 γδ T cells. However, we did observe that DAP12 expression was associated with CD16 expression. Flow cytometry data from D14 phenotyping confirmed that intracellular DAP12 is higher in CD16+ γδ T cells compared to CD16- γδ T cells from the same culture. RNA-sequencing also provides additional evidence that DAP12/TYROBP was expressed at higher levels in CD16+ BCMA-TAC γδ T cells.

RNA-seq was used to investigate the gene expression profiles of CD16+ vs CD16- BCMA-TAC Vδ2 cells from 4 donors. Similar to previous results, we found that CD16+ γδ T cells upregulate NKRs, KIRs, and DAP12[66,67]. Furthermore, CD16+ γδ T cells downregulate several genes associated with the Th17 phenotype[67]. Indeed, Th17-associated transcription factor RORC is also downregulated in CD16+ γδ T cells. These results were unexpected because co-culture of BCMA-TAC γδ T cells –containing both CD16+ and CD16 cells– with MM tumour cells induces a Th1-like cytokine response, with nominal produce of IL-10 and IL-17. The functional significance of Th17-associated transcription factor expression in CD16- cells is therefore unclear. However, human γδ T cells maintain phenotypic plasticity between Th1 and Th17 subsets in the periphery, and while Th17 differentiation is rare in healthy humans, it can be observed in highly immunosuppressive environments such as TB granulomas[39,40] and tumours[25]. While our BCMA-TAC γδ T cells have minimal expression of IL-17 in our *in vitro* tumour co-culture model, our assays are focused on short-term functional attributes of γδ T cells activated by TAC ligation binding (cytotoxicity, cytokine production). The expression of Th17-associated transcripts in BCMA-TAC CD16- γδ T cells may indicate they are prepared to

rapidly differentiate into Th17 cells upon immunosuppressive signals found in tumour microenvironments (e.g IL-6, IL-23, IL-17[142]). Th17 differentiation of γδ T cells would likely be disadvantageous for cancer immunotherapy applications, as Th17 γδ T cells have a regulatory pro-tumour phenotype[25]. Therefore, further investigation is required into the Th1 and Th17 plasticity of engineered γδ T cells in cancer immunotherapy models, where γδ T cells are exposed to immunosuppressive environments.

CD16+ γδ T cells have been identified as primarily having a TEMRA phenotype[66,67]. Our RNA-seq results also suggest CD16+ γδ T cells have features of TEMRA cells, including downregulating genes associated with proliferation and T cell differentiation – potentially indicating terminal differentiation. Accordingly, phenylalanine and tryptophan biosynthesis and metabolism are reduced in CD16+ γδ T cells. The depletion of tryptophan and phenylalanine has been associated with low proliferation phenotype in conventional T cells[132]. Thus, while CD16+ γδ T cells display a highly cytotoxic Th1 phenotype capable of responding to numerous stress ligands on tumour cells, they would also be expected to have limited proliferative capacity. Based on these characteristics, the ideal application of CD16+ γδ T cells in engineered ACT may be a therapeutic strategy where central memory γδ T cells are administered to the patient, which differentiate into a highly cytotoxic Th1-like CD16+ TEMRA phenotype following *in vivo* expansion either though pharmaceutical interventions or genetic engineering strategies. However, manufacturing highly proliferative central memory γδ T cells is a challenge, as demonstrated by poor *in vivo* expansion of published engineered γδ T cell therapies[90,91]. Furthermore, signalling pathways and transcription factors to target for differentiation of Vδ2 T

cells into a CD16+ subset remain unknown, thus limiting the ability to develop strategies to induce *in vivo* differentiation of highly cytotoxic CD16+ γδ T cells.

CD16+ γδ T cells bridge the innate and adaptive immune response via their phagocytic and antigen presentation capacity[62]. Antibody opsonization of bacterial[62] or tumour[61] targets leads to ADCP and antigen presentation to αβ T cells. While γδ T cells have been shown to endocytose and present peptides from the environment and induce modest αβ T cell expansion[78], phagocytosis and presentation of larger particulates and cells seem to require antibody opsonization[62] – implicating the CD16+ subset. Indeed, our CD16+ BCMA-TAC γδ T cells upregulate genes related to the phagosome and antigen processing and present presentation pathways. Particularly, genes related to MHC-II epitope loading and MHC-II itself, are upregulated, which is typically associated with professional APCs[143]. Upregulation of antigen presentation-associated proteins (e.g MHC-II, CD86) occurs in γδ T cells following TCR stimulation, and suggests that CD16+ BCMA-TAC γδ T cells would be licensed for antigen presentation in response to antibody opsonized targets[61]. Antigen presentation of tumour targets by engineered γδ T cells may represent a unique strategy to reduce target antigen loss and increase engineered T cell therapy efficacy by engaging the host immune system.

Future Directions

While we demonstrated that non-transduced γδ T cells manufactured from αβ-depleted PBMCs leads to γδ T cell cultures with high purity and comparable expansion to non-depleted cultures, this manufacturing strategy also must be assessed in the context of virus transduction. Given that viral transduction of certain γ-retroviral and lentiviral constructs was associated with the outgrowth of αβ T cells, future experiments should investigate whether transduction in αβ-

depleted PBMCs leads to an outgrowth of residual αβ T cells leftover from purification. If αβ T cell outgrowth is identified in transduced αβ-depleted cultures, this issue may be circumvented by postponing the transduction day until the αβ T cell population has contracted (e.g Day 7 – 9) or re-applying depleted-PBMCs to a second MACS purification column on D0 to removal residual αβ T cells.

We encountered several technical issues with our Daratumumab tumour ICS assays. Namely, BCMA-TAC γδ T cells degranulated when co-cultured with CD38-negative tumour cells lines loaded with Daratumumab, which may be caused by CD16 cross-linking to plate-bound Daratumumab. The presence of Daratumumab was also noted to decrease degranulation of BCMA-TAC γδ T cells following co-culture with BCMA-positive tumor lines, which may indicate that maximum short-term degranulation capacity of BCMA-TAC γδ T cell cultures has already been reached via TAC ligation to BCMA, and engagement of CD16 via Daratumumab functioned in an inhibitory manner. Inhibitory effects of Daratumumab could potentially be caused by fratricide mediated via CD38 expressed on neighbouring γδ T cell fratricide or through monovalent FcγR interactions from soluble Daratumumab. Consequently, assays analyzing the BCMA-TAC γδ T cell response to antibody-opsonized tumour cells should use an antibody pre-loading strategy, whereby antibody is loaded onto tumour cells in a separate tube and excess soluble antibody is washed prior to tumour cells transfer to experimental wells. Pre-loading antibody in a separate tube may prevent plate-bound Daratumumab from inducing degranulation in CD38-negative controls, while also limiting the potential inhibitory activity of soluble Daratumumab. Using tumour cell lines with low BCMA expression may also be preferable models for observing the effect of dual CD16 and TAC stimulation in short-term

degranulation assays. Furthermore, using a monoclonal antibody that has been well-validated in the literature to induce ADCC or ADCP for γδ T cells (e.g Rituximab[50,59]), would be useful as a positive control for future antibody opsonization assays with BCMA-TAC γδ T cells.

In our manufacturing experiments, we observed low levels of CD27+ BCMA-TAC γδ T cells, indicative of an effector memory or TEMRA γδ T cell phenotype with limited proliferative capacity. A major limitation of *in vivo* engineered γδ T cell therapy experiments in the literature is limited *in vivo* persistence of γδ T cells[90–92]. A manufacturing strategy that primarily generates CD27+ central memory BCMA-TAC γδ T cells with high proliferative capacity may be preferable for establishing a durable anti-tumour response. Non-engineered Vγ9Vδ2 T cells manufactured from umbilical cord blood have reproducibly been reported to generate cultures with >70% CD27+ central memory γδ T cells[87]. Indeed, cord blood Vγ9Vδ2 cells are primarily a naïve memory phenotype, while circulating Vγ9Vδ2 T cells from adult PBMCs are primarily central memory T cells[144,145] that differentiate into effector memory T cells upon *ex vivo* expansion[140]. Naïve cord blood Vγ9Vδ2 T cells may be biased to generate central memory T cells central memory T cells because fetal Vγ9Vδ2 T cells must rapidly expand during the first year of life to populate the circulating repertoire. In addition to manufacturing central memory TAC Vγ9Vδ2 T cells for adoptive cell transfer, *in vivo* persistence may be further supported by integrating an IL-15 expression cassette into γ-retroviral TAC constructs for co-expression upstream or downstream of a T2A cleavage site. Recent experiments by Park et al. demonstrate that exogenous IL-15 administration enhanced *in vivo* persistence of adoptively transferred Vγ9Vδ2 T cells – more so than IL-2[92] – indicating that endogenous production of IL-15 by engineered TAC γδ T cells may support long-term proliferation and persistence.

We've shown that BCMA-TAC γδ T cell degranulation is enhanced when stimulated via both TAC and CD16, suggesting that a cancer immunotherapy that takes advantage of both signalling receptors may be beneficial to anti-tumour cytotoxicity. CD16 stimulation is also required to initiate antigen presentation functions in γδ T cells, and therefore may also represent a strategy to engage the endogenous host immune response. Although our attempts to assess the efficacy of a Daratumumab combination therapy have had limited success, we could attempt to recapitulate dual stimulation in in TAC γδ T cells by replacing the CD4 transmembrane and cytoplasmic domain of the gRV-BCMA-TAC#1195 construct with an FcRγ domain – similar to KIR2DS2 in the KIR-TAC gRV#1240 construct. FcRγ is a co-adaptor protein for CD16 with ITAM regions for receptor signal transduction[146] and may induce similar effector functions to CD16 stimulation in γδ T cells upon tumour ligand recognition when integrated into the TAC construct.

Conclusion

We have investigated the feasibility of BCMA-TAC engineered γδ T cell therapies for targeting Multiple Myeloma. We demonstrate that γδ T cells can be engineered with a BCMA-TAC γ-retroviral vector, and αβ-depleted at the end of culture to generate purified highly transduced BCMA-TAC γδ T cells. Our engineered BCMA-TAC γδ T cells rapidly and specifically eradicate *in vitro* MM tumour cells and generate Th1-associated cytokines in response to tumour co-culture.

We also assessed the potential for using an engineered γδ T cell and monoclonal antibody combination therapy. A combination therapy would take advantage of CD16-expression on γδ T cells, and the integration of monoclonal antibodies into front-line cancer treatments. BCMA-TAC γδ T cells express CD16 and have enhanced degranulation in response to CD16 and TAC dual stimulation. However, when we assessed the *in vitro* efficacy of a Daratumumab and engineered BCMA-TA γδ T cell therapy, it was unclear whether Daratumumab could improve killing or degranulation.

Thus, my investigations have confirmed the feasibility of manufacturing BCMA-TAC γδ T cells and their utility in eradicating BCMA-positive tumor *in vitro*. However, the benefit of combined therapy with monoclonal antibodies remains uncertain.

Supplementary

Supplementary Table 1A: CD16+ vs. CD16- Upregulated DEG

ENSEMBL ID	SYMBOL	GENENAME	log2fc	padj
ENSG00000224550	NA	NA	2.95	0.011
ENSG00000162383	SLC1A7	solute carrier family 1 member 7	2.88	0.013
ENSG00000203747	FCGR3A	Fc fragment of IgG receptor IIIa	2.56	0.005
ENSG00000242473	KIR2DP1	killer cell immunoglobulin like receptor, two Ig domains pseudogene 1	2.22	0.019
ENSG00000125498	KIR2DL1	killer cell immunoglobulin like receptor, two Ig domains and long cytoplasmic tail 1	2.14	0.009
ENSG00000167618	LAIR2	leukocyte associated immunoglobulin like receptor 2	1.92	0.033
ENSG00000071967	CYBRD1	cytochrome b reductase 1	1.90	0.005
ENSG00000221957	KIR2DS4	killer cell immunoglobulin like receptor, two Ig domains and short cytoplasmic tail 4	1.86	0.008
ENSG00000162825	NBPF20	NBPF member 20	1.78	0.02
ENSG00000205336	ADGRG1	adhesion G protein-coupled receptor G1	1.75	0.003
ENSG00000113269	RNF130	ring finger protein 130	1.62	0.023
ENSG00000162747	FCGR3B	Fc fragment of IgG receptor IIIb	1.58	0.016
ENSG00000270617	URGCP-MRPS24	URGCP-MRPS24 readthrough	1.42	0.024
ENSG00000147459	DOCK5	dedicator of cytokinesis 5	1.40	0.015
ENSG00000105370	LIM2	lens intrinsic membrane protein 2	1.31	0.006
ENSG00000127951	FGL2	fibrinogen like 2	1.30	<0.001
ENSG00000172460	PRSS30P	serine protease 30, pseudogene	1.23	0.006
ENSG00000011600	TYROBP	transmembrane immune signaling adaptor TYROBP	1.07	<0.001
ENSG00000182985	CADM1	cell adhesion molecule 1	1.06	<0.001
ENSG00000133067	LGR6	leucine rich repeat containing G protein-coupled receptor 6	1.05	0.016
ENSG00000196139	AKR1C3	aldo-keto reductase family 1 member C3	1.02	<0.001
ENSG00000109956	B3GAT1	beta-1,3-glucuronyltransferase 1	1.00	0.029
ENSG00000129595	EPB41L4A	erythrocyte membrane protein band 4.1 like 4A	0.99	0.017
ENSG00000100427	MLC1	modulator of VRAC current 1	0.96	<0.001
ENSG00000103056	SMPD3	sphingomyelin phosphodiesterase 3	0.89	0.002
ENSG00000170962	PDGFD	platelet derived growth factor D	0.86	0.011
ENSG00000168229	PTGDR	prostaglandin D2 receptor	0.84	<0.001
ENSG00000173930	SLCO4C1	solute carrier organic anion transporter family member 4C1	0.84	0.009
ENSG00000189430	NCR1	natural cytotoxicity triggering receptor 1	0.80	0.013
ENSG00000154734	ADAMTS1	ADAM metallopeptidase with thrombospondin type 1 motif 1	0.79	0.027
ENSG00000206190	ATP10A	ATPase phospholipid transporting 10A (putative)	0.77	<0.001
ENSG00000171101	SIGLEC17P	sialic acid binding Ig like lectin 17, pseudogene	0.75	0.045
ENSG00000169583	CLIC3	chloride intracellular channel 3	0.75	<0.001
ENSG00000204161	TMEM273	transmembrane protein 273	0.72	<0.001
ENSG00000126822	PLEKHG3	pleckstrin homology and RhoGEF domain containing G3	0.71	<0.001
ENSG00000198821	CD247	CD247 molecule	0.71	<0.001
ENSG00000152229	PSTPIP2	proline-serine-threonine phosphatase interacting protein 2	0.69	0.026
ENSG00000113721	PDGFRB	platelet derived growth factor receptor beta	0.69	<0.001
ENSG00000115523	GNLY	granulysin	0.69	0.042
ENSG00000176845	METRNL	meteorin like, glial cell differentiation regulator	0.67	0.011
ENSG00000109787	KLF3	Kruppel like factor 3	0.65	<0.001
ENSG00000083444	PLOD1	procollagen-lysine,2-oxoglutarate 5-dioxygenase 1	0.63	0.001
ENSG00000196914	ARHGEF12	Rho guanine nucleotide exchange factor 12	0.62	0.001
ENSG00000107679	PLEKHA1	pleckstrin homology domain containing A1	0.62	0.04
ENSG00000272655	NA	NA	0.62	0.021
ENSG00000180739	S1PR5	sphingosine-1-phosphate receptor 5	0.60	0.013
ENSG00000006756	ARSD	arylsulfatase D	0.59	0.04
ENSG00000145730	PAM	peptidylglycine alpha-amidating monooxygenase	0.55	0.002
ENSG00000075234	TTC38	tetratricopeptide repeat domain 38	0.53	<0.001
ENSG00000004468	CD38	CD38 molecule	0.53	<0.001
ENSG00000132718	SYT11	synaptotagmin 11	0.53	0.048
ENSG00000189319	FAM53B	family with sequence similarity 53 member B	0.52	<0.001
ENSG00000105327	BBC3	BCL2 binding component 3	0.52	0.013
ENSG00000168209	DDIT4	DNA damage inducible transcript 4	0.52	0.023

Supplementary Table 1B: CD16+ vs. CD16- Downregulated DEG

ENSEMBL ID	SYMBOL	GENENAME	log2fc	padj
ENSG00000157404	KIT	KIT proto-oncogene, receptor tyrosine kinase	-4.60	<0.001
ENSG00000148848	ADAM12	ADAM metallopeptidase domain 12	-4.46	<0.001
ENSG00000143365	RORC	RAR related orphan receptor C	-4.28	<0.001
ENSG00000080573	COL5A3	collagen type V alpha 3 chain	-4.11	0.001
ENSG00000111536	IL26	interleukin 26	-4.03	<0.001
ENSG00000049768	FOXP3	forkhead box P3	-3.90	0.001
ENSG00000214279	SCART1	scavenger receptor family member expressed on T cells 1	-3.47	<0.001
ENSG00000104267	CA2	carbonic anhydrase 2	-3.37	<0.001
ENSG00000017427	IGF1	insulin like growth factor 1	-3.19	0.009
ENSG00000162594	IL23R	interleukin 23 receptor	-2.84	<0.001
ENSG00000162630	B3GALT2	beta-1,3-galactosyltransferase 2	-2.74	0.001
ENSG00000136193	SCRN1	secernin 1	-2.68	<0.001
ENSG00000107282	APBA1	amyloid beta precursor protein binding family A member 1	-2.62	<0.001
ENSG00000167664	TMIGD2	transmembrane and immunoglobulin domain containing 2	-2.61	<0.001
ENSG00000148053	NTRK2	neurotrophic receptor tyrosine kinase 2	-2.59	0.018
ENSG00000144290	SLC4A10	solute carrier family 4 member 10	-2.47	<0.001
ENSG00000016391	CHDH	choline dehydrogenase	-2.45	0.039
ENSG00000184613	NELL2	neural EGFL like 2	-2.29	<0.001
ENSG00000104951	IL4I1	interleukin 4 induced 1	-2.25	0.004
ENSG00000138795	LEF1	lymphoid enhancer binding factor 1	-2.19	<0.001
ENSG00000182010	RTKN2	rhotekin 2	-2.13	0.001
ENSG00000270249	NA	NA	-2.13	0.049
ENSG00000156299	TIAM1	TIAM Rac1 associated GEF 1	-1.81	0.038
ENSG00000029534	ANK1	ankyrin 1	-1.79	0.004
ENSG00000095397	WHRN	whirlin	-1.77	0.043
ENSG00000169508	GPR183	G protein-coupled receptor 183	-1.60	0.03
ENSG00000204482	LST1	leukocyte specific transcript 1	-1.15	0.004
ENSG00000109943	CRTAM	cytotoxic and regulatory T cell molecule	-1.13	0.034
ENSG00000114554	PLXNA1	plexin A1	-0.94	0.002
ENSG00000120738	EGR1	early growth response 1	-0.93	0.047
ENSG00000286169	AHRR	aryl-hydrocarbon receptor repressor	-0.89	0.005
ENSG00000142102	PGGHG	protein-glucosylgalactosylhydroxylysine glucosidase	-0.87	<0.001
ENSG00000168056	LTBP3	latent transforming growth factor beta binding protein 3	-0.82	0.002
ENSG00000161996	WDR90	WD repeat domain 90	-0.72	0.019
ENSG00000119537	KDSR	3-ketodihydrosphingosine reductase	-0.71	<0.001
ENSG00000168685	IL7R	interleukin 7 receptor	-0.70	<0.001
ENSG00000136997	MYC	MYC proto-oncogene, bHLH transcription factor	-0.67	<0.001
ENSG00000172197	MBOAT1	membrane bound O-acyltransferase domain containing 1	-0.66	0.045
ENSG00000124813	RUNX2	RUNX family transcription factor 2	-0.66	0.028
ENSG00000120254	MTHFD1L	methylenetetrahydrofolate dehydrogenase (NADP+ dependent) 1 like	-0.63	0.007
ENSG00000042493	CAPG	capping actin protein, gelsolin like	-0.61	0.002
ENSG00000163519	TRAT1	T cell receptor associated transmembrane adaptor 1	-0.57	0.02
ENSG00000132382	MYBBP1A	MYB binding protein 1a	-0.52	0.012
ENSG00000166669	ATF7IP2	activating transcription factor 7 interacting protein 2	-0.52	0.01
ENSG00000178921	PFAS	phosphoribosylformylglycinamidine synthase	-0.52	<0.001
ENSG00000188677	PARVB	parvin beta	-0.51	0.022

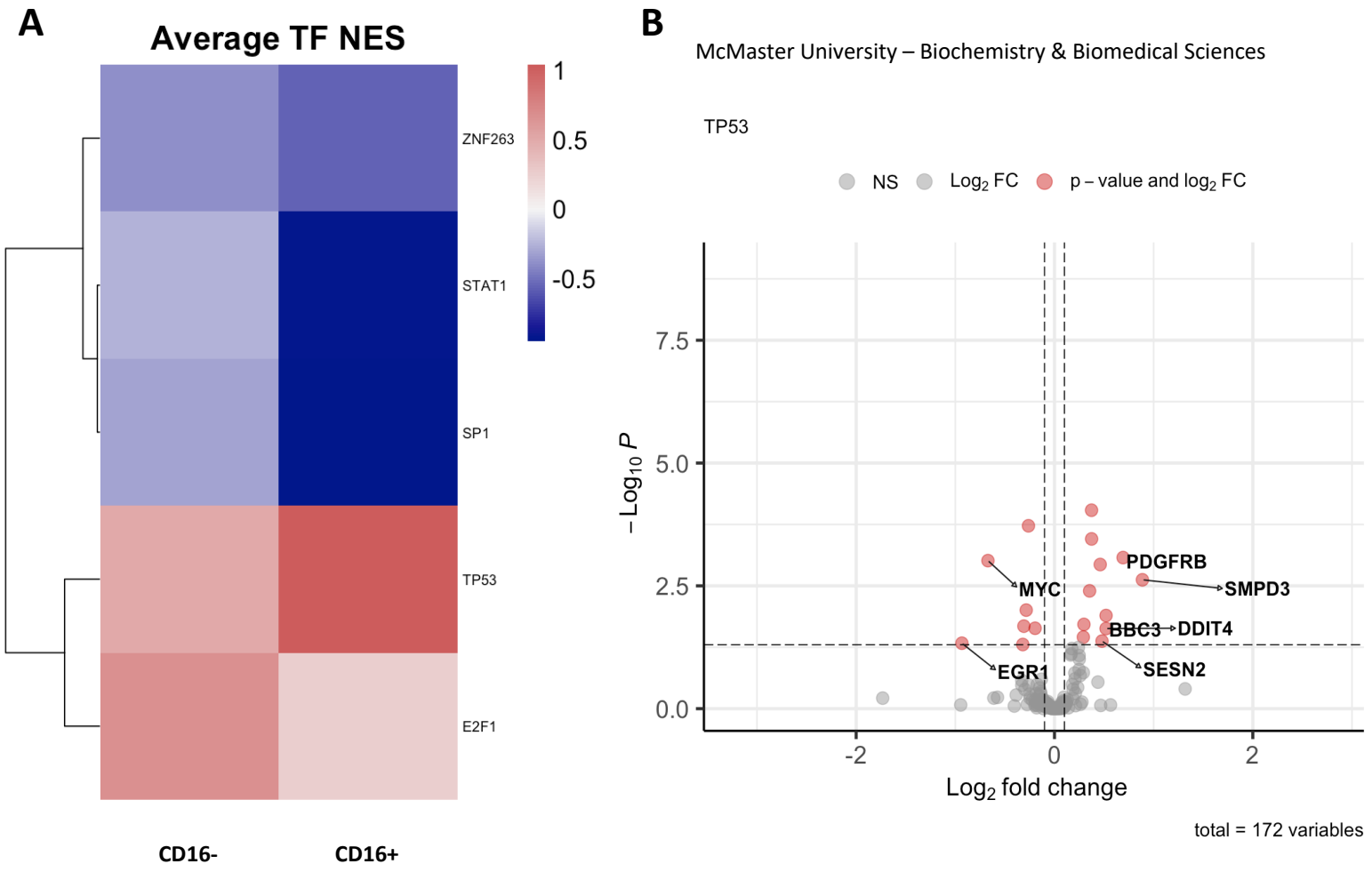

***Supplementary Figure 1**: Transcription factor prediction for CD16+ DEGs using dorothea. **A)** Predicted transcription factors associated and their mean Normalized Enriches Score (NES) in CD16- or CD16+ Vd2 fractions. **B)** Volcano plot of genes associated with upregulated transcription factor pathway TP53.*
Coloured point cut-off: p > 0.05, |LFC| > 0.1.
***C)** Volcano plot of genes associated with downregulated transcription factor pathway STAT1 (left) or SP1 (right).*

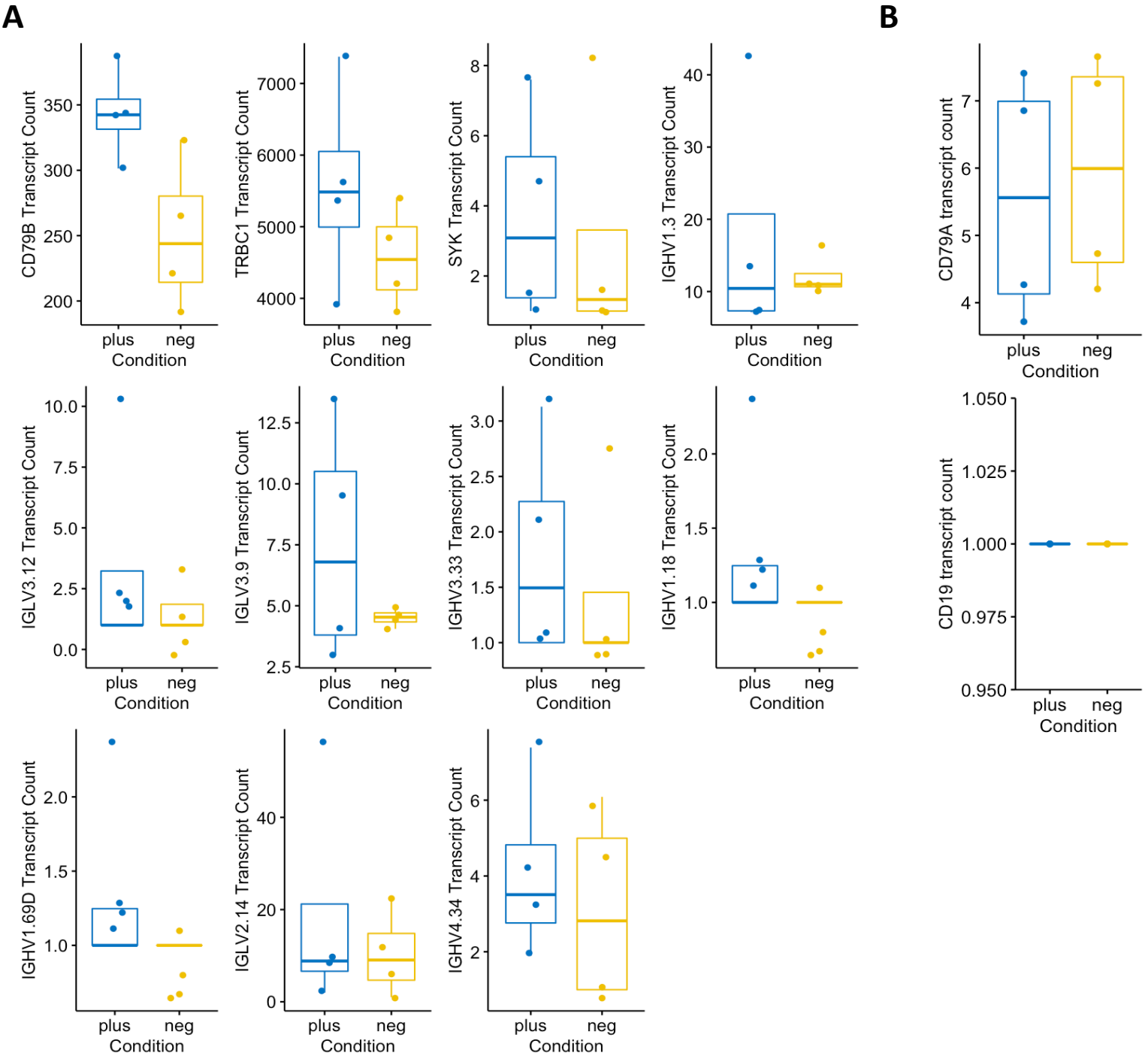

Supplementary Figure 2: *Normalized transcript counts of genes associated with Immunoglobulin complex GO pathway or B cells. Immunoglobulin and B cell transcript counts are low. CD79B has relatively high transcript counts, but other B cell lineage transripts are lowly or not expressed. Normalized transcripts include a pseudocount of 1.* ***A)*** *Immunoglobulin complex GO pathway genes* ***B)*** *B cell marker genes.*

Works Cited

1. Sonneveld, P. & Broijl, A. Treatment of relapsed and refractory multiple myeloma. *Haematologica* vol. 101 396–406 (2016).

2. Morgan, G. J., Walker, B. A. & Davies, F. E. The genetic architecture of multiple myeloma. *Nature Reviews Cancer* vol. 12 335–348 (2012).

3. Mitsiades, C. S., Mitsiades, N. S., Munshi, N. C., Richardson, P. G. & Anderson, K. C. The role of the bone microenvironment in the pathophysiology and therapeutic management of multiple myeloma: Interplay of growth factors, their receptors and stromal interactions. *Eur. J. Cancer* **42**, 1564–1573 (2006).

4. Tamura, H. *et al.* Marrow stromal cells induce B7-H1 expression on myeloma cells, generating aggressive characteristics in multiple myeloma. *Leukemia* **27**, 464–472 (2013).

5. Moreau, P. *et al.* Multiple myeloma: ESMO Clinical Practice Guidelines for diagnosis, treatment and follow-up. *Ann. Oncol.* (2017) doi:10.1093/annonc/mdx096.

6. Pulte, E. D. *et al.* FDA Approval Summary: Lenalidomide as Maintenance Therapy After Autologous Stem Cell Transplant in Newly Diagnosed Multiple Myeloma. *Oncologist* **23**, 734–739 (2018).

7. Durie, B. G. M. *et al.* Bortezomib with lenalidomide and dexamethasone versus lenalidomide and dexamethasone alone in patients with newly diagnosed myeloma without intent for immediate autologous stem-cell transplant (SWOG S0777): a randomised, open-label, phase 3 trial. *Lancet* **389**, 519–527 (2017).

8. Leblanc, R., Hollmann, S. & Tay, J. Canadian cost analysis comparing maintenance therapy with bortezomib versus lenalidomide for patients with multiple myeloma post autologous stem cell transplant. *J. Popul. Ther. Clin. Pharmacol.* (2016).

9. Ghobrial, I. *et al.* Immunotherapy in Multiple Myeloma: Accelerating on the Path to the Patient. *Clinical Lymphoma, Myeloma and Leukemia* (2019) doi:10.1016/j.clml.2019.02.004.

10. Bahlis, N. *et al.* Daratumumab Plus Lenalidomide and Dexamethasone (D-Rd) Versus Lenalidomide and Dexamethasone (Rd) in Patients with Newly Diagnosed Multiple Myeloma (NDMM) Ineligible for Transplant: Updated Analysis of Maia. *Blood* **134**, 1875–1875 (2019).

11. Harada, H. *et al.* Phenotypic difference of normal plasma cells from mature myeloma cells. *Blood* **81**, 2658–2663 (1993).

12. Nijhof, I. S. *et al.* Upregulation of CD38 expression on multiple myeloma cells by all-trans retinoic acid improves the efficacy of daratumumab. *Leukemia* **29**, 2039–2049 (2015).

13. Malavasi, F. *et al.* Evolution and function of the ADP ribosyl cyclase/CD38 gene family in

physiology and pathology. *Physiological Reviews* vol. 88 841–886 (2008).

14. Raedler, L. A. Darzalex (Daratumumab): First Anti-CD38 Monoclonal Antibody Approved for Patients with Relapsed Multiple Myeloma. *Am Heal. Drug Benefits* **9**, 70–73 (2016).

15. Zhou, H. *et al.* The efficacy and safety of anti-CD19/CD20 chimeric antigen receptor- T cells immunotherapy in relapsed or refractory B-cell malignancies:a meta-analysis. *BMC Cancer* **18**, 929 (2018).

16. Shah, N., Chari, A., Scott, E., Mezzi, K. & Usmani, S. Z. B-cell maturation antigen (BCMA) in multiple myeloma: rationale for targeting and current therapeutic approaches. *Leukemia* vol. 34 985–1005 (2020).

17. Brudno, J. N. *et al.* T cells genetically modified to express an anti–B-Cell maturation antigen chimeric antigen receptor cause remissions of poor-prognosis relapsed multiple myeloma. *J. Clin. Oncol.* **36**, 2267–2280 (2018).

18. Raje, N. *et al.* Anti-BCMA CAR T-cell therapy bb2121 in relapsed or refractory multiple myeloma. *N. Engl. J. Med.* (2019) doi:10.1056/NEJMoa1817226.

19. NC, M. *et al.* Idecabtagene Vicleucel in Relapsed and Refractory Multiple Myeloma. *N. Engl. J. Med.* **384**, 705–716 (2021).

20. Berdeja, J. G. *et al.* Ciltacabtagene autoleucel, a B-cell maturation antigen-directed chimeric antigen receptor T-cell therapy in patients with relapsed or refractory multiple myeloma (CARTITUDE-1): a phase 1b/2 open-label study. *Lancet* **398**, 314–324 (2021).

21. Helsen, C. W. *et al.* The chimeric TAC receptor co-opts the T cell receptor yielding robust anti-tumor activity without toxicity. *Nat. Commun.* **9**, (2018).

22. K, B. *et al.* Development of a B-cell maturation antigen-specific T-cell antigen coupler receptor for multiple myeloma. *Cytotherapy* (2021) doi:10.1016/J.JCYT.2021.05.007.

23. Dopfer, E. P. *et al.* The CD3 conformational change in the γδ T cell receptor is not triggered by antigens but can be enforced to enhance tumor killing. *Cell Rep.* **7**, 1704–1715 (2014).

24. Chien, Y., Meyer, C. & Bonneville, M. γδ T Cells: First Line of Defense and Beyond . *Annu. Rev. Immunol.* **32**, 121–155 (2014).

25. Silva-Santos, B., Serre, K. & Norell, H. γδT cells in cancer. *Nature Reviews Immunology* vol. 15 683–691 (2015).

26. Pizzolato, G. *et al.* Single-cell RNA sequencing unveils the shared and the distinct cytotoxic hallmarks of human TCRVδ1 and TCRVδ2 γδ T lymphocytes. *Proc. Natl. Acad. Sci. U. S. A.* **116**, 11906–11915 (2019).

27. Hviid, L. *et al.* High frequency of circulating γδ T cells with dominance of the V(δ)1 subset in a healthy population. *Int. Immunol.* (2000) doi:10.1093/intimm/12.6.797.

28. Cairo, C. *et al.* Impact of age, gender, and race on circulating γδ T cells. *Hum. Immunol.*

(2010) doi:10.1016/j.humimm.2010.06.014.

29. McVay, L. D. & Carding, S. R. Extrathymic origin of human gamma delta T cells during fetal development. *J. Immunol.* **157**, 2873–82 (1996).

30. Ravens, S. *et al.* Human γδ T cells are quickly reconstituted after stem-cell transplantation and show adaptive clonal expansion in response to viral infection. *Nat. Immunol.* **18**, 393–401 (2017).

31. Gertner-Dardenne, J. *et al.* Human Vγ9Vδ2 T Cells Specifically Recognize and Kill Acute Myeloid Leukemic Blasts. *J. Immunol.* **188**, 4701–4708 (2012).

32. Castella, B. *et al.* Anergic bone marrow Vγ9Vδ2 T cells as early and long-lasting markers of PD-1-targetable microenvironment-induced immune suppression in human myeloma. *Oncoimmunology* **4**, e1047580 (2015).

33. Di Lorenzo, B., Ravens, S. & Silva-Santos, B. High-throughput analysis of the human thymic Vδ1+ T cell receptor repertoire. *Sci. data* (2019) doi:10.1038/s41597-019-0118-2.

34. Fritz, G. Targeting the Mevalonate Pathway for Improved Anticancer Therapy. *Curr. Cancer Drug Targets* **9**, 626–638 (2009).

35. Silva-Santos, B., Mensurado, S. & Coffelt, S. B. γδ T cells: pleiotropic immune effectors with therapeutic potential in cancer. *Nature Reviews Cancer* vol. 19 392–404 (2019).

36. Boutin, L. & Scotet, E. Towards deciphering the hidden mechanisms that contribute to the antigenic activation process of human Vγ9Vd2 T cells. *Frontiers in Immunology* vol. 9 (2018).

37. Rigau, M. *et al.* Butyrophilin 2A1 is essential for phosphoantigen reactivity by gd T cells. *Science (80-.).* **367**, (2020).

38. Peigné, C.-M. *et al.* The Juxtamembrane Domain of Butyrophilin BTN3A1 Controls Phosphoantigen-Mediated Activation of Human Vγ9Vδ2 T Cells. *J. Immunol.* **198**, 4228–4234 (2017).

39. Peng, M. *et al.* Interleukin 17-producing γδ T cells increased in patients with active pulmonary tuberculosis. *Cell. Mol. Immunol.* **5**, 203–208 (2008).

40. Okamoto Yoshida, Y. *et al.* Essential Role of IL-17A in the Formation of a Mycobacterial Infection-Induced Granuloma in the Lung. *J. Immunol.* **184**, 4414–4422 (2010).

41. Happel, K. I. *et al.* Cutting Edge: Roles of Toll-Like Receptor 4 and IL-23 in IL-17 Expression in Response to Klebsiella pneumoniae Infection . *J. Immunol.* **170**, 4432–4436 (2003).

42. Ribeiro, S. T., Ribot, J. C. & Silva-Santos, B. Five layers of receptor signaling in γδ T-cell differentiation and activation. *Frontiers in Immunology* vol. 6 (2015).

43. Di Carlo, E. *et al.* Mechanisms of the antitumor activity of human Vγ9Vδ2 T cells in combination with zoledronic acid in a preclinical model of neuroblastoma. in *Molecular*

Therapy vol. 21 1034–1043 (Nature Publishing Group, 2013).

44. Raulet, D. H. Roles of the NKG2D immunoreceptor and its ligands. *Nature Reviews Immunology* vol. 3 781–790 (2003).

45. Lança, T. *et al.* The MHC class Ib protein ULBP1 is a nonredundant determinant of leukemia/lymphoma susceptibility to γδ T-cell cytotoxicity. *Blood* **115**, 2407–2411 (2010).

46. Kong, Y. *et al.* The NKG2D ligand ULBP4 binds to TCRγ9/δ2 and induces cytotoxicity to tumor cells through both TCRγδ and NKG2D. *Blood* **114**, 310–317 (2009).

47. Trichet, V. *et al.* Complex Interplay of Activating and Inhibitory Signals Received by Vγ9Vδ2 T Cells Revealed by Target Cell β 2 -Microglobulin Knockdown . *J. Immunol.* **177**, 6129–6136 (2006).

48. Coscia, M. *et al.* Dysfunctional Vγ9Vδ2 T cells are negative prognosticators and markers of dysregulated mevalonate pathway activity in chronic lymphocytic leukemia cells. *Blood* **120**, 3271–3279 (2012).

49. Lafarge, X. *et al.* Expression of MHC class I receptors confers functional intraclonal heterogeneity to a reactive expansion of γδ T cells. *Eur. J. Immunol.* **35**, 1896–1905 (2005).

50. Gertner-Dardenne, J. *et al.* Bromohydrin pyrophosphate enhances antibody-dependent cell-mediated cytotoxicity induced by therapeutic antibodies. *Blood* (2009) doi:10.1182/blood-2008-08-172296.

51. Sawaisorn, P. *et al.* Antigen-Presenting Cell Characteristics of Human γδ T Lymphocytes in Chronic Myeloid Leukemia. *Immunol. Invest.* (2019) doi:10.1080/08820139.2018.1529039.

52. Xiao, L. *et al.* Large-scale expansion of Vγ9Vδ2 T cells with engineered K562 feeder cells in G-Rex vessels and their use as chimeric antigen receptor–modified effector cells. *Cytotherapy* (2018) doi:10.1016/j.jcyt.2017.12.014.

53. Liu, M. *et al.* Trastuzumab enhanced the cytotoxicity of Vγ9Vδ2 T cells against zoledronate-sensitized osteosarcoma cells. *Int. Immunopharmacol.* (2015) doi:10.1016/j.intimp.2015.06.002.

54. Lafont, V., Liautard, J., Liautard, J. P. & Favero, J. Production of TNF-α by Human Vγ9Vδ2 T Cells Via Engagement of FcγRIIIA, the Low Affinity Type 3 Receptor for the Fc Portion of IgG, Expressed upon TCR Activation by Nonpeptidic Antigen. *J. Immunol.* (2001) doi:10.4049/jimmunol.166.12.7190.

55. da Silva, F. P., Aloulou, M., Benhamou, M. & Monteiro, R. C. Inhibitory ITAMs: a matter of life and death. *Trends Immunol.* (2008) doi:10.1016/j.it.2008.05.001.

56. Patel, K. R., Roberts, J. T. & Barb, A. W. Multiple Variables at the Leukocyte Cell Surface Impact Fc γ Receptor-Dependent Mechanisms. *Frontiers in immunology* (2019) doi:10.3389/fimmu.2019.00223.

57. Hamerman, J. A., Ni, M., Killebrew, J. R., Chu, C. L. & Lowell, C. A. The expanding roles of ITAM adapters FcRγ and DAP12 in myeloid cells. *Immunological Reviews* vol. 232 42–58 (2009).

58. Getahun, A. & Cambier, J. C. Of ITIMs, ITAMs, and ITAMis: Revisiting immunoglobulin Fc receptor signaling. *Immunological Reviews* (2015) doi:10.1111/imr.12336.

59. Braza, M. S., Klein, B., Fiol, G. & Rossi, J. F. γδT-cell killing of primary follicular lymphoma cells is dramatically potentiated by GA101, a type II glycoengineered anti-CD20 monoclonal antibody. *Haematologica* (2011) doi:10.3324/haematol.2010.029520.

60. Capietto, A.-H., Martinet, L. & Fournié, J.-J. Stimulated γδ T Cells Increase the In Vivo Efficacy of Trastuzumab in HER-2 + Breast Cancer . *J. Immunol.* (2011) doi:10.4049/jimmunol.1100681.

61. Himoudi, N. *et al.* Human γδ T Lymphocytes Are Licensed for Professional Antigen Presentation by Interaction with Opsonized Target Cells. *J. Immunol.* **188**, 1708–1716 (2012).

62. Barisa, M. *et al.* E. coli promotes human Vγ9Vδ2 T cell transition from cytokine-producing bactericidal effectors to professional phagocytic killers in a TCR-dependent manner. *Sci. Rep.* **7**, 1–12 (2017).

63. Mantegazza, A. R., Magalhaes, J. G., Amigorena, S. & Marks, M. S. Presentation of Phagocytosed Antigens by MHC Class I and II. *Traffic* (2013) doi:10.1111/tra.12026.

64. Wu, Y. *et al.* Human γδ T Cells: A Lymphoid Lineage Cell Capable of Professional Phagocytosis. *J. Immunol.* **183**, 5622–5629 (2009).

65. Meuter, S., Eberl, M. & Moser, B. Prolonged antigen survival and cytosolic export in cross-presenting human γδ T cells. *Proc. Natl. Acad. Sci. U. S. A.* **107**, 8730–8735 (2010).

66. Angelini, D. F. *et al.* FcγRIII discriminates between 2 subsets of Vγ9Vδ2 effector cells with different responses and activation pathways. *Blood* (2004) doi:10.1182/blood-2004-01-0331.

67. Ryan, P. L. *et al.* Heterogeneous yet stable Vδ2(+) T-cell profiles define distinct cytotoxic effector potentials in healthy human individuals. *Proc. Natl. Acad. Sci.* **113**, 14378–14383 (2016).

68. Tice, J. A. *et al. Chimeric Antigen Receptor T-Cell Therapy for B- Cell Cancers: Effectiveness and Value*. *Institute for Clinical and Economic Review* https://icer-review.org/wp-content/uploads/2017/07/ICER_CAR_T_Final_Evidence_Report_032318.pdf (2017).

69. Shlomchik, W. D. Graft-versus-host disease. *Nature Reviews Immunology* vol. 7 340–352 (2007).

70. Kernan, N. *et al.* Clonable T lymphocytes in T cell-depleted bone marrow transplants correlate with development of graft-v-host disease. *Blood* **68**, 770–773 (1986).

71. Born, W. K., Kemal Aydintug, M. & O'brien, R. L. Diversity of γδ T-cell antigens. *Cellular and Molecular Immunology* vol. 10 13–20 (2013).

72. Gentles, A. J. *et al.* The prognostic landscape of genes and infiltrating immune cells across human cancers. *Nat. Med.* **21**, 938–945 (2015).

73. Alnaggar, M. *et al.* Allogenic Vγ9Vδ2 T cell as new potential immunotherapy drug for solid tumor: a case study for cholangiocarcinoma. *J. Immunother. Cancer* **7**, 36 (2019).

74. Xu, Y. *et al.* Allogeneic Vγ9Vδ2 T-cell immunotherapy exhibits promising clinical safety and prolongs the survival of patients with late-stage lung or liver cancer. *Cell. Mol. Immunol.* (2020) doi:10.1038/s41423-020-0515-7.

75. Airoldi, I. *et al.* γδ T-cell reconstitution after HLA-haploidentical hematopoietic transplantation depleted of TCR-αβ+/CD19+ lymphocytes. *Blood* **125**, 2349–2358 (2015).

76. Arruda, L. C. M., Gaballa, A. & Uhlin, M. Impact of gd T cells on clinical outcome of hematopoietic stem cell transplantation: Systematic review and meta-analysis. *Blood Advances* vol. 3 3436–3448 (2019).

77. Arruda, L. C. M., Gaballa, A. & Uhlin, M. Impact of γδ T cells on clinical outcome of hematopoietic stem cell transplantation: systematic review and meta-analysis. *Blood Adv.* **3**, 3436–3448 (2019).

78. Capsomidis, A. *et al.* Chimeric Antigen Receptor-Engineered Human Gamma Delta T Cells: Enhanced Cytotoxicity with Retention of Cross Presentation. *Mol. Ther.* **26**, 354–365 (2018).

79. Nada, M. H., Wang, H., Workalemahu, G., Tanaka, Y. & Morita, C. T. Enhancing adoptive cancer immunotherapy with Vγ2Vδ2 T cells through pulse zoledronate stimulation. *J. Immunother. Cancer* **5**, (2017).

80. Joalland, N. *et al.* Combined chemotherapy and allogeneic human Vγ9Vδ2 T lymphocyte-immunotherapies efficiently control the development of human epithelial ovarian cancer cells in vivo. *Oncoimmunology* **8**, e1649971 (2019).

81. Serrano, R., Wesch, D. & Kabelitz, D. Activation of Human γδ T Cells: Modulation by Toll-Like Receptor 8 Ligands and Role of Monocytes. *Cells* **9**, 713 (2020).

82. Correia, D. V. *et al.* Highly active microbial phosphoantigen induces rapid yet sustained MEK/Erk- and PI-3K/Akt-mediated signal transduction in anti-tumor human γδ T-cells. *PLoS One* **4**, (2009).

83. Ribot, J. C., Ribeiro, S. T., Correia, D. V., Sousa, A. E. & Silva-Santos, B. Human γδ Thymocytes Are Functionally Immature and Differentiate into Cytotoxic Type 1 Effector T Cells upon IL-2/IL-15 Signaling. *J. Immunol.* **192**, 2237–2243 (2014).

84. Van Acker, H. H. *et al.* Interleukin-15 enhances the proliferation, stimulatory phenotype, and antitumor effector functions of human gamma delta T cells. *J. Hematol. Oncol.* **9**, 1–13 (2016).

85. DOMAE, E. *et al.* IL-15, but Not IL-2, Induces Proliferative Activity of Human Ex Vivo Expanded Vγ9Vδ2 T Cells. *J. Oral Tissue Eng.* **15**, 143–148 (2018).

86. Viey, E. *et al.* Chemokine Receptors Expression and Migration Potential of Tumor-infiltrating and Peripheral-expanded Vγ9Vδ2 T Cells From Renal Cell Carcinoma Patients. *J. Immunother.* **31**, 313–323 (2008).

87. Cairo, C. *et al.* Human cord blood γδ T cells expressing public Vγ2 chains dominate the response to bisphosphonate plus interleukin-15. *Immunology* **138**, 346–360 (2013).

88. Kunzmann, V. *et al.* Stimulation of γδ T cells by aminobisphosphonates and induction of antiplasma cell activity in multiple myeloma. *Blood* **96**, 384–392 (2000).

89. Sebestyen, Z., Prinz, I., Déchanet-Merville, J., Silva-Santos, B. & Kuball, J. Translating gammadelta (γδ) T cells and their receptors into cancer cell therapies. *Nature Reviews Drug Discovery* vol. 19 169–184.

90. Ang, W. X. *et al.* Electroporation of NKG2D RNA CAR Improves Vγ9Vδ2 T Cell Responses against Human Solid Tumor Xenografts. *Mol. Ther. - Oncolytics* (2020) doi:10.1016/j.omto.2020.04.013.

91. Rozenbaum, M. *et al.* Gamma-Delta CAR-T Cells Show CAR-Directed and Independent Activity Against Leukemia. *Front. Immunol.* (2020) doi:10.3389/fimmu.2020.01347.

92. Park, J. A., Santich, B. H., Xu, H., Lum, L. G. & Cheung, N.-K. K. V. Potent ex vivo armed T cells using recombinant bispecific antibodies for adoptive immunotherapy with reduced cytokine release. *J. Immunother. Cancer* **9**, e002222 (2021).

93. Fisher, J. *et al.* Avoidance of On-Target Off-Tumor Activation Using a Co-stimulation-Only Chimeric Antigen Receptor. *Mol. Ther.* **25**, 1234–1247 (2017).

94. Overbey, E. G. *et al.* NASA GeneLab RNA-seq consensus pipeline: standardized processing of short-read RNA-seq data. *iScience* **24**, 102361 (2021).

95. Krueger, F. Trim Galore!: A wrapper tool around Cutadapt and FastQC to consistently apply quality and adapter trimming to FastQ files. *Babraham Inst.* (2015).

96. Andrews, S. FastQC. *Babraham Bioinforma.* (2010).

97. Ewels, P., Magnusson, M., Lundin, S. & Käller, M. MultiQC: Summarize analysis results for multiple tools and samples in a single report. *Bioinformatics* (2016) doi:10.1093/bioinformatics/btw354.

98. Dobin, A. *et al.* STAR: Ultrafast universal RNA-seq aligner. *Bioinformatics* (2013) doi:10.1093/bioinformatics/bts635.

99. Li, B. & Dewey, C. N. RSEM: Accurate transcript quantification from RNA-Seq data with or without a reference genome. *BMC Bioinformatics* (2011) doi:10.1186/1471-2105-12-323.

100. Love, M. I., Huber, W. & Anders, S. Moderated estimation of fold change and dispersion for RNA-seq data with DESeq2. *Genome Biol.* (2014) doi:10.1186/s13059-014-0550-8.

101. Ritchie, M. E. *et al.* Limma powers differential expression analyses for RNA-sequencing and microarray studies. *Nucleic Acids Res.* (2015) doi:10.1093/nar/gkv007.

102. Blighe, K., Rana, S. & Lewis, M. EnhancedVolcano: Publication-ready volcano plots with enhanced colouring and labelin. *R-Package* (2019).

103. Yu, G., Wang, L. G., Han, Y. & He, Q. Y. ClusterProfiler: An R package for comparing biological themes among gene clusters. *Omi. A J. Integr. Biol.* (2012) doi:10.1089/omi.2011.0118.

104. Garcia-Alonso, L., Holland, C. H., Ibrahim, M. M., Turei, D. & Saez-Rodriguez, J. Benchmark and integration of resources for the estimation of human transcription factor activities. *Genome Res.* (2019) doi:10.1101/gr.240663.118.

105. Puente-Santamaria, L., Wasserman, W. W. & Del Peso, L. TFEA.ChIP: A tool kit for transcription factor binding site enrichment analysis capitalizing on ChIP-seq datasets. *Bioinformatics* (2019) doi:10.1093/bioinformatics/btz573.

106. Wickham, H. *et al.* Welcome to the Tidyverse. *J. Open Source Softw.* (2019) doi:10.21105/joss.01686.

107. Thomas, L. & Miller, A. Package 'leaps'. Regression subset selection. *CRAN R Project* (2020).

108. Cribari-Neto, F. & Zeileis, A. Beta regression in R. *J. Stat. Softw.* (2010) doi:10.18637/jss.v034.i02.

109. Kondo, M. *et al.* Expansion of human peripheral blood γδ T cells using zoledronate. *J. Vis. Exp.* (2011) doi:10.3791/3182.

110. Van Acker, H. H. *et al.* The role of the common gamma-chain family cytokines in γδ T cell-based anti-cancer immunotherapy. *Cytokine and Growth Factor Reviews* vol. 41 54–64 (2018).

111. Alexander, A. A. Z. *et al.* Isopentenyl pyrophosphate-activated CD56+ γδ T lymphocytes display potent antitumor activity toward human squamous cell carcinoma. *Clin. Cancer Res.* (2008) doi:10.1158/1078-0432.CCR-07-4912.

112. Mellor, J. D., Brown, M. P., Irving, H. R., Zalcberg, J. R. & Dobrovic, A. A critical review of the role of Fc gamma receptor polymorphisms in the response to monoclonal antibodies in cancer. *Journal of Hematology and Oncology* vol. 6 1–10 (2013).

113. Chekmasova, A. A. *et al.* A Novel and Highly Potent CAR T Cell Drug Product for Treatment of BCMA-Expressing Hematological Malignances. *Blood* **126**, 3094–3094 (2015).

114. Friedman, K. M. *et al.* Effective Targeting of Multiple B-Cell Maturation Antigen–Expressing Hematological Malignances by Anti-B-Cell Maturation Antigen Chimeric Antigen Receptor T Cells. *Hum. Gene Ther.* **29**, 585–601 (2018).

115. Dussault, N. *et al.* Immunomodulation of human B cells following treatment with intravenous immunoglobulins involves increased phosphorylation of extracellular signal-regulated kinases 1 and 2. *Int. Immunol.* **20**, 1369–1379 (2008).

116. Hastie, T., Tibshirani, R., James, G. & Witten, D. Chapter 6.1.2 Stepwise Selection. in *An Introduction to Statistical Learning* (Springer Texts, 2013).

117. Wang, W. & Zou, W. Amino Acids and Their Transporters in T Cell Immunity and Cancer Therapy. *Mol. Cell* **80**, 384–395 (2020).

118. Johnson, M. O. M. E. *et al.* Distinct Regulation of Th17 and Th1 Cell Differentiation by Glutaminase-Dependent Metabolism. *Cell* **175**, 1780 (2018).

119. Capone, A. & Volpe, E. Transcriptional Regulators of T Helper 17 Cell Differentiation in Health and Autoimmune Diseases. *Front. Immunol.* **0**, 348 (2020).

120. Donnelly, R. P. *et al.* Interleukin-26: An IL-10-related cytokine produced by Th17 cells. *Cytokine Growth Factor Rev.* **21**, 393 (2010).

121. Michel, M.-L. *et al.* Interleukin 7 (IL-7) selectively promotes mouse and human IL-17–producing γδ cells. *Proc. Natl. Acad. Sci. U. S. A.* **109**, 17549 (2012).

122. Zhou, A. X., Hed, A. El, Mercer, F., Kozhaya, L. & Unutmaz, D. The Metalloprotease ADAM12 Regulates the Effector Function of Human Th17 Cells. *PLoS One* **8**, 81146 (2013).

123. V, S. *et al.* IL-4-induced gene 1 maintains high Tob1 expression that contributes to TCR unresponsiveness in human T helper 17 cells. *Eur. J. Immunol.* **44**, 654–661 (2014).

124. BH, Y. *et al.* Foxp3(+) T cells expressing RORγt represent a stable regulatory T-cell effector lineage with enhanced suppressive capacity during intestinal inflammation. *Mucosal Immunol.* **9**, 444–457 (2016).

125. Molinier-Frenkel, V., Prévost-Blondel, A. & Castellano, F. The IL4I1 Enzyme: A New Player in the Immunosuppressive Tumor Microenvironment. *Cells* **8**, 757 (2019).

126. McAleer, J. P. & Kolls, J. K. Mechanisms controlling Th17 cytokine expression and host defense. *J. Leukoc. Biol.* (2011) doi:10.1189/jlb.0211099.

127. Truong, K.-L. *et al.* Killer-like receptors and GPR56 progressive expression defines cytokine production of human CD4 + memory T cells. *Nat. Commun. 2019 101* **10**, 1–15 (2019).

128. Wistuba-Hamprecht, K., Haehnel, K., Janssen, N., Demuth, I. & Pawelec, G. Peripheral blood T-cell signatures from high-resolution immune phenotyping of γδ and αβ T-cells in younger and older subjects in the Berlin Aging Study II. *Immun. Ageing 2015 121* **12**, 1–12 (2015).

129. Sato, K. *et al.* Th17 functions as an osteoclastogenic helper T cell subset that links T cell activation and bone destruction. *J. Exp. Med.* **203**, 2673 (2006).

130. TV, S., Z, H., E, M., J, V. & VB, K. Chondroitin sulphate inhibits NF-κB activity induced by interaction of pathogenic and damage associated molecules. *Osteoarthr. Cartil.* **25**, 166–174 (2017).

131. Bishnoi, M., Jain, A., Hurkat, P. & Jain, S. K. Chondroitin sulphate: a focus on osteoarthritis. *Glycoconjugate J. 2016 335* **33**, 693–705 (2016).

132. AK, S. Amino acids and immune response: a role for cysteine, glutamine, phenylalanine, tryptophan and arginine in T-cell function and cancer? *Pathol. Oncol. Res.* **21**, 9–17 (2015).

133. Farrington, L. A. *et al.* Opsonized antigen activates Vδ2+ T cells via CD16/FCγRIIIa in individuals with chronic malaria exposure. *PLOS Pathog.* **16**, e1008997 (2020).

134. Junqueira, C. *et al.* γδ T cells suppress Plasmodium falciparum blood-stage infection by direct killing and phagocytosis. *Nat. Immunol. 2021 223* **22**, 347–357 (2021).

135. Yang, R. *et al.* IL-12 Expands and Differentiates Human Vγ2Vδ2 T Effector Cells Producing Antimicrobial Cytokines and Inhibiting Intracellular Mycobacterial Growth. *Front. Immunol.* **0**, 913 (2019).

136. Yin, S. *et al.* Hyperactivation and in situ recruitment of inflammatory Vδ2 T cells contributes to disease pathogenesis in systemic lupus erythematosus. *Sci. Reports 2015 51* **5**, 1–12 (2015).

137. Nedellec, S., Sabourin, C., Bonneville, M. & Scotet, E. NKG2D Costimulates Human Vγ9Vδ2 T Cell Antitumor Cytotoxicity through Protein Kinase Cθ-Dependent Modulation of Early TCR-Induced Calcium and Transduction Signals. *J. Immunol.* (2010) doi:10.4049/jimmunol.1000373.

138. Mayer, M. P. & Bukau, B. Hsp70 chaperones: Cellular functions and molecular mechanism. *Cell. Mol. Life Sci.* **62**, 670 (2005).

139. Kleiveland, C. R. Peripheral Blood Mononuclear Cells. *Impact Food Bioact. Heal. Vitr. Ex Vivo Model.* 161–167 (2015) doi:10.1007/978-3-319-16104-4_15.

140. Berglund, S., Gaballa, A., Sawaisorn, P., Sundberg, B. & Uhlin, M. Expansion of gammadelta T cells from cord blood: A therapeutical possibility. *Stem Cells Int.* **2018**, (2018).

141. PATAKAS, A., LONDON, T. & COSIMO, E. Modified car-t. (2019).

142. Ramstead, A. G. & Jutila, M. A. Complex Role of γδ T-Cell-Derived Cytokines and Growth Factors in Cancer. *J. Interf. Cytokine Res.* **32**, 563 (2012).

143. Roche, P. A. & Furuta, K. The ins and outs of MHC class II-mediated antigen processing and presentation. *Nat. Rev. Immunol. 2015 154* **15**, 203–216 (2015).

144. Rosa, S. C. De *et al.* Ontogeny of γδ T Cells in Humans. *J. Immunol.* **172**, 1637–1645 (2004).

145. Davey, M. S. *et al.* The human Vδ2+ T-cell compartment comprises distinct innate-like Vγ9+ and adaptive Vγ9- subsets. **9**, 1–14 (2018).

146. Nimmerjahn, F. & Ravetch, J. V. Fcγ receptors as regulators of immune responses. *Nat. Rev. Immunol. 2007 81* **8**, 34–47 (2008).